Functional analysis of the *Drosophila* gene *smallish (CG43427)*

PhD Thesis

for the award of the degree

"doctor rerum naturalium"

in the GGNB program Genes and Development

at the Georg August University Göttingen,

Faculty of Biology

Submitted by

Seyed Amir Hamze Beati

born in Henstedt-Ulzburg, Germany

Göttingen, 2013

PhD Thesis Committee

Prof. Dr. Andreas Wodarz (Uni-Med)

Department of Anatomy and Cell Biology (Stem Cell Biology)

Georg-August-University, Göttingen

Prof. Dr. Ernst Wimmer (Uni-Bio)

Department of Developmental Biology

Georg-August-University, Göttingen

Prof. Dr. Reinhard Schuh (MPI-bpc)

Department of Molecular Developmental Biochemistry (Molecular Organogenesis)

Max Planck Institute for Biophysical Chemistry, Göttingen

Day of PhD examination: 13th march 2013

AFFIDAVIT

I hereby declare that I prepared the thesis "Functional analysis of the *Drosophila* gene *smallish (CG43427)*" on my own with no other sources and aids than quoted.

Seyed Amir Hamze Beati

Göttingen, January 31st 2013

TABLE OF CONTENTS

Acknowledgments

Firstly, I would like to thank Prof. Dr. Andreas Wodarz for giving me the opportunity to do my PhD thesis in his lab. I really appreciate the helpful discussions, ideas, support and that I had the possibility to develop my own ideas. Thank you.

I further would like to thank Prof. Dr. Ernst Wimmer and Prof. Dr. Reinhard Schuh for being part of my thesis committee and for the helpful discussions and suggestions during my committee meetings.

In addition I would like to thank the GGNB program “Genes and Development” for organization, helpful discussions and the nice atmosphere at the retreats and the GZMB, CMPB and DFG for funding this project.

I am grateful to Shigeo Hayashi for providing pSrc antibody, Kaoru Saigo for the Src42A antibody and *Src42A* mutants and Michael A. Simon for providing *Src64B* mutants.

Meinen besonderen Dank möchte ich allen der Abteilung Stammzellbiologie widmen. Es war eine sehr schöne Zeit in der ich viel gelernt habe und vorallem auch sehr viel Spaß gehabt habe. Mona, ich weiß du magst nicht vorne stehen, aber vielen Dank für deine stetige Hilfsbereitschaft und das Klonieren von unklonierbaren Konstrukten (ich bin mir sicher selbst Titin wäre vor dir nicht sicher!). Karen, dir danke ich für das gegenseitige Aufbauen während unserer beider Arbeiten, dein stets offenes Ohr und vorallem für deine Freundschaft. Vielen Dank dafür! Jaffer möchte ich für das coolste „Fellowship“ des Universums danken. Ganz besonderen Dank auch für die vielen Korrekturen. Thanks Bro! Oh Carolina, dir danke ich natürlich auch für die zahlreichen lustigen Abende mit unserem Kumpel Jack und dem stetigem Versuch das Ameisensterben zu stoppen. Sascha, auch wenn du schon zu den „Ehemaligen“ gehörst danke ich dir für eine coole Zeit im Labor, auch wenn dein Musikgeschmack echt grenzwertig ist… Bei Katja (Krusty) möchte ich mich gerne für den „Motivationsschub“ in der Endphase dieser Arbeit bedanken! Patricia, vielen Dank für den ganzen bürokratischen Teil und mein erstes Whisky Seminar. Das wird definitiv sehr bald wiederholt! Ich möchte mich weiterhin bei Katja (Curthi) und Claudia für die stetige Hilfe im Labor und die jährlichen BBQs bedanken, sowie Julia für das super Fliegenfutter! Manu danke ich für die Diskussionen und Ideen. Natürlich gilt besonderer Dank auch Ieva, Marilena, Gang, Nils und Tobi. Ihr seit mir alle sehr ans Herz gewachsen und werde die gemeinsame Zeit mit euch nicht

vergessen. Ich werde diese als eine meiner positivsten in Erinnerung behalten. Mein weiterer Dank gilt auch den Molekularen Onkologen für die gemeinsame Zeit auf unserem Flur, den netten Gesprächen bei der Kaffeerunde und den zahlreichen Aktivitäten außerhalb des Labors.

Mein besonderer Dank gilt meiner Familie und meinen Freunden. Ihr habt mir immer den Rücken gestärkt, mich unterstützt und motiviert sobald es nötig war. Dies hat mir letztlich sehr geholfen alle Tiefs zu durchstehen. Vielen, vielen Dank!

Abstract

The establishment and maintenance of cell polarity is crucial for the function of many cell types in multicellular organisms. Especially in epithelial tissues, cell polarity is connected to the regulation of cell adhesion and regulated by a complex hierarchy of highly conserved proteins. These can be subdivided into three groups of genes, the *bazooka* and *crumbs* groups, which encode apically localizing proteins, and the *discs large* group that encodes laterally localizing tumor suppressor proteins. Among these classes of proteins, Bazooka (Baz), the *Drosophila* homolog of vertebrate Par-3, plays a predominant role as shown by genetic epistasis experiments.

In a yeast two-hybrid screen we identified the protein encoded by the annotated gene *CG43427* which we named *smallish (smash),* as a new interaction partner of Baz. The gene product of *smash* possesses a C-terminal PDZ binding motif and a LIM domain close to the C-terminus. Endogenous Smash colocalizes with Baz apically in epithelial cells, a region harboring the adherens junctions (AJs). Co-immunoprecipitation of Baz and an N-terminally tagged version of Smash-PI (an isoform encoding for the last 889 amino acids of Smash) has confirmed that these proteins interact *in vivo* in embryos.

To analyze the function of *smash* during the development of *Drosophila*, we generated two different knockout alleles by transdeletion, one representing a null allele and the other a C-terminal truncation affecting the part of the protein carrying the LIM domain and the PDZ binding motif. We found that *smash* is not an essential gene, as homozygous mutants for both alleles are viable and fertile. The subcellular localization of polarity markers such as Baz were not affected upon *smash* knockout. On the other hand, overexpression of Smash using the UAS/Gal4 system and transgenes encoding for N-terminally GFP-tagged versions of Smash caused lethality in embryonic and larval stages. Rare eclosing escaper flies were decreased in body size. Overexpression of Smash in epithelial cells resulted in reduction of the apical surface area, indicating that Smash may function in apical constriction, a process important for morphogenetic rearrangements in epithelia. Overexpression of Smash during eye development caused a rough eye phenotype and reduction of eye size. Upon ubiquitous overexpression of Smash in embryos, many embryonic cuticles exhibited anterior and dorsal holes.

Following up on these findings, we showed that the non-receptor tyrosine kinase Src42A binds N-terminally GFP-tagged versions of Smash-PI *in vitro* in S2 cells and is furthermore able to phosphorylate GFP-Smash-PI. Endogenous Smash protein was found to be tyrosine phosphorylated *in vivo* in embryos as well. Domain deletion versions of Src42A still showed binding to Smash, indicating different binding mechanisims provided by the fact that tyrosine phosphorylation of Smash was only abolished upon deletion of the kinase domain.

A double mutant for *Src64B*, the second Src kinase encoded by the *Drosophila* genome, and *smash* is lethal. However, embryonic cuticles did not show defects and epithelial integrity appeared intact.

List of figures

List of tables

1 Introduction

1.1 Cell polarity

The polarization of a cell regulates various aspects of cell behaviour, such as the shape of the cell, the unequal distribution of organelles or the alignment of the cytoskeleton. Cell membranes are furthermore composed of different types of lipids, which also represents a type of polarization. A very important feature of polarization is provided by the asymmetric localization of different proteins or protein complexes. Many types of cells are polarized, e.g. neurons, oocytes or stem cells, to mention a few.

Epithelial cells represent a highly polarized cell type and have important functions in forming physiological and mechanical barriers (Suzuki and Ohno, 2006) and in shaping a metazoan organism by delineating different compartments (Knust and Bossinger, 2002). The plasma membrane of epithelial cells can be subdivided into two distinct domains: the apical membrane domain facing the environment or a lumen and the basolateral membrane domain, which is in contact with neighboring cells and the basal substratum. These two membrane domains are segregated by highly elaborated adherens junctions (AJs). Fig.1 shows a schematic of an ectodermal epithelial cell of *Drosophila melanogaster* (*Drosophila*) in comparison with an ectodermal epithelial cell of vertebrates.

The region containing the AJs is also referred to as the zonula adherens (ZA). A region slightly above the ZA is called marginal zone or subapical region (SAR), which harbours proteins which have been identified as homologs of vertebrate tight junction (TJ) proteins. However, TJs are absent in *Drosophila* which in contrast features septate junctions (SJ) at the lateral membrane, which are not formed in vertebrates (Fig.1). Within these membrane domains three main protein complexes had been identified over the past two decades, which localize in a highly polarized fashion to these distinct regions. These complexes will be discussed in more detail in the following pages with regard to their function in ectodermal epithelia.

As mentioned above, another highly polarized cell type is represented by stem cells. The *Drosophila* ventral neural ectoderm (VNE) is the origin for *Drosophila* neuroblasts (NB), which will give rise to the nervous system of the animal. Here, NBs divide asymmetrically, which leads to the generation of two daughter cells, another NB and a ganglion mother cell (GMC). The latter cell will

divide once more and give rise to a pair of neuron or glial cells, whereas the NB will continue dividing (Wodarz and Huttner, 2003; Wodarz, 2005). In the VNE, individual neuroectodermal cells are determined to become NBs via Notch/Delta signaling and delaminate from the epithelium into the embryo (Doe, 2008). A very important point is that the NB will inherit the polarization of the neuroectodermal cells, which indicates that those proteins needed for polarization are not just important for epithelial cells but also for other types of cells.

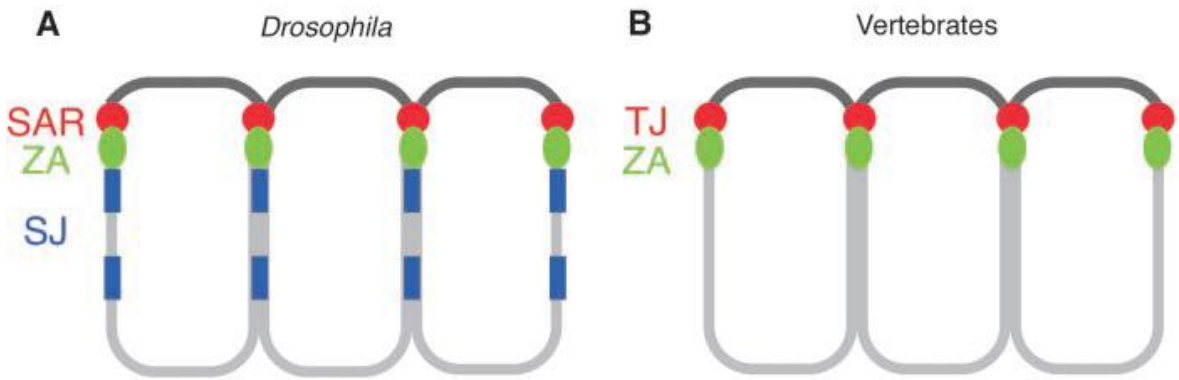

Fig.1: Organization of epithelial cells in comparison between *Drosophila* and vertebrates

(A) Epithelial cells of *Drosophila* can be distinct into different regions: an apical membrane domain facing the environment or a lumen, and a basolateral membrane domain which is in contact with neighboring cells as well as with the basal substratum. Both domains are segregated by AJs, which is a belt-like structure encircling the cell, also referred to as ZA. Apical to the ZA a region is defined as SAR or marginal zone. The latter region harbours protein homologs of vertebrates which form TJs (B). Although TJs are not formed in *Drosophila*, proteins localizing to this region share some functions. In comparison *Drosophila* exhibits SJs, which are absent in vertebrates. Adapted from Knust and Bossinger, 2002.

As mentioned above epithelial cells are highly polarized and depend on three identified groups of proteins or genes which are involved in the correct formation and maintenance of epithelial integrity. The gene products of two of the three groups were found to be localized apically in epithelial cells, regions referred to as the apical membrane domain and the ZA. Gene products of the third group have been shown to localize to the lateral membrane domain and the SJs. The apical protein complexes belong to gene products of the *bazooka* (*baz*) and the *crumbs* (*crb*) group. The *discs large* (*dlg*) group represents proteins of tumor suppressor genes, which have been found to localize at the lateral membrane and the SJs. These three groups have been shown

to be crucial for the establishment of epithelial cell polarity as well as their maintenance and will be discussed in more detail below (Johnson and Wodarz, 2003).

Proteins belonging to the *baz* group of genes are Baz, which is the *Drosophila* homolog of vertebrate Partitioning defective 3 (Par3), *Drosophila* atypical Protein Kinase C (DaPKC) and the adaptor protein *Drosophila* Partitioning defective 6 (DPar6). Baz and DPar6 are scaffolding proteins, which exhibit PDZ domains (name derived from PSD-95, Dlg and ZO-1). PDZ domains are one of the most common protein-protein binding domains (Sheng and Sala, 2001; Te Velthuis and Bagowski, 2007). They consist of about 80-90 amino acids, which contain six anti-parallel β-strands and two α-helices (Fanning and Anderson, 1999). They bind to C-terminal peptide motifs and internal sequences resembling a C-terminus and are also described to bind phospholipids (Harris and Lim, 2001; Jeleń et al., 2003). Baz, DaPKC and DPar6 are also referred to as the Par complex, since they had been found to form a protein complex *in vivo* (Wodarz et al., 2000; Petronczki and Knoblich, 2001). The binding of Baz to DPar6 and DaPKC is important for their initial recruitment to the apical plasma membrane (Harris and Peifer, 2005; Horikoshi et al., 2009). Later DaPKC phosphorylates Baz at serine 980 and thereby releases it from the complex. DaPKC and DPar6 remain in the SAR due to the binding of DPar6 to Crb (Morais-de-Sá et al., 2010; Walther and Pichaud, 2010), whereas Baz localizes to the AJs (Nam and Choi, 2003; Harris and Peifer, 2005; Horikoshi et al., 2009; McCaffrey and Macara, 2009; Morais-de-Sá et al., 2010; Walther and Pichaud, 2010). DPar6 acts as a regulatory subunit of DaPKC with evidence showing that it negatively influences its kinase activity (Atwood et al., 2007), which is of importance for the maintenance of apical membrane identity. For example phosphorylation of Lethal giant larvae (Lgl, which is a member of the *dlg* group) and Par1 leads to their exclusion from the apical membrane (Betschinger et al., 2003; Plant et al., 2003; Yamanaka et al., 2003; Hurov et al., 2004; Kusakabe and Nishida, 2004; Suzuki et al., 2004). However, it was found that DaPKC phosphorylates the cytoplasmic tail of Crb at four serine/threonine residues (Sotillos et al., 2004), but the *in vivo* function of this modification remains unknown (Huang et al., 2009). As mentioned above, phosphorylation of Baz results in its dissociation from the Par complex and relocalization to the AJs. Here Baz can bind to Armadillo (Arm, the *Drosophila* homolog of β-Catenin (β-Cat)) and Echinoid (an immunoglobulin-superfamily adhesion molecule) (Wei et al., 2005) and to a phosphatase PTEN (Von Stein et al., 2005). Here Baz has been proposed to function in the recruitment of cadherin-catenin clusters for the formation of AJs (McGill et al., 2009). With regards to this, *baz* loss of function alleles result in a loss of AJs components and the phenotype resembles the loss of function of *arm* (Müller and Wieschaus, 1996). Furthermore, apical polarity

markers are reduced and were found to be mislocalized along the basolateral membrane domain. Cells are rounded up and the epithelium becomes multilayered. As a consequence these cells begin to die through apoptosis (Bilder et al., 2003).

The *crb* group, which is the second group of proteins localizing to the apical plasma membrane domain, consists of Crb, which is the only transmembrane protein (among the so far identified members of the three groups) with a huge extracellular domain consisting of EGF and LamG domains. It exhibits a short intracellular tail of 37 amino acids containing a highly conserved C-terminal PDZ binding motif (ERLI), which recruits Stardust (Sdt, encoding for a membrane associated guanylate kinase (MAGUK)) as a member of the *crb* group to the apical membrane. Aside from a single PDZ domain, Sdt exhibits a L27 and a SH3 domain and recruits PATJ (Pals1-associated TJ protein) to the apical membrane, which also contains a L27 domain as well as four PDZ domains. Crb is localized slightly apical to the AJs in the SAR (Tepass, 1996) and *crb* mutants show loss of apical membrane identity and the AJs, whereas overexpression leads to an increase of the apical membrane domain (Wodarz et al., 1993, 1995).

The *dlg* group of tumor suppressor genes is composed of Dlg and Scribble (Scrib), which exhibit several PDZ domains, as well as Lgl, a WD40 domain containing protein. These polarity markers are located at the lateral plasma membrane. Scrib was also described to exist in a cytoplasmic pool (Bilder and Perrimon, 2000; Bilder et al., 2000). In contrast to proteins of the apical networks, members of the *dlg* group have not been described to bind to each other. Mutations in these genes show abnormal cell shapes and loss of the ZA accompanied by a multilayered epithelium (Bilder and Perrimon, 2000; Bilder et al., 2000, 2003; Tanentzapf and Tepass, 2003). A very important difference to mutations in the *baz* and *crb* group is an enlarged apical membrane domain, which is reduced or lost in mutations of the latter genes. Furthermore mutations in genes of the *dlg* group do not lead to apoptosis of these cells (Bilder and Perrimon, 2000; Bilder et al., 2000, 2003). Fig.2 shows a schematic of an epithelial cell with the main identified polarity markers which play a role in establishing or maintaining epithelial polarity and integrity.

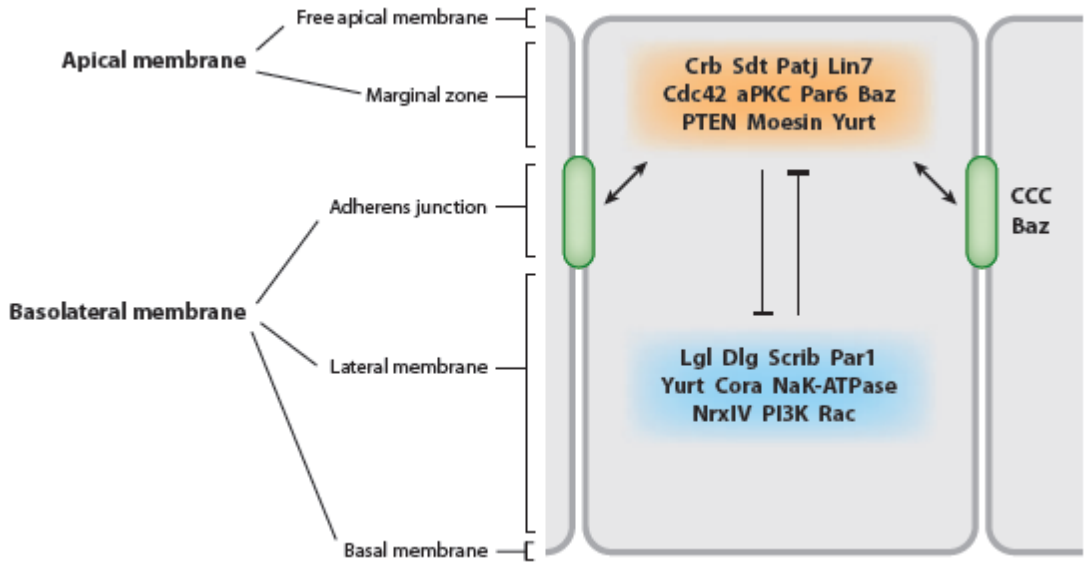

Fig.2: Localization of distinctive protein markers in *Drosophila* epithelial cells

Different distinguishable regions of the epithelium are indicated on the left side of the scheme. Members of the *baz* and *crb* group are shown in orange and those of the *dlg* group are shown in blue. Baz was also identified to be an AJ marker, where it recruits cadherin-catenin clusters (CCC). Arrows indicate the interaction between AJ markers and apical polarity determinants, negative regulatory mechanisms are indicated between proteins of the lateral membrane domain and apical polarity proteins. Adapted from Tepass, 2012.

Genetic experiments revealed that *baz* gene function is most likely upstream of other identified genes that encode for polarity markers so far. As mutations in *crb* or *sdt*, as well as *baz,* show quite similar phenotypes, defects in *baz* mutants become apparent slightly earlier. Furthermore Crb mislocalizes in *baz* mutants, but Baz is localized correctly in *crb* mutants (Müller and Wieschaus, 1996; Müller, 2000; Bilder et al., 2003). In this context it was shown that Baz recruits Sdt to the plasma membrane. This direct interaction is dependent on aPKC activity, as phosphorylation of Baz at serine 980 causes dissociation of Sdt from the complex. Expression of a respective non-phosphorylatable Baz transgene caused phenotypes similar to *crb* and *sdt* mutants (Krahn et al., 2010a). It has been shown that proteins of these complexes interact in a dynamic manner (some examples had been discussed above). One important regulatory mechanism was identified by genetic experiments, where it was found that apical determinants antagonize the function of laterally localized proteins, and vice versa. For example zygotic *crb scrib* double mutants somehow show suppression of the *crb* single mutant phenotype to a large extent,

indicating the interaction between these two different groups (Bilder et al., 2003). However, zygotic *dlg baz* double mutants show quite a similar phenotype to *baz* single mutants, underlining the epistatic importance of *baz* in the establishment of cell polarity (Bilder et al., 2003; Tanentzapf and Tepass, 2003).

There are many more factors which are important for the establishment and maintenance of epithelial polarity and integrity. For example Yurt (Yrt), Coracle (Cora), the NaK-ATPase and NrxIV have been shown to be necessary for proper SJ formation and are implicated in tube size control of tracheal cells, which also represent a type of an ectodermal epithelium (Laprise et al., 2010). Since Echinoid was recently shown to fuction upstream of the Hippo pathway (Yue et al., 2012), which in general is a pathway described for being important for tissue growth and organ size (Cherret et al., 2012), the establishment of cell polarity and junction formation must be regarded as a highly dynamic process.

1.2 Cell adhesion

AJs, which have already been mentioned in the previous chapter, are important for cell-cell adhesion. They are composed of E-Cadherin (E-Cad), a transmembrane protein which is important for the homophilic cell-cell adhesion and its intracellular associated Catenins. The extracellular domain of E-Cad forms *trans* dimers with E-Cad proteins of the plasma membrane of the neighboring cell and *cis* dimers with E-Cad proteins of the same cell. Intracellular, E-Cad binds to β-Cat which in turn binds to α-Catenin (α-Cat). The complex of E-Cad-β-Cat-α-Cat is also referred to as cadherin-catenin complex (see chapter before). α-Cat associates with Actin and it was believed that these interactions form a stable link between AJs and the cytoskeleton. Nelson and co-workers have shown in 2005 that the function of AJs in cell adhesion is much more dynamic and that a quaternary complex of E-Cad-β-Cat-α-Cat-Actin cannot exist simultaneously (Drees et al., 2005; Gates and Peifer, 2005; Yamada et al., 2005). It was shown that a monomeric form of α-Cat binds to the E-Cad-β-Cat complex, whereas a dimeric form of α-Cat does not bind to this complex anymore. In contrast, these homodimers show high binding affinity for Actin. Furthermore α-Cat homodimers can suppress the activity of the Arp2/3 complex, which is important for the nucleation of Actin branches. However, the physiological relevance of this property is not known. Fig.3 shows the classical view of cell-cell adhesion as described above and

Fig.4 shows an illustration of the revised model of how AJs may be connected tightly or transiently to the cytoskeleton.

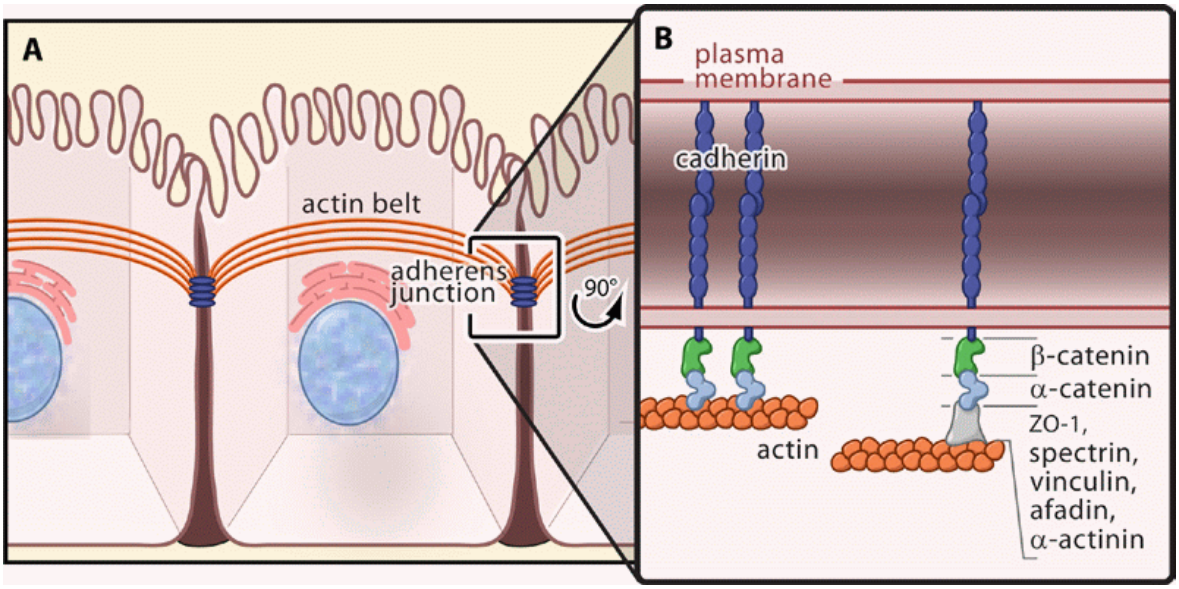

Fig.3: Classical model of cell-cell adhesion

(A) AJs are important for cell-cell adhesion. Here, E-Cad as a transmembrane protein forms *cis* and *trans* dimers. The latter are important for cell-cell contacts. (B) Intracellularly, E-Cad associates with β-Cat, which in turn binds to α-Cat. Since α-Cat binds to Actin it was believed that this binding forms a stable link between AJs and the cytoskeleton. Other Actin binding proteins like ZO-1 or Afadin have been proposed to play a role in this link as well, as many of them can associate with α-Cat. Adapted from Gates and Peifer, 2005.

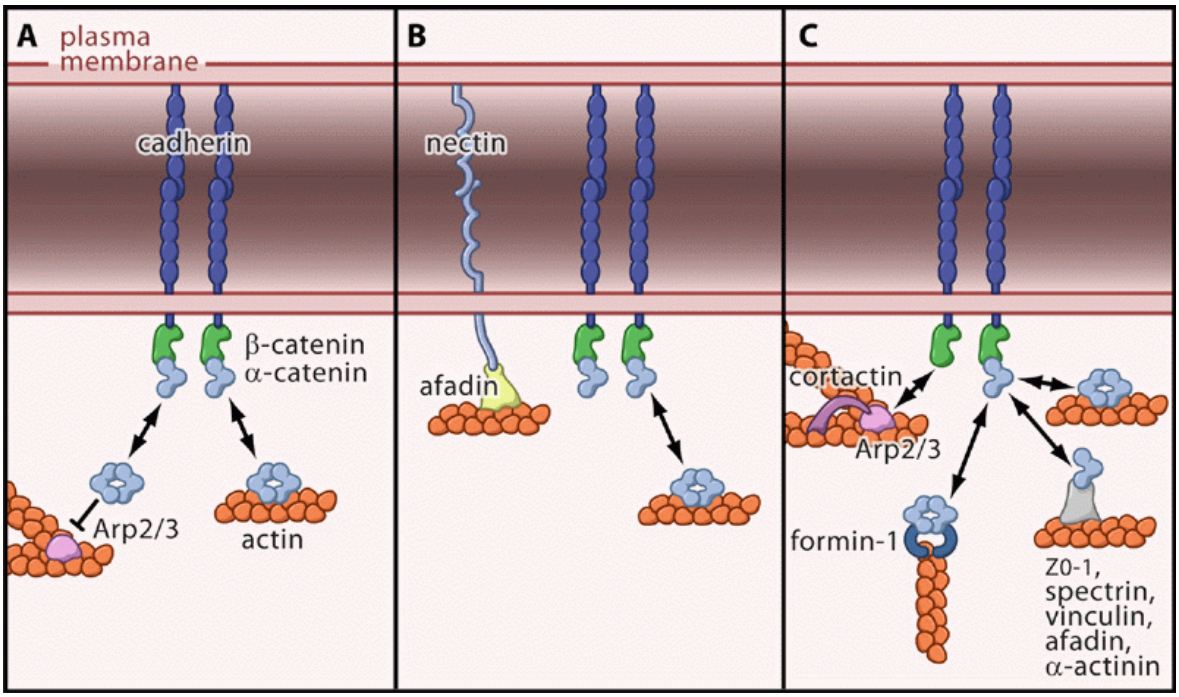

Fig.4: Revised models showing possibilities of the linkage between AJs and the cytoskeleton

(A) Summarized revised interactions of the cadherin-catenin complex. α-Cat associates with E-Cad-β-Cat in a monomeric form, whereas its dimeric form dissociates from this complex and shows binding to Actin. However, homodimers of α-Cat can antagonize the activity of the Arp2/3 complex. (B) A possible link between AJs and the cytoskeleton could be through Nectins. These transmembrane proteins belong to the immunoglobulin-superfamily adhesion molecules. Nectins form dimers as well and associate with Afadin intracellularly, which in turn binds to Actin, providing a second link between AJs and the cytoskeleton. (C) A more complex model includes many protein-protein interactions which thereby form a transient link between AJs and the cytoskeleton, which is highly dynamic. Adapted from Gates and Peifer, 2005.

The remodelling and interplay of AJs and the Actin cytoskeleton is of fundamental importance, as processes like apical constriction, where the Actin/Myosin ring beneath the AJs contracts to mediate cell shape changes, are needed for morphogenetic processes. e.g., during gastrulation the mesoderm invaginates due to repositioning of the AJs by contraction forced by the Actin/Myosin network. When AJ function is abolished by depletion of β-Cat, the Actin/Myosin ring still contracts, but cell shape change does not take place (Dawes-Hoang et al., 2005). These findings strongly indicate that a physical link between AJs and the cytoskeleton must somehow exist.

1.3 Src kinases

Src family kinases (SFKs) are known to be important for several cell biological processes, e.g. cell migration, cell-shape changes, cell-substratum and cell-cell interactions. SFKs are considered to function in the modulation of the Actin based cytoskeleton, which represents a determinant of cell shape change and cell migration (Boschek et al., 1981; Brown and Cooper, 1996). Furthermore, Src activity is involved in the alteration of the cadherin-catenin complex as tyrosine phosphorylation of β-Cat or other AJs associated proteins causes weakening of the linkage to the Actin cytoskeleton (Takeda et al., 1995; Lilien et al., 2002). Phosphorylation of the cadherin-catenin complex correlates with loss of epithelial character, detachment of cells and gain in invasiveness (Behrens et al., 1993; Hamaguchi et al., 1993; Lilien et al., 2002). Several proteins are known to bind Src kinases for being substrates for them. Many of them are associated with the cytoskeleton and AJs (Thomas and Brugge, 1997). Vertebrate Fes/Fer tyrosine kinases share some substrates with SFKs, among them p120ctn, β-Cat (Piedra et al., 2003) and Cortactin, which is the activator of Arp2/3 (Wu and Parsons, 1993; Kim and Wong, 1998).

The vertebrate family of Src non-receptor tyrosine kinases comprehends of 9 members. These are subdivided into three groups: Src, Yes and Fyn. Each group comprises three members which are widely expressed in a variety of cells (Thomas and Brugge, 1997). The *Drosophila* genome encodes for two Src kinases, *Src42A*, the closest homolog to vertebrate *c-Src* (Takahashi et al., 1996), and *Src64B* (Simon et al., 1985; Takahashi et al., 1996).

Src non-receptor tyrosine kinases are composed of three main domains: an N-terminal Src homology 3 domain (SH3), a structural motif known to associate with proline rich regions, a Src homology 2 domain (SH2) for binding phosphotyrosine, followed by the tyrosine kinase domain. Other structural features of Src kinases are a myristoylation site at the N-terminus, which is functioning as a membrane anchor, an autophosphorylation site which is important for activation and a second tyrosine phosphorylation site at the C-terminus, which is targeted by C-terminal Src kinase (Csk), an endogenous Src inhibitory factor (Ia et al., 2010). Phosphorylation results in an intramolecular binding of Src, where the SH2 domain binds to this phosphotyrosine, resulting in a conformational change which inactivates the kinase (Engen et al., 2008). The domain structure of *Drosophila* Src42A is depicted in the results section (see Fig.31 A) and Fig.5 shows the common structure of Src kinases.

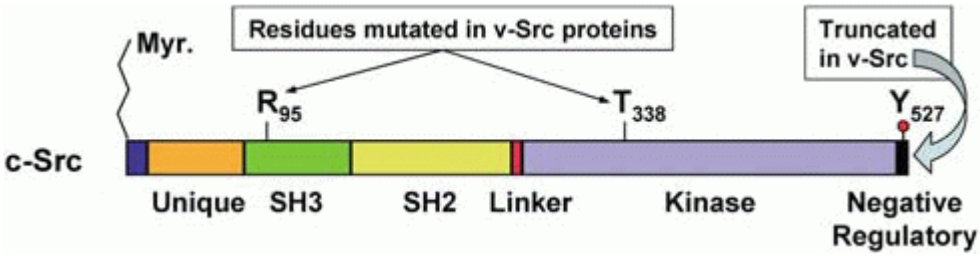

Fig.5: Structure of Src kinases

Figure depicts overall domain structure of c-Src kinase, the closest homolog of *Drosophila* Src42A. The N-terminus shows a myristoylation site, important for membrane anchoring. An SH3 domain is located in the N-terminal part, followed by an SH2 domain, important for intramolecular binding of the C-terminal tyrosine, after Csk dependent phosphorylation. The tyrosine kinase domain locates at the C-terminus of the kinase. Identfied mutations in v-Src are indicated. Adapted from Parsons and Parsons, 2004.

Members of SFKs are good candidate genes for the regulation of AJ remodelling. In cultured epithelial cells activated Src was shown to downregulate E-Cad, thereby leading to dissociation of cells, a process also referred to as epithelial mesenchymal transition (EMT) (Behrens et al., 1993; Boyer et al., 1997; Thomas and Brugge, 1997).

Drosophila Src42A localizes along the plasma membrane in epithelial cells, whereas activated Src42A (pSrc) colocalizes with DE-Cad/Arm at the AJs. Evidence was provided by Shindo et al., that Src42A is preferentially activated at AJs of epithelia undergoing morphogenetic rearrangements. They showed that Src42A can influence DE-Cad in two distinct, and disparate, ways. First it antagonizes DE-Cad mediated cell adhesion, while on the other hand positively influencing the transcription of DE-Cad in a TCF dependent manner. These findings propose a model where activation of Src42A at the AJs is mediating AJs turnover, thereby promoting their rearrangement and remodelling of the epithelial tissue. With regard to this it was shown that expression of activated Src42A increased expression of Escargot (Esg), which is a target of Wg/Arm signaling in the trachea, whereas mutants for *Src42A* showed reduced Esg expression. This suggests that Src42A is acting through the Arm/TCF pathway, because this phenotype was suppressed by co-expression of dominant negative TCF (TCFΔN) (Chihara and Hayashi, 2000; Llimargas, 2000; Shindo et al., 2008). However, the function of Srcs in Wg signaling appears to be limited, since double mutants for *Src42A* and *Src64B* do not exhibit segmentation defects, which is a characteristic of mutations in these genes.

Src42A and *Src64B* were shown to have redundant functions in germband retraction and dorsal closure (Tateno et al., 2000), which is a process where two lateral epithelial cell sheets migrate towards each other closing the big gap at the dorsal side which remains after germband retraction (see further down for more details). Double mutants frequently exhibit broken longitudinal tracts and commissures, and optic lobe/Bolwig's organ and trachea formation was found to be disrupted as well (Takahashi et al., 2005). In comparison, the respective single mutants do not exhibit severe defects in these processes/structures. In this context, *Src42A* and *Src64B* have been shown to interact genetically and functionally with *shotgun*, which encodes for DE-Cad, and *arm*. Here Src42A and Src64B can trigger cytosolic and nuclear accumulation of Arm. Co-IP experiments revealed that DE-Cad and Arm form a ternary complex with Src42A (Takahashi et al., 2005; Shindo et al., 2008). Upon Src42A knockdown it was shown that Arm remained at cellular junctions, whereas nuclear as well as cytosolic fractions were lower in comparison to the wt situation (Desprat et al., 2008). Src42A and Src64B functions had been shown to play roles in WNT5/Derailed signaling, as double mutants for *Src42A* and *Src64B* exhibit comparable commissural phenotypes similar to *Wnt5* and *derailed* mutants (see also above), which could be suppressed or enhanced by Src gain- and loss-of-function, respectively. A physical interaction between Derailed and Src64B had been shown in this context as well (Wouda et al., 2008).

As mentioned above, *Src42A* and *Src64B* have been shown to have some redundant functions with regard to morphogenetic processes like dorsal closure. However, some functions have been shown, where only one single Src kinase is involved. For example mutations in *Src64B* result in reduction in female fertility, which is due to nurse cell fusion and ring canal defects (Dodson et al., 1998), whereas Src42A is supposed to have just minor, if at all, functions during oogenesis (Takahashi et al., 2005). Src64B was also shown to be important for proper cellularization of the *Drosophila* embryo (Thomas and Wieschaus, 2004; Strong and Thomas, 2011). In contrast Src42A was confirmed to modulate mitochondrial Citrate synthase (CS) activity negatively *in vivo*, as mutants show increased CS activity (Chen et al., 2008). *Src42A* mutants show high frequency of lethality before hatching, whereas *Src64B* single mutants are viable (Dodson et al., 1998; Lu and Li, 1999; Tateno et al., 2000; Takahashi et al., 2005; O'Reilly et al., 2006). However one hypomorphic *Src42A* allele is reported ($Src42A^{JP45}$) which shows some escapers exhibiting mild dorsal cleft phenotypes (Tateno et al., 2000). Src42A was shown to regulate receptor tyrosine kinase (RTK) signaling and JUN Kinase (JNK) activity (Lu and Li, 1999; Tateno et al., 2000). *Src42A* single mutants exhibit defects in mouthpart formation (Tateno et al., 2000) and defects in leading

edge cells: the actomyosin cable is disrupted, phosphotyrosine levels are weaker and dorsal closure is slightly defective, where 8% show small holes at embryonic stage 16, where the dorsal hole should be already closed (see Fig.7 B) (Murray et al., 2006). Transcripts of *Src42A* accumulate in high levels in neighboring cells upon wound induction and wound-induced genes like *Ddc* and *ple* show widespread wounding induced transcription in *Src42A* mutants (Juarez et al., 2011). It was shown that Src42A is acting cell autonomously and inhibiting *Ddc* expression when its constitutively active form is expressed.

Src42A was recently shown by two groups to be involved in the elongation of the dorsal trunk of the tracheal network (Förster and Luschnig, 2012; Nelson et al., 2012; Ochoa-Espinosa et al., 2012). *Src42A* single mutants, as well as expression of dominant negative Src42A (Src42AKM), leads to a shortened dorsal trunk. Expression of Src42A, as well as its constitutively active form, leads to an extended dorsal trunk respectively. DE-Cad recycling at AJs is affected in *Src42A* single mutants, indicating that defective junction remodelling leads to cell shape changes. The apical surface area of *Src42A* mutants is significantly reduced. Src42A dependent anisotropic expansion along the longitudinal axis was shown to be a main driving force for elongation and overall apical expansion. Furthermore, it was demonstrated that this expansion process is cell autonomous by expressing Src42A transgenes via the UAS/Gal4 system in three different compartments in the *Src42A* mutant background. Expansion had been shown consequently in expressing cells (Förster and Luschnig, 2012). The short trunk phenotype of *Src42A* single mutants is epistatic to several genes which are involved in dorsal trunk development, and overelongated dorsal trunk phenotypes of respective mutants is not due to increased Src42A activity, indicating a parallel or downstream pathway where Src42A acts. Fig. 6 depicts the model of these new findings.

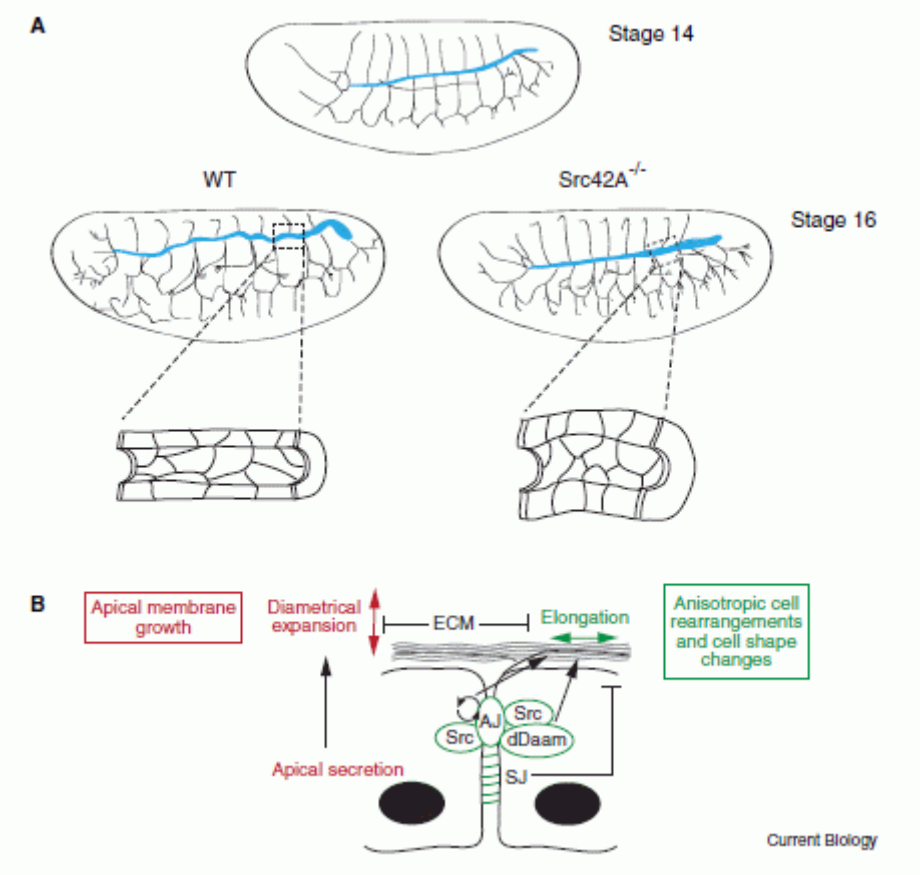

Fig. 6: Model of dorsal trunk elongation with regard to Src42A function

(A) Shown in blue is the tracheal dorsal trunk. After stage 14 of embryogenesis the dorsal trunk elongates, which is depicted in the wt embryo. Mutants for *Src42A* show a shortened dorsal trunk phenotype. The magnified area indicates the function of Src42A in the anisotropic expansion of dorsal trunk cells in the longitudinal axis. (B) Model summarizes findings of Förster and Luschnig, 2012 and Nelson et al. of how Src42A acts in apical membrane growth, as well as in the cell shape changes. Adapted from Ochoa-Espinosa et al., 2012.

The dorsal closure defects, which have been observed in double mutants for *Src42A* and *Src64B*, indicate functional redundancy with regard to this morphogenetic process. Dorsal closure is the last big morphogenetic process during *Drosophila* embryogenesis, where two epidermal lateral sheets extend to the dorsal side meet and fuse, thereby closing the big dorsal hole which remains after germband retraction. During dorsal closure the amnioserosa and yolk sac are enclosed inside the embryo as a consequence. The process where the leading edge cells meet at the dorsal midline is regulated in part through the remodelling of adherens junctions, which is leading to

their fusion. An important signaling pathway for dorsal closure was shown to be JNK signaling (Jacinto et al., 2002). Fig.7 depicts the process of dorsal closure.

Src42A is proposed to act upstream of JNK signaling. Members of the SFK family cooperate to regulate JNK activity: double mutants in *Src42A* and *tec29* as well as *Src42A* and *Src64B* (as described above) give dorsal open phenotypes, whereas single mutants do not (Tateno et al., 2000; Takahashi et al., 2005). Furthermore *tec29 Src42A* double mutants show loss of *dpp* and *puc* expression at the leading edge, which are downstream effectors of JNK signaling (see Fig.7 C) (Tateno et al., 2000). Mutations of *dfer* and *Src42A* together are causing total failure of dorsal closure (Murray et al., 2006).

Src42A was shown to act together with *DCas* in integrin-dependent effector pathways. Simultaneous reduction of *Src42A* and *DCas* functions caused blistered wing phenotypes in adult escapers. This phenotype had been reported for mutants in the integrin subunits *multiple edematous wings* (*mew*) and *inflated* (*if*) as well (Bloor and Brown, 1998), and embryonic cuticles displayed dorsal closure and anterior cuticle defects (Tikhmyanova et al., 2010). Analysis of Src and Focal adhesion kinase (Fak56) revealed overlapping and distinct contributions in inhibiting neuromuscular junction growth, which is transduced by the integrin signaling pathway (Tsai et al., 2008). Src42A was also shown to be important for the Draper pathway. Here association of Shark and Draper is mediated by Src42A, since Draper is a Src substrate. This binding promotes activation of downstream phagocytic signaling events (Ziegenfuss et al., 2008).

All these data nicely demonstrate that Src non-receptor tyrosine kinases, as well as SFKs in general, are implicated in many different cellular and morphogenetic processes, where AJs are undergoing rearrangements and are remodelled. Many of those genes do not exhibit dramatic phenotypes as in contrast their combinations do. This demonstrates that these kinases have many overlapping functions, indicating a highly dynamic and complex network.

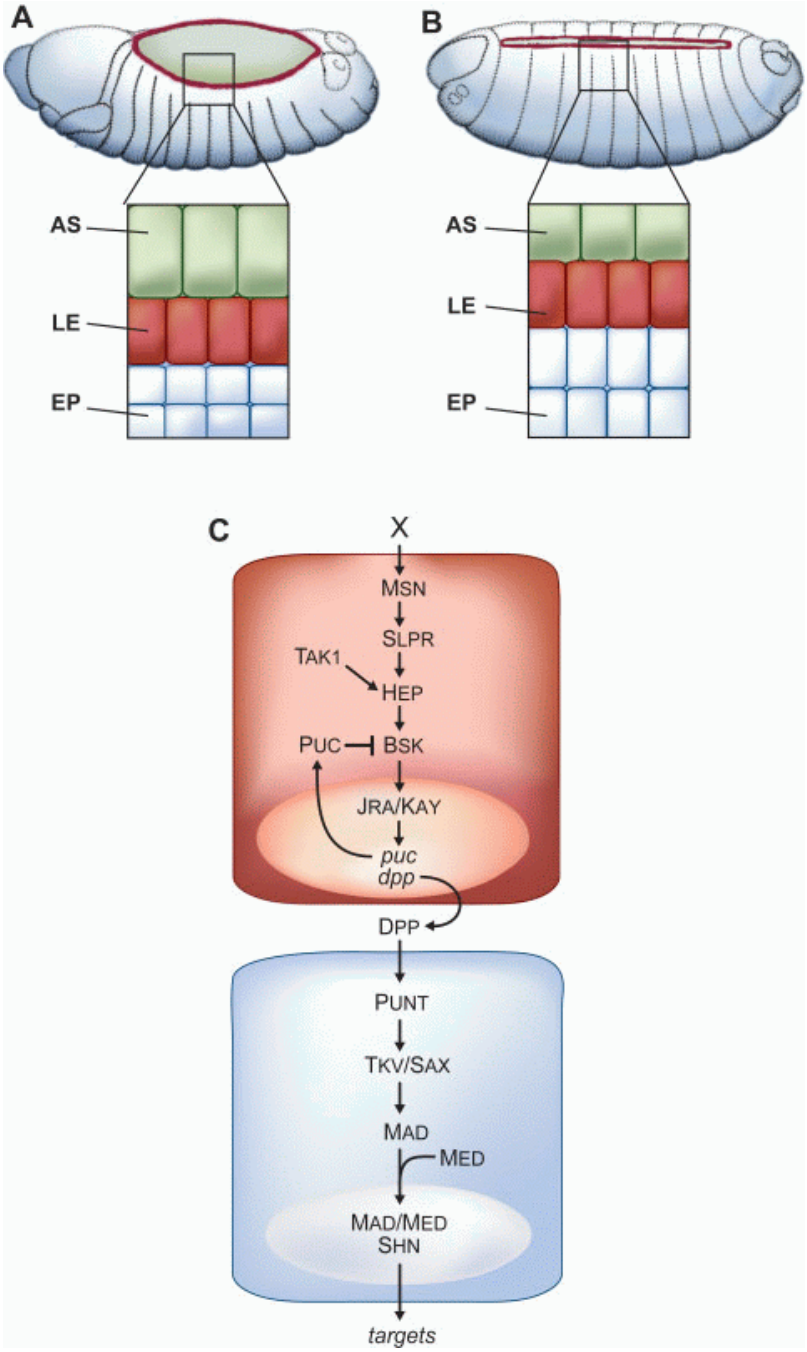

Fig.7: Dosal closure and JNK signaling

(A) Shown is an embryo at developmental stage 14, where a big dorsal hole remains as a consequence of germband retraction. Amnioserosa cells (AS) are marked in green, leading edge cells (LE) are labeled in red which represent the most dorsal epithelial cell row. (B) After embryonic stage 15, the dorsal hole is closed by the process of dorsal closure, and both leading edge cell rows build a seam at the dorsal midline. (C) JNK signaling is important for dorsal closure. The result of the JNK pathway is the secretion of Dpp at the leading edge and expression of *puc*, which encodes a dual phosphatase dephosphorylating Bsk (JNK) in a negative feedback loop. Adapted from VanHook and Letsou, 2008.

1.4 LMO7

The family of PDZ and LIM domain containing proteins comprises ten members possessing PDZ domains and at least one LIM domain. LIM domains (name derived from *C.elegans lin-11*, rat *ISL-1* and *C.elegans mec-3*) (Way and Chalfie, 1988; Freyd et al., 1990; Karlsson et al., 1990) act as protein-protein binding interfaces. The domain is approximately 55 amino acids in size and characterized by a highly conserved histidine/cysteine motif important for the binding of two zinc ions, thereby forming a two-zinc-finger-like structure (Bach, 2000; Kadrmas and Beckerle, 2004; Te Velthuis et al., 2007). PDZ and LIM family proteins are thought to be involved in Z-Band formation of muscles through their PDZ domains, which can bind to α-Actinin or β-tropomyosin. However, PDZ and LIM domain containing proteins are associated with the cytoskeleton directly or indirectly as well (Harris and Lim, 2001; Kadrmas and Beckerle, 2004). The group of PDZ and LIM domain encoding genes consists of four subgroups: the ALP subfamily (ALP, Elfin, Mystique, and RIL), the Enigma subfamily (Enigma, Enigma Homolog, and ZASP), LIM kinases (LIMK1 and LIMK2), and the LIM only protein 7 (LMO7). The latter protein will be discussed in more detail. *LMO7* was initially linked as a candidate gene to breast cancer progression, due to implication of human genomic region 13q21-22 in cancer development (Rozenblum et al., 2002) and was found to be upregulated in several human tumors, among them lymphnode metastasis in breast cancer (Sasaki et al., 2003).

LMO7 contains an intramolecular PDZ domain, a C-terminal LIM domain and a Calponin homology domain (CH). A partial consensus sequence for a putative F-box motif has been described earlier (Cenciarelli et al., 1999), which fails to be detected by current prediction programs (Te Velthuis et al., 2007). Coiled coil domains are predicted for some *LMO7* gene products as well, which is species dependent. So far, functional analysis of these domains has not been reported for LMO7. The *LMO7* gene (on chromosome 13q22 in humans, see above) was duplicated through evolution and the gene product of its paralog *LIMCH1* (on chromosome 4p13 in humans) shows 64% identical amino acid sequence of the CH domain and 60% homology of the LIM domain, respectively. However, LIMCH1 does not contain an additional PDZ domain. Beside these domains three regions with high homology have been identified within LMO7 and LIMCH1. These regions may indicate the existence of domains within these proteins, which have not been identified yet (Friedberg, 2009, 2010). *LIMCH1* was found to be upregulated in *PIK3CA*-mutated tumors (Cizkova et al., 2010). *LIMCH1* was described to be expressed in the presomitic mesoderm, however, targeted mutations for *LIMCH1* have not been reported yet (Sewell et al., 2010). *LMO7* exhibits a

splice variant lacking the LIM domain in mice brain cDNA (Tanaka-Okamoto et al., 2009), whereas *LIMCH1* shows splice variants lacking the CH domain (Friedberg, 2009). Homologs of *LMO7* have been identified in invertebrates. *temporarily assigned gene 204* (*tag204*) was found to be the *LMO7* homolog in *C.elegans* and *CG31534* (now annotated as *CG43427*) encoding the *Drosophila* homolog respectively. These homologs show high conservation in regard to the C-terminal LIM domain but the invertebrate homologs do not exhibit PDZ and CH domains (Te Velthuis et al., 2007). A domain structure of full length vertebrate LMO7 is shown in Fig.9 A.

Studies indicated that LMO7 is likely involved in the formation and maintenance of epithelial architecture by remodelling the Actin cytoskeleton. The LIM domain has been shown to interact with Afadin (which in turn associates with Nectins). LMO7 binds to α-Actinin (an Actin binding protein). These interactions are thought to modulate a link between the cell adhesion complex of E-Cad and the Nectin network. Furthermore Afadin can directly associate with F-Actin, therefore creating a second link between LMO7 and the Actin cytoskeleton. Antibodies against LMO7 showed expression in various rat tissues including the heart, lung, small intestine, kidney, brain, liver, spleen, and skeletal muscle. Staining of LMO7 showed colocalization with Afadin in the region of the AJs in epithelial cells of rat gallbladder (see Fig.8), supporting the biochemical data. It was furthermore shown that E-Cad, β-Cat and α-Cat co-immunoprecipitate with LMO7, even in *afadin*$^{-/-}$ ES cells, supporting the hypothesis that LMO7 connects Nectins with the E-Cad adhesion complex. Whether LMO7 can directly associate with the Actin cytoskeleton remains unclear, but CH domains can bind to Actin bundles directly, thereby suggesting a role of LMO7 in direct association with the Actin cytoskeleton (Ooshio et al., 2004).

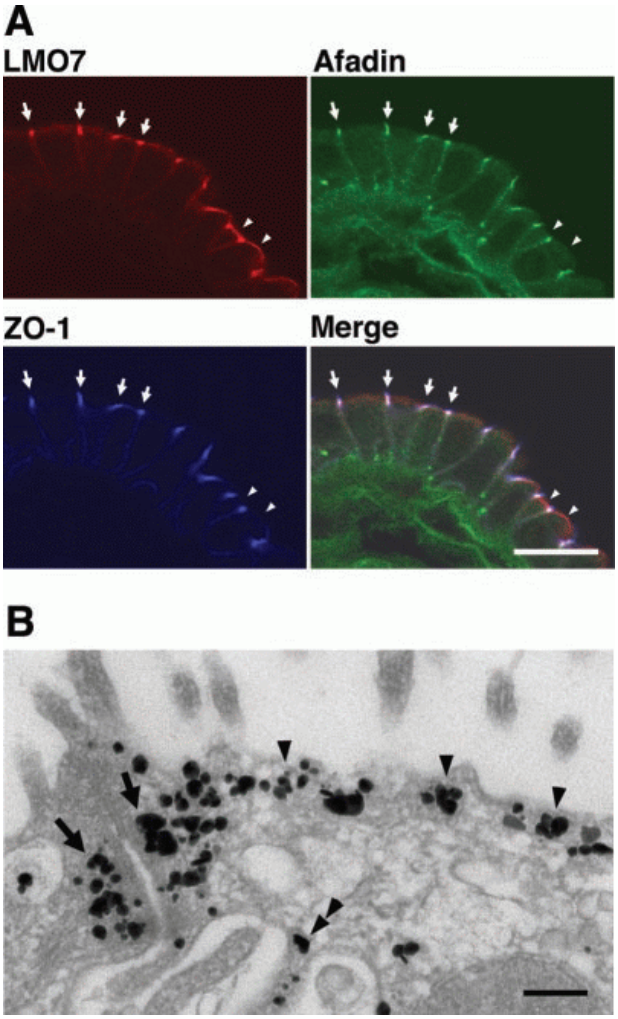

Fig.8: Localization of LMO7 in epithelial cells of rat gallbladder

(A) Localization of LMO7 in epithelial cells of rat gallbladder. Afadin localizes to AJs, where LMO7 is detected as well (arrows), slightly basal to the TJ marker ZO-1. LMO7 is additionally detected at the cytoplasmic faces of the apical membrane (arrowheads). Scalebar represents 10 µm. (B) Immunoelectron microscopy revealed that LMO7 localizes to the AJs (arrows) and at the cytoplasmic faces of the apical membrane (arrowheads). Scalebar represents 0.1 µm. Adapted from Ooshio et al., 2004.

A large deletion of around 800 kb, covering *Uchl3* and *LMO7* gene loci, resulted in lethality for about 40% of mice between birth and weaning and surviving homozygotes showed muscular degeneration and growth retardation, as well as retinal degeneration. The latter phenotype is suggested to be caused likely by the *Uchl3* knockout. Respective single mutants show the same retinal degeneration defects. Although the proportion of muscles to body weight was proportionate in the *Uchl3 LMO7* knockout mice, nuclei were elongated and increased in their

amount by a factor of 2 in thigh muscle fibers (Semenova et al., 2003). These observations are consistent with an expression analysis performed in mice, where *LMO7* mRNA was detected in somites and the eye, respectively (Ott et al., 2008).

LMO7 knockdown in the zebrafish *Danio rerio* causes defects in the cardiac conduction system, including arrhythmia and heart delocalization. The latter could indicate a possible function of LMO7 for neural crest cells and their migration. Severe defects which had been observed were shorter embryos and strongly bent tails. Severe elongation defects were found later in development. Some extreme phenotypes exhibited upon *LMO7* knockdown were head defects. Rescue experiments showed that these phenotypes were observed upon the morpholino injection. The knockdown was targeted against the 5'UTR of *LMO7*, whereas *LMO7* RNA was coinjected without the respective UTR (Ott et al., 2008).

LMO7 is transcribed in the lung, heart, brain and kidney. An alternative splice form, lacking the LIM domain, was identified in a mouse brain cDNA library (Tanaka-Okamoto et al., 2009). It was shown, that transforming growthfactor-β1 (TGF-β1) induces expression of *LMO7* while enhancing invasiveness of rat ascites hepatoma cells. Furthermore, TGF-β1 induced this alternatively spliced variant of *LMO7S,* lacking the C-terminal LIM domain (Nakamura et al., 2005). LMO7 localizes to the luminal surface of epithelial cells. The PDZ domain is essential for the apical localization, because *LMO7* deficient mice lacking the PDZ domain showed cytosolic mislocalization of LMO7. These *LMO7* knockout mice were viable and fertile, and had been indistinguishable in appearance, size, growth, development and behaviour from their littermates. Lung sections of 14-week old *LMO7* deficient mice showed irregular epithelial sheets, respiratory bronchioles and alveolar ducts. However, although the position of AJs was slightly deviated, E-Cad and its associated Catenins, as well as Afadin and Nectins were localizing at the AJs, indicating that *LMO7* function is not required for proper AJs formation. Mice at an age of 90 weeks deficient for *LMO7* showed development of adenocarcinomas to an extent of about 22%, whereas $LMO7^{+/-}$ mice developed lung cancer to 13%. It was shown that cultured tumor cell lines deficient for *LMO7* possess chromosome abnormalities and cause tumor formation *in vivo* when injected into nude mice. These observations indicate tumor suppressor roles for *LMO7* (Tanaka-Okamoto et al., 2009). With regards to these observations, human lung adenocarcinomas showed that *LMO7* expression was decreased with tumor progression (Nakamura et al., 2011).

Beside the tumor suppressor functions of LMO7 and its localization at the AJs, LMO7 was furthermore shown to be involved in gene expression. Upon *LMO7* knockdown in cell culture it was found that around 4000 genes showed altered expression. Among these the muscle relevant genes *emerin* was identified (Holaska et al., 2006). LMO7 was reported to bind the LEM domain protein Emerin, in which mutations cause Emery-Dreifuss muscular dystrophy. This disease was reported as well for mutations in LMNA, which encodes an A-type lamin (Nagano et al., 1996; Emery, 2000; Bengtsson and Wilson, 2004). LMO7 activates the transcription of muscle-relevant genes as well as the expression of the *emerin* gene itself (see above). The binding of LMO7 to Emerin inhibits LMO7 function in *emerin* expression, indicating a negative feedback mechanism (Holaska and Wilson, 2006; Holaska et al., 2006). Furthermore Emerin is required for nuclear localization of LMO7. Emery-Dreifuss muscular dystrophy has been linked to *LMO7* since one isolated missense mutant of *emerin* (P183H), is deficient in LMO7 binding. However, three other gene products of mutations in *emerin* were still found associating with LMO7 (Holaska et al., 2006). Recently it was shown that LMO7 can directly bind to the promoters of *Pax3*, *MyoD* and *Myf5*, suggesting that LMO7 is directly involved in their expression. This interaction is suppressed by Emerin, providing a mechanism of how Emerin inhibits LMO7 function (Dedeic et al., 2011).

Fig.9 B shows a summarized model of LMO7 functions in cell-cell adhesion as well as its nuclear role in expression of muscle-relevant genes.

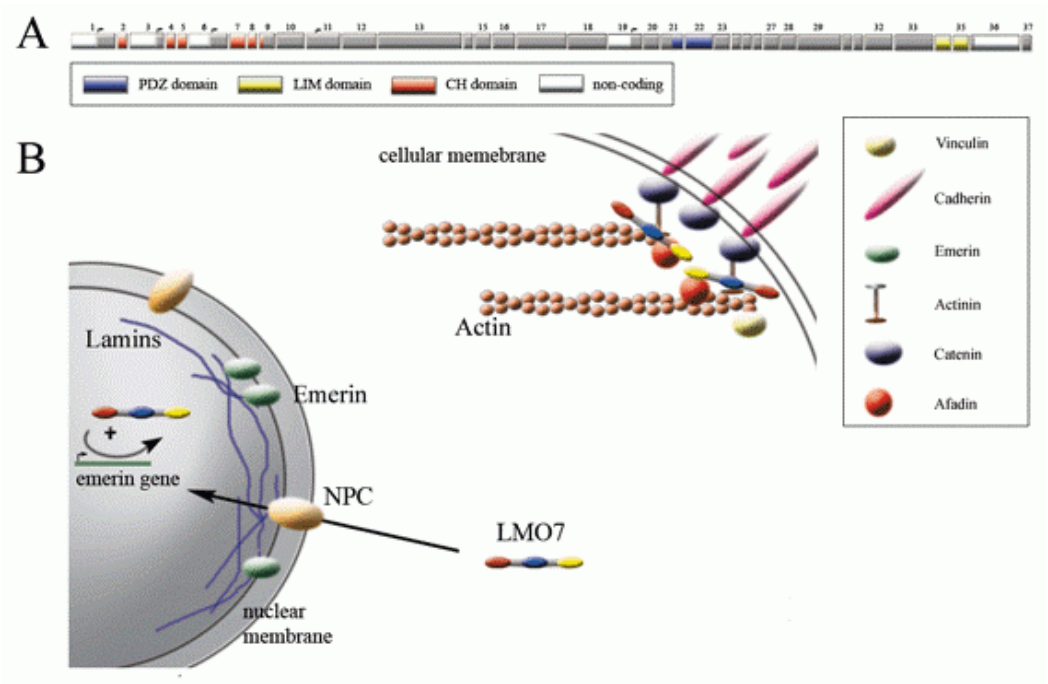

Fig.9: LMO7 structure and function

(A) Structure of full length LMO7. CH domains were identified at the N-terminus of the protein, a PDZ domain is found as well as a C-terminal LIM domain. Described splice variants of *LMO7* are not shown. (B) Summarized functions of LMO7 at AJs and in the nucleus. LMO7 associates with α-Actinin at one hand while binding to Afadin at the other. Since Afadin associates with F-Actin and α-Actinin with Catenins, LMO7 is suggested to build a link between the E-Cad adhesion complex and Nectins, which bind to Afadin. LMO7 might be able to associate directly with Actin bundles as well by the CH domain. A second function of LMO7 is its involvement in the expression of muscle-relevant genes and *emerin*. The gene product of *emerin* was furthermore shown to bind LMO7, thereby inhibiting expression of target genes. This is most likely by recruiting LMO7 to the nuclear envelope, where Emerin localizes. LMO7 was shown recently to directly bind promoters of *Pax3*, *MyoD* and *Myf5*. Adapted from Te Velthuis and Bagowski, 2007.

1.5 *smallish (CG43427)*

As already described in the first two chapters of the introduction, *baz* gene function was found to be implicated in the establishment of cell polarity of many types of tissues (e.g. ectodermal epithelia and NBs) as well into the formation of AJs of epithelial cells. Baz was found in a complex with DaPKC and DPar6, referred as the Par complex (Wodarz et al., 2000; Petronczki and Knoblich, 2001). The Par complex is important for the apical membrane identity at first, whereas release of Baz by DaPKC phosphorylation causes relocalization of Baz at the AJs, where Baz was shown to recruit cadherin-catenin clusters, thereby being implicated in the formation of these cell-cell contact sites (Wei et al., 2005; McGill et al., 2009). As *baz* gene function was shown to be epistatic to other polarity markers it is suggested that Baz is a key player in mediating cell polarity. As the past years revealed several new binding partners of Baz, thereby identifying new cellular pathways were Baz is functioning, its overall role remains elusive in many aspects.

To unriddle the function of Baz in the establishment of cell polarity in more detail, a yeast two-hybrid screen was performed for the identification of new binding partners of the protein (Ramrath, 2002). Three different regions of Baz were chosen as baits, among them the N-terminal oligomerization domain (Benton and Johnston, 2003), the C-terminus, as well as the intramolecular region encoding for the three PDZ domains. The latter one is of interest for this work, because one potential binding partner identified was binding to this PDZ domain containing region within Baz. The potential interactor identified as prey was the C-terminus of the annotated

gene *CG31534*, which was not described so far. The C-terminus encoded for a LIM domain and a PDZ binding motif of class I (S/T $X^{‡}\Phi^{§}$ -COOH), which made this hit very interesting. PDZ binding motifs are the counterpart of PDZ domains, which can bind into a hydrophobic pocket within the PDZ domain (Harris and Lim, 2001). Furthermore *CG31534* turned out to be likely the *Drosophila* homolog of vertebrate *LMO7* (see 1.4), which was already implicated functioning at AJs in vertebrates. A detailed scheme of the yeast two-hybrid screen is shown in the results section (see Fig.12).

CG31534 is located on the right arm of the third chromosome. However, in 2008 only two splice variants were annotated for *CG31534*: one encoding for 889aa (98.8 kDa), which resembled the full length form of the protein and a second isoform encoding for 849aa (94.4 kDa) respectively. This isoform was lacking the LIM domain by use of an alternative spliced exon containing a premature stop signal, which was also reported for a *LMO7* (*LMO7S*) specific neuronal isoform (Nakamura et al., 2005). By 2009 the gene prediction for *CG31534* was changed in a way that four isoforms were annotated, encoding for two additional isoforms. They were slightly deviated from the two isoforms mentioned above with minor changes affecting the C-terminus, thereby exhibiting 8 additional amino acids in the region N-terminal to the LIM domain, as well as a change affecting the N-terminus of the full length isoform by use of an alternative ATG, causing a slightly larger protein. Altogether *CG31534* was encoding four protein isoforms, CG31534-PA, CG31534-PB, CG31534-PC (857aa, 95.3 kDa) and CG31534-PD (932aa, 103.5 kDa), respectively. Of major interest had been only the two protein isoforms PA and PD due to the lack of the C-terminal region carrying the LIM domain and the PDZ binding motif in the two isoforms PB and PC, which was identified in the yeast two-hybrid screen as prey.

Unluckily, the gene annotation of *CG31534* was still not correct at this time. In 2011 (nearly at the end of the regular time limit of this work given by the GGNB doctoral program), a new gene annotation release of flybase (gene annotation release 5.40) indicated that the neighboring gene *CG31531*, located 5' to *CG31534*, is part of the same transcription unit. We confirmed by PCR, using embryonic cDNA as template, that both transcription units indeed resemble a single gene, spanning approximately 52 kb (3R 485,301 – 537,915). A detailed gene map of the current gene annotation of *CG43427* is shown in Fig.17 B in the results section. Most biochemical data produced within this work were performed with the shorter protein isoform CG31534-PA, which is now CG43427-PI, reflecting only two third of the C-terminus of the full length protein. More recent data generated were performed using the larger isoform, annotated as CG43427-PM,

encoding for 1533aa (168.9 kDa) and additionally possessing two coiled coil domains in the N-terminal region (see also Fig.12 in the results section).

At the start of the thesis some preliminary data had been obtained in two diploma works before (Neugebauer, 2007; Beati, 2009). Endogenous CG31534 protein was detected apical in ectodermal epithelia, which was already a good hint. In cell culture experiments it was shown that Baz can recruit CG31534, which localized in the cytoplasm without Baz, to the cell cortex. *In vivo* binding of Baz and CG31534 was shown later by Co-IP experiments using embryonic lysates expressing an N-terminally GFP tagged version of CG31534-PA. However, mutations generated in both works for *CG31534* were viable and fertile (Beati, 2009), which is also a characteristic for the respective *LMO7* knockout in mice (Tanaka-Okamoto et al., 2009).

1.6 Scope of the thesis

The aim of the thesis was the analysis of the gene function of *CG43427 (smallish, (smash))* during the development of *Drosophila*. Smash was identified as a new potential binding partner of the cell polarity regulator Baz (Ramrath, 2002). Preliminary work showed that endogenous Smash protein colocalizes with Baz in the region of the AJs. As both proteins associate *in vivo*, we wanted to further analyse the function of *smash* with regard to epithelial cell polarity. A knockout of *smash* was generated before with regard to the old gene annotation. This allele is viable and fertile but did not show polarity defects. This allele cannot be considered as a classical null, because N-terminal parts might be still expressed. Thus we generated a mutation for *smash*, affecting the entire genomic locus by FLP/FRT mediated transdeletion. This full knockout allele was analysed for its viability and for potential polarity defects. Flies lacking the entire genomic locus are still viable and fertile and do not show obvious defects.

All preliminary data had been obtained with the short isoform Smash-PI. As *smash* encodes a larger isoform we wanted to analyse potential gain of function phenotypes. Accordingly, the respective *smash* isoform had to be cloned and transgenic flies were subsequently generated. Overexpression of the respective large isoform caused a dramatic increase in the lethality score and embryonic cuticles showed anterior and dorsal holes.

Beside the interaction of Smash and Baz, other binding partners of Smash had been of interest. Preliminary data showed that Smash binds to the non-receptor tyrosine kinase Src42A (Beati, 2009). Based on this finding, we wanted to continue to investigate the developmental relevance of this interaction. *Src42A* has been implicated to function in dorsal closure and other morphogenetic processes. Thus we analyzed whether *smash* might also function in pathways coordinating dorsal closure. With regard to this we focussed on *Src64B* as well. *Src42A* is known to function redundantly with *Src64B* in morphogenetic processes like dorsal closure (see 1.3). Of interest had been double mutant combinations of *smash* with *Src42A* or *Src64B* respectively. A double mutant with *Src64B* is lethal. However, cell polarity was not affected and embryonic cuticles did not show the dorsal open phenotype.

2 Material and methods

2.1 Chemicals and materials

2.1.1 Chemicals and enzymes

Used chemicals were purchased from following companies:

Acros, Geel, Belgium; *Baker*, Deventer, Netherlands; *Biomol*, Hamburg, Germany; *Bio-RAD*, Munich, Germany; *Difco*, Detroit, U.S.A.; *Fluka*, Buchs, Swiss; *Gibco/BRL Life Technologies*; Karlsruhe, Germany; *Gruessing*, Filsum, Germany; *Merck*, Darmstadt, Germany; *Riedel-de Haên*, Seelze, Germany; *Roth*, Karlsruhe, Germany; *Serva*, Germany; *Sigma-Aldrich*, Steinheim, *Machery-Nagel*, Dueren, Germany.

Demineralized water was used for solutions, buffers, etc., which were autoclaved if necessary.

Enzymes were purchased from following companies:

Boehringer/Roche Diagnostics, Mannheim, Germany; *MBI Fermentas*, St. Leon-Rot, Germany; New England *Biolabs*, Schwalbach-Taunus, Germany, *Invitrogen*, Karlsruhe, Germany; Promega, Madison, USA.

2.1.2 Kit systems

The following kits were used in this work:

Nucleobond AX100, *Macherey-Nagel*
NucleoSpin Extract II, *Macherey Nagel*
pENTR™/D-TOPO® Cloning Kit, *Invitrogen*
Gateway® LR ClonaseTM II Enzyme Mix, *Invitrogen*
BM Chemiluminescence Blotting Substrate, *Roche Diagnostics*

2.1.3 Photo and picture analysis

Light microscopy:	Axio Imager, *Carl Zeiss Jena GmbH,* Germany
Fluorescence binocular:	Leica MZ 16 FA
Confocal microscopy:	LSM 510 Meta, *Carl Zeiss Jena GmbH,* Germany
X-ray films:	Fuji Medical X-Ray Film „Super RX“, *Fuji,* Tokyo, Japan
X-ray film developer and fixer:	Tenetal Roentogen, *Tenetal*, Norderstedt, Germany
Operating Systems:	Macintosh iMac, *Apple*, Ismaning, USA Microsoft Windows XP and Windows Vista, *Microsoft*, Redmont, USA
Image processing:	GIMP, GNU General Public License (GPL) Inkscape, GNUGeneral Public License (GPL) IrfanView (Proprietary Freeware)
Sequence und primer analysis:	DNA-Star Lasergene V7, *DNASTAR Inc.*Madison, USA

2.1.4 Bacterial strains and cell culture lines

Bacterial strains and cell culture lines which were used for this work are listed in Table 1.

Table 1: Used bacterial strains and cell lines

Cell line	Usage
E.coli DH5α	Amplification and purification of plasmid DNA
E.coli XL-1 blue	
E.coli Bl21	Expression and purification of recombinant proteins
E.coli Top 10 one shot	Transformation of DNA after pENTR™/D-TOPO® cloning reaction
S2 cells	Transfection for biochemical experiments

2.1.5 Plasmids

Used plasmids and their properties are listed in Table 2.

Table 2: Used plasmids and their properties

Plasmid	Property
pENTR™/D-TOPO®	plasmid for gateway cloning; insertion of PCR products with 5' CACC overhang
pPGW	Destinationvector for gateway cloning; N-terminal tagged with GFP; under control of UASp promotor
pPWG	Destinationvector for gateway cloning; C-terminal tagged with GFP; under control of UASp promotor
pUASpGW	Destinationvector for gateway cloning; N-terminal tagged with GFP; under control of UASp promotor; contains attp site
pUASpWG	Destinationvector for gateway cloning; C-terminal tagged with GFP; under control of UASp promotor; contains attp site
pPWH	Destinationvector for gateway cloning; C-terminal tagged with HA; under control of UASp promotor
pHGWA	Destinationvector for gateway cloning; N-terminal tagged with His and GST + C-terminal His tag; under control of T7 promotor

2.1.6 Buffers and medium

Buffers and reagents for histology:

PBS:
140 mM NaCl
10 mM KCl
2 mM KH_2PO_4
6.4 mM Na_2HPO_4 x $2H_2O$
pH 7.3

4% Formaldehyde in PBS:
39.75 ml PBS
5.25 ml 37% Formaldehyde

1x Triton salt solution:
1l dH_2O
0.3 ml Triton X-100
4 g NaCl

PBTw:	PBS with 0.1% Tween20
NHS:	Normal Horse Serum (*Gibco*)
Mowiol:	5 g Mowiol 20 ml PBS 10 ml Glycerol
Hoyers mountant:	30 g Gumarabic 50 ml dH_2O 200 g Chloralhydrate 20 g glycerol

Before use 800 µl hoyers mountant were gently mixed with 640 µl lactic acid.

Buffers for molecular biological methods:

TE-Buffer:	10 mM Tris HCl 0.5 mM EDTA pH 8.0
TAE-Puffer:	40 mM Tris acetate Acetic Acid 1 mM EDTA pH 7.4

Buffers for DNA purification from *E.coli*:

S1 buffer:	50 mM TrisHCl 10 mM EDTA 100 µg/ml RNase A pH 8.0

S2 buffer: 200 mM NaOH
1% SDS

S3 buffer: 2.8 M Potassium acetate (CH_3CO_2K)
pH 5.1

Buffers S1 and S3 are stored at 4°C.

Buffers for DNA purification from flies:

Squishing buffer: 25 mM NaCl
1 mM EDTA
10 mM TrisHCl
pH 8.0

Quick Fly Genomic DNA Prep

Buffer A: 100 mM TrisHCl
pH 7.5
100 mM EDTA
100 mM NaCl
0.5% SDS

Buffer for protein biochemical experiments:

Lysis buffers

LLBVII buffer: 150 mM NaCl
1% Igepal
50 mM Tris HCl
pH 8.0

TNT buffer: 150 mM NaCl

50 mM Tris HCl

1% Triton X-100

pH 8.0

TNT buffer (high salt): 500 mM NaCl

50 mM Tris HCl

1% Triton X-100

pH 8.0

Proteinase inhibitors:

1 mg/ml Aprotinin

1 mg/ml Leupeptin

1 mg/ml Pepstatin A

0.5 M Pefabloc SC

Proteinase inhibitors were added to the lysis buffer in a concentration of 1:500.

Phosphatase inhibitors:

500 mM Sodiumorthovanadate

50 mM Phenyloxide

Halt Phosphatase Inhibitor Cocktail (Thermo Scientific)

Phosphatase inhibitors were added to the lysis buffer to a concentration of 1:500, phosphatase inhibitor cocktail was used 1:100.

SDS gelelectrophoresis and Western blotting:

2x SDS loading buffer:	0.2% Bromophenolblue
	200 mM beta mercaptoethanol
	20% glycerol
	4% SDS
	100 mM Tris HCl
	pH 6.8
1x SDS buffer:	192 mM glycine
	25 mM Trisbase
	0.1% SDS
Transfer buffer:	25 mM TrisHCl
	192 mM glycine
	20% (v/v) methanol
TBST:	150 mM NaCl
	1 mM Tris HCl
	0.2% Tween20
	pH 8.0

Blocking buffer:	TBST containing 3% skim milk and 1% BSA
Blocking buffer:	TBST containing 5% BSA

Culture mediums:

LB medium:	0.5% (w/v) yeast extract 1% Trypton 1% NaCl
SOC-Medium:	20 g Trypton 5 g yeast extract 0.5 g NaCl 10 ml 0.25 M KCl 5 ml 2 M $MgCl_2$ 20 ml 1 M glucose filled up to 1l volume with dH_2O pH 7.0
S2 medium:	Schneider's *Drosophila* Medium (Gibco) 10% Serum, insect cell tested (Sigma) PenStrep (Gibco)

2.1.7 Primers

Table 3 lists primers that were used for this work. Primers were ordered from *metabion international AG*, Martinsried and BioTez GmbH, Berlin.

Table 3: Used primers and their application

name	sequence [5' - 3']	[°C]	application
M13 forward	GTAAAACGACGGCCAG	51	sequencing of pENTRTM/D-TOPO®
M13 reverse	CAGGAAACAGCTATGAC	47	sequencing of pENTRTM/D-TOPO®
UASp forward	GGCAAGGGTCGAGTCGATAG	58	sequencing of gateway® destination vectors
pPTagW rev	GGTATAATGTTATCAAGCTC	46	sequencing of gateway® destination vectors
eGFP N rev	CGGACACGCTGAACTTGTG	57	sequencing of gateway® destination vectors
eGFP C for	CAAAGACCCCAACGAGAAG	54	sequencing of gateway® destination vectors
piggyBac 5' outside	CAATTTTACGCAGAC TATCTTTCTAGGG	57	screening for mutants after transdeletion
CG31534 genomic-e03181-R	CCGATATATGCTCACCTCATGC	56	screening for mutants after transdeletion
piggyBac 3' outside	CGTACGTCACAATATGATTATCTTTCT AGG	56	screening for mutants after transdeletion
CG43427 PBACRB test	GTCGCGGCGCTGCCATGATCATCG	68	screening for mutants after transdeletion
UP Primer	GACGGGACCACCTTATTTTATTCTATC ATG	59	screening for mutants after transdeletion
CG43427 genomic for P(XP) test	CACACTCCGCCCCATTTTTATATCC	60	screening for mutants after transdeletion
check ATG I CG43427 for	GTGCAGATCCATCACGGATGC	60	test for successful deletion of the first ATG of CG43427
check ATG I CG43427 rev	GCGCAATGGAAAACTCACCA	58	test for successful deletion of the first ATG of CG43427
check ATG II CG43427 for	CATGTCACGCCCACCTCATC	59	test for successful deletion of the second ATG of CG43427
check ATG II CG43427 rev	GCACCGGCCTTAAATGCTTG	58	test for successful deletion of the second ATG of CG43427
Control_CG9769_ forward	CCGCACTATCGATAGGCCC	58	control primers for downstream neighboring gene CG9769
Control_CG9769_ reverse	CATGCAGCCGCTCTTGC	58	control primers for downstream neighboring gene CG9769
Src42A-DeltaSH3-F	GCAGGTGCCAACGTC GGA TCC GGT GGA GGT AAATCAATCGAAGCA	75	deletes SH3 domain, introduces BamHI restriction site
Src42A-DeltaSH3-R	TGCTTCGATTGATTTACCTCCA CCGGATCCGACGTTGGCACCTGC	75	deletes SH3 domain, introduces BamHI restriction site
Src42A-DeltaSH2-F	AAATCAATCGAAGCA GGA TCC GGT GGA GGT GTCCAGATCGAGAAG	72	deletes SH2 domain
Src42A-DeltaSH2-R	CTTCTCGATCTGGACACCTCCA CCGGATCCTGCTTCGATTGATTT	72	deletes SH2 domain
Src42A-DeltaKinase-F	ATCGACAGAACATCC GGA TCC GGT GGA GGT GAAGACTTCTATACA	71	deletes tyrosine kinase domain
Src42A-DeltaKinase-R	TGTATAGAAGTCTTCACCTCCA CCGGATCCGGATGTTCTGTCGAT	71	deletes tyrosine kinase domain

Src42A-YF-F	ACA TCT GAT CAG AGC GAC TTC AAA GAG GCG CAA GCC TAC	71	mutates last tyrosine to phenylalanine, deletes StuI restriction site
Src42A-YF-R	GTAGGCTTGCGCCTCTTTG AAGTCGCTCTGATCAGATGT	79	mutates last tyrosine to phenylalanine, deletes StuI restriction site
Mut Y64F for LIM	GGACGAGAGCCCATC TTT GAGAATGTCAGCTCG	68	mutates tyrosine 64 of CG43427-RI to phenylalanine
Mut Y64F rev LIM	CGAGCTGACATTCTC AAA GATGGGCTCTCGTCC	68	
Mut Y152F for LIM	CAAGCAGAGCCCTAC TTC CAAGTGCCGAAGGCC	72	mutates tyrosine 152 of CG43427-RI to phenylalanine
Mut Y152F rev LIM	GGCCTTCGGCACTTG GAA GTAGGGCTCTGCTTG	72	
Mut Y162F for LIM	GCCACGGAGCCCTAC TTC GATGCCCCCAAGCAT	74	mutates tyrosine 162 of CG43427-RI to phenylalanine
Mut Y162F rev	ATGCTTGGGGGCATC GAA GTAGGGCTCCGTGGC	74	
Mut Y244F for LIM	TCATCGGACAACACC TTC GAGACCATATCGAAC	66	mutates tyrosine 244 of CG43427-RI to phenylalanine
Mut Y244F rev	GTTCGATATGGTCTC GAA GGTGTTGTCCGATGA	66	
Mut Y601F for LIM	GGCCTGGAGCCAGAT TTC GCTGTTAGCACGAGG	71	mutates tyrosine 601 of CG43427-RI to phenylalanine
Mut Y601F rev LIM	CCTCGTGCTAACAGC GAA ATCTGGCTCCAGGCC	71	
Y685F Mut for LIM	CAGCAGCGGAAGAGT TTT GACAGCCAACAGACC	69	mutates tyrosine 685 of CG43427-RI to phenylalanine
Y685F Mut rev LIM	GGTCTGTTGGCTGTC AAA ACTCTTCCGCTGCTG	69	
LIM delta prr1 for	GTAGGGCTGATGGAG GCA GCA AAGGAAAAG GCA GCA GCA GCA GCA ACCGAGAGTCCGATT	79	exchanges prolines in proline rich region 1 to glycines
LIM delta prr1 rev	AATCGGACTCTCGGTTGCTGCTG CTGCTGCCTTTTCCTTTGCTGCC TCCATCAGCCCTAC	79	
LIM delta prr2 for	CAGTCAGAGGCCACA GCA GCA GCA TTG GCA GCA GCA GCATCGACCGCCCAAGTG	81	exchanges prolines in proline rich region 2 to glycines
LIM delta prr2 rev	CACTTGGGCGGTCGATG CTGCTGCTGCCAATGCTGCTGCTGT GGCCTCTGACTG	81	
Lim seq1	CTACCAAGTGCCGAAGGCCACG	64	sequencing of CG43427-RI
Lim seq2	CTCGCCAGAGCAGTGAGCACTAC	63	sequencing of CG43427-RI
Lim seq3	GCATGCATATCACCAGATGGAC	57	sequencing of CG43427-RI

2.1.8 Primary antibodies

Primary antibodies, which were used for immunofluorescence staining (IF), Western blotting (WB) and Immunoprecipitation (IP), are listed in Table 4. Secondary antibodies and fluorochrome conjugated phalloidin for F-actin staining are listed in Table 5.

Table 4: Primary antibodies

antibody	species	application	source / company
Actin	rabbit	WB 1:2000	Sigma A2066
Smash intra (DE02088)	rabbit	IF 1:500; WB 1:2000; IP	Wodarz, unpublished
Smash N-term (DE12095)	guinea pig	IF 1:500; WB 1:1000	Beati, unpublished
Bazooka (DE99646)	rabbit	IF 1:2000; WB 1:2000; IP	Wodarz et al., 1999
DE-Cadherin (DCAD2)	rat	IF 1:5; WB 1:5, IP	Developmental Studies Hybridoma Bank (DSHB)
Discs Large (4F3)	mouse	IF 1:20	
Armadillo (N2 7A1)	mouse	IF 1:20; WB 1:50	
α-Catenin (D-CAT1)	rat	IF 1:50	
GFP	mouse	IF 1:2000; WB 1:2000; IP	Invitrogen Molecular Probes # A11120
GFP	rabbit	IF 1:2000; WB 1:2000; IP	Invitrogen Molecular Probes # A11122
HA	mouse	WB 1:2000	Roche # 11 583 816 001
Phosphotyrosine (PT-66)	mouse	IF 1:1000; WB 1:1000	Sigma P3300
Src42A	rabbit	IF 1:1000	Takahashi et al., 2005
pSrc	rabbit	IF 1:1000	Shindo et al., 2008
BrdU (MoBu-1)	mouse	IF 1:500	Abcam (ab8039)
mCherry (1C51)	mouse	IF 1:500	Abcam (ab125096)

Table 5: antibodies and fluorochrome conjugated phalloidin

antibody	species	application	company
Peroxidase-AffiniPure Goat Anti-Mouse IgG + IgM (H+L)	goat	1:10.000	Jackson ImmunoResearch (115-035-068)
Peroxidase-AffiniPure Goat Anti-Rabbit IgG, (H+L)	goat	1:10.000	Jackson ImmunoResearch (111-035-144)
Peroxidase-AffiniPure Goat Anti-Rat IgG + IgM, (H+L)	goat	1:10.000	Jackson ImmunoResearch (112-035-068)
Alexa Fluor® 488 Goat Anti-Mouse IgG1 (γ1)	goat	1:200	Invitrogen Life Technologies A21121
Alexa Fluor® 555 Anti-Mouse IgG (H+L)	goat	1:200	Invitrogen Life Technologies A21422

Alexa Fluor® 647 Goat Anti-Mouse IgG (H+L)	goat	1:200	Invitrogen Life Technologies A21235
Alexa Fluor® 488 Goat Anti-Rabbit IgG (H+L)	goat	1:200	Invitrogen Life Technologies A11008
Alexa Fluor® 555 Goat Anti-Rabbit IgG (H+L)	goat	1:200	Invitrogen Life Technologies A21428
Alexa Fluor® 647 Goat Anti-Rabbit IgG (H+L)	goat	1:200	Invitrogen Life Technologies A21244
Alexa Fluor® 488 Goat Anti-Rat IgG (H+L)	goat	1:200	Invitrogen Life Technologies A11006
Alexa Fluor® 555 Goat Anti-Rat IgG (H+L)	goat	1:200	Invitrogen Life Technologies A21434
Alexa Fluor® 647 Goat Anti-Rat IgG (H+L)	goat	1:200	Invitrogen Life Technologies A21247
Alexa Fluor® 488 Goat Anti-Guinea Pig IgG (H+L), highly cross-adsorbed	goat	1:200	Invitrogen Life Technologies A11073
Alexa Fluor® 555 Goat Anti-Guinea Pig IgG (H+L), highly cross-adsorbed	goat	1:200	Invitrogen Life Technologies A21435
Alexa Fluor® 647 Goat Anti-Guinea Pig IgG (H+L), highly cross-adsorbed	goat	1:200	Invitrogen Life Technologies A21450
Alexa Fluor® phalloidin 488		1:100	Invitrogen Life Technologies A12379
Alexa Fluor® phalloidin 568		1:100	Invitrogen Life Technologies A12380
Alexa Fluor® phalloidin 647		1:100	Invitrogen Life Technologies A22287

2.1.9 Fly stocks

Used fly stocks and donors are listed below in Table 6.

Table 6: Fly stocks

Stock	Plain text genotype	Description	Reference
Oregon R		wildtype	Wodarz stock collection
white^{1118}	w[1118]	white eyes	Bloomington #5905
daughterless Gal4	w[1118]; P{da-GAL4.w[-]}3	Gal4 driver line; ubiquitous expression under control of *daughterless* promotor; 3rd chromosome	Bloomington #8641

engrailed Gal4	y[1] w[*]; P{w[+mW.hs]=en2.4-GAL4}e16E P{w[+mC]=UAS-FLP1.D}JD1	Gal4 driver line; expression under control of *engrailed* promotor in stripes; 2nd chromosome	Bloomington #6356
daughterless Gal4	w[*]; P{w[+mW.hs]=GAL4-da.G32}UH1	Gal4 driver line; ubiquitous expression under control of *daughterless* promotor; 2nd chromosome	Wodarz stock collection
tubulin Gal4	Y[1] w[*]; P{w[+mC]=tubP-GAL4}LL7/TM3, Sb[1]	Gal4 driver line; ubiquitous expression under control of *tubulin* promotor; 3rd chromosome	Bloomington #5138
patched Gal4	W[*]; P{w[+mW.hs]=GawB}ptc[559.1]	Gal4 driver line; expression under control of *patched* promotor in stripes; 2nd chromosome	Bloomington #2017
hsFlp;; actin > CD2 > Gal4, UAS RFP	P{ry[+t7.2]=hsFLP}12, y[1] w[*]; P{w[.mC]=Act5C(CD2)Gal4}17bFO1, UAS RFP /TM3, Sb[1]	Gal4 driver line, expression under control of *actin* promotor in clones	Wodarz stock collection
y^1, w, hsFlp*; Sco/CyO	P{ry[+t7.2]=hsFLP}12, y[1] w[*]; sna[Sco]/CyO	Flipase under control of heat shock promotor; used for transdeletions	Bloomington #1929
P{XP}^{d00921}	P{XP}CG43427d00921	P{XP} insertion at position 3R:485,651 [-]; used for transdeletion of entire *smash* gene locus	Exelixis Collection, Harvard
PBac{WH}^{f00542}	PBac{WH}CG43427f00542	piggyBac insertion at position 3R:531,436 [+]; used for transdeletion of *CG31534*	Exelixis Collection, Harvard
PBac{RB}^{e03181}	PBac{RB}CG43437e03181	piggyBac insertion at position 3R:537,071 [-]; used for both transdeletions	Exelixis Collection, Harvard
Df(3R)ED5066	w[1118]; Df(3R)ED5066, P{w[+mW.Scer\FRT.hs3]=3'.RS5+3.3'}ED5066/TM6C, cu[1] Sb[1]	Deleted segment 82C5--82E4; deficient for *smash* gene locus	Bloomington #8092
$smash^{4.1}$	smash[4.1]	*smash* mutant allele; C-terminally truncated; homozygous viable	this work
$smash^{35}$	smash[35]	*smash* null allele; homozygous viable	this work
$Src64B^{KO}$	Src64B[KO]	*Src64B* nullallele	O'Reilly et al., 2006
$Src42A^{26-1}$	Src42A[26-1]	*Src42A* nullallele	Takahashi et al., 2005
Gla/CyO	w[1118]; In(2LR)Gla, wg[Gla-1] Bc[1]/CyO	Balancer for the 2nd chromosome	Bloomington #5439
If/CyO ; MKRS/TM6B	w[1118]; If/CyO; MKRS/TM6B[Tb1]	Balancer for 2nd and 3rd chromosome	Wodarz stock collection
Br/CyO ; TM2/TM6B	w[*], Br/CyO ; TM2/TM6B[Tb1]	Balancer for 2nd and 3rd chromosome	Wodarz stock collection
TM3/TM6B	w[*]; TM3, Sb[1] Ser[1]/TM6B, Tb[1]	Balancer line for the 3rd chromosome	Bloomington #2537
TM3[*tw-GFP*]/TM6B	w[*]; TM6B, Tb[1]/TM3, Sb[1], Ser[1], twist-GFP	Balancer line for the 3rd chromosome	Wodarz stock collection (B.Shilo)
UASt GFP-Smash-PI	UASt-GFP-Smash-PI	GFP-Smash-PI under control of UASt promotor; 3rd chromosome	Neugebauer, 2007
UASt GFP-Smash-PM	UASt GFP-Smash-PM[10]	GFP-Smash-PMunder control of UASt promotor; 2nd chromosome	this work
y^1, w^{1118};; attp 22A3	y[1] w[1118]; PBac{y[+]-attP-3B}VK00037	attP docking site for phiC31 integrase-mediated transformation; 22A3, 2L:1582820	Bloomington #9752
UAS GFP-Smash-PI	UAS GFP-Smash-PI	GFP-Smash-PI under control of UASp promotor; 2rd chromosome (22A3)	this work
UAS GFP-Smash-PM	UAS GFP-Smash-PM	GFP-Smash-PM under control of UASp promotor; 2nd chromosome (22A3)	this work
UAS Src42A-HA	UAS Src42A-HA[11]	Src42A-HA under control of UASp promotor, 2nd chromosome	this work

UAS Src64B-HA	UAS Src64B-HA[6]	Src64B-HA under control of UASp promotor, 2nd chromosome	this work
UAS Src42AYF-HA5	UAS Src42AYF-HA[5]	Src42AYF-HA under control of UASp promotor, 2nd chromosome	this work
UAS Src42AYF-HA6	UAS Src42AYF-HA[6]	Src42AYF-HA under control of UASp promotor, 2nd chromosome	this work
UAS mCD8::GFP	w[*]; P{y[+t7.7] w[+mC]=10XUAS-mCD8::GFP}attP2	mCD8-GFP under control of UAS promotor, 2nd chromosome	Bloomington #32184

2.1.10 Fly breeding

Flies were raised on standard medium and kept at 25°C, unless stated otherwise. Embryo collections were performed by keeping flies in cages on apple juice agar plates, which were coated with yeast.

Standard medium consists of 356 g corn groats, 47.5 g soybean flour, 84 g dry yeast, 225 g malt extract, 75 ml 10% nipagin, 22.5 ml propanoic acid, 28 g agar, 200 g sugar beet molasses and 4.9 l H_2O.

2.2 Genetic methods

2.2.1 Separation of DNA fragments via gel electrophoresis

DNA exhibits a negative charge associated with the phospho groups it contains. This allows DNA to migrate in an electric field to the positively charged anode. 1% agarose gels containing ethidiumbromide (EtBr), a chemical intercalating with DNA that can be visualized under UV light is widely used to resolve DNA samples. The DNA is separated based upon its length and secondary structure, which can be formed by circular DNA (e.g. plasmids). The size can be determined by using a DNA standard, which is loaded in a separate lane on the gel.

1% agarose gel is made with 1 g agarose, which is solved in 100 ml of TAE buffer in a microwave. 1 µl of EtBr (1%) is added and the solution poured into a gel chamber. After hardening DNA can be loaded and separation takes place at 110V for 20 – 25 min.

2.2.2 Polymerase Chain Reaction (PCR)

The polymerase chain reaction (PCR) is a method allowing the amplification of specific DNA sequences, using primers (oligonucleotides) consisting of 18 – 30 nucleotides. The technique became available when the thermophilic bacterium *Thermophilus aquaticus* was discovered. This bacterium features a heat resistant DNA polymerase, afterwards called Taq polymerase. A disadvantage of this enzyme is a lack of "proofreading" activity, leading to a significant error rate. A second polymerase was isolated from the archae bacterium *Pyrococcus furiosus*, which features a heat resistant DNA polymerase too. This enzyme exhibits a proofreading activity. This Pfu polymerase is widely used for the cloning of DNA.

For the use of the PCR it is necessary to generate a pair of primers, which target the DNA sequence of interest from 5' to 3' and 3' to 5', respectively. After denaturation at 95°C the DNA will be available in a single stranded form. After decreasing the temperature, the DNA will associate primarily with the added primers, because they are added in an excess. The temperature for this annealing step is dependent on the sequence of the primer. Afterwards, the DNA polymerase binds to the primer and a temperature shift to 72°C leads to the activation of the enzyme and the subsequent synthesis of the complementary DNA strand by the use of dNTPs (deoxynucleosidetriphosphates). Repeating these steps denaturation- annealing – elongation, DNA can be easily amplified.

An example PCR can be set up as followed:

100 ng template DNA

4 µl oligonucleotides (10 pmol, forward and reverse)

2 µl dNTPs (10 mM)

10 µl polymerase buffer (5x)

1 µl polymerase

filled up to a volume of 50 µl with dH_2O

Table 7 shows an example for a PCR program.

Table 7: Example for PCR program

step	time	temperature [°C]
I denaturation	5 min	95
II denaturation	30 sec	95
III annealing	30 sec	dependent on sequence of the respective primer
IV elongation	dependent on length of DNA sequence to be amplified Taq polymerase 30 - 60 sec = 1 kb Pfu polymerase 90 sec = 1 kb	72
V	*repeat from step II for 34 times*	
VI final elongation	10 - 20 min	72
VII end of reaction		4

2.2.3 Mutagenesis PCR

Mutagenesis PCRs were adapted from the QuickChange II site directed mutagenesis kit (Stratagene).

By the use of PCR it is possible to generate targeted mutations of DNA constructs. Point mutations of single nucleotides can be achieved by designing primers, which are not fully complementary to the template DNA. Thereby the coding nucleotide triplet is changed to generate the desired mutation, meaning that during the annealing step these nucleotides will pair in a wrong way (e.g. G with T or A). This triplet within the primer is flanked by 15 nucleotides on the 5’ and 3’ end. This primer has a length of 33 nucleotides, which guarantees annealing of the oligonucleotide carrying the desired base pair change.

Furthermore it is possible to delete whole domains, by “looping” them out. In this case the 5’ sequence of the primer is binding the template in front of the region, which is wished to be deleted and the 3’ end binds after this region. In between this two 15 nucleotide long sequences 12 additional nucleotides can be added, which have a spacer function. The sequence can encode for G – A – G – A. It is important that the deleted DNA construct stays in frame, thereby not leading to a false translated protein. For this kind of PCR, the elongation time has to be adapted

to the length of the whole plasmid, because the polymerase has to amplify the full construct. The PCR product needs to be digested by a restriction enzyme DpnI, which recognizes and digests only methylated DNA (GA^MT^MC, which is modified in that way by *E.coli*). This step is necessary to get rid of the non mutated template DNA. The mutated PCR product will be transformed into *E.coli* DH5α.

2.2.4 Transformation of DNA into chemically competent *E.coli*

Chemically competent *E.coli* cells (e.g. XL 1 blue) are thawed on ice. 50 µl of bacteria are transformed with DNA and incubation on ice takes place for 30 min. The cells will be heatshocked for 45 sec at 42°C and incubated on ice again for 3 min. 250 µl of prewarmed SOC medium is given to the cells which will be incubated at 37°C for 45 min while shaking. The mixture is plated on LB agar plates containing an appropriate antibiotic for selection.

2.2.5 Isolation of DNA out of an agarose gel

After separating DNA by use of gel electrophoresis, bands can be cut out and the DNA isolated and purified. For this purpose the NucleoSpin Extract II kit (Macherey Nagel) was used and purification was according to the manufacturer protocol. DNA was eluted with 15 – 30 µl NE Buffer.

2.2.6 Purification of DNA out of a PCR product

Purification was performed with the NucleoSpin Extract II kit (Macherey Nagel). DNA was eluted with 15 – 25 µl of NE Buffer.

2.2.7 pENTR™/D-TOPO® cloning

The principle of the pENTR™/D-TOPO® cloning (Invitrogen) is to generate a pENTR™/D-TOPO® vector in the first step, which contains an insert of interest (e.g. coding sequence for *CG43427-RM*). This vector can be used afterwards for Gateway® cloning to exchange the gateway cassette from a destination vector with the insert of the pENTR™/D-TOPO® vector. This reaction is catalyzed by an enzyme called clonase, which recognizes attL sites upstream and downstream of the pENTR insert/gateway cassette thereby mediating their recombination. Successful recombination is selected by the change of antibiotic resistance. The pENTR™/D-TOPO® vector carries a resistance gene against kanamycin, and the destination vectors against ampicillin. Fig.10 shows the principle of the pENTR™/D-TOPO® / Gateway® cloning system.

For the cloning as such it is necessary to design a forward primer with a CACC overlap at its 5' end. This signal will be recognized by the topoisomerase, which is included in the reaction mix with the pENTR™/D-TOPO® vector. For the reverse primer it has to be decided, whether one wants to work with N-terminal or C-terminal tags. In the latter case the primer has to stop with the last coding nucleotide triplet encoding for an amino acid. For N-terminal tags it is important to add a nucleotide triplet encoding for a stop signal (e.g. TAA).

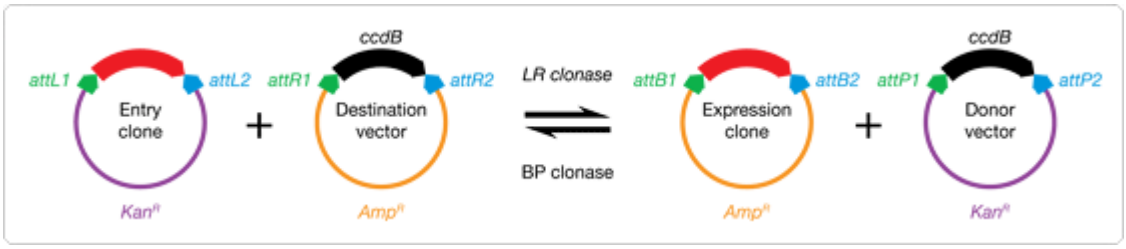

Fig.10: Principle of Gateway® cloning

An insert from the pENTR™/D-TOPO® vector is shuttled to a Gateway® destination vector, mediated by the reversible reaction of the clonase. Selection is performed by the change of antibiotic resistence from kanamycin to ampicillin (source: http://de-de.invitrogen.com/site/de/de/home/Products-and-Services/Applications/Cloning/Gateway-Cloning/Clonase-Enzyme.html).

For the pENTR™/D-TOPO® reaction, 2 µl of freshly purified PCR product were mixed with 0.5 µl of salt solution and 0.5 µl of linearized pENTR vector. Incubation took place for 5 – 6 min at room temperature. Transformation was done into the *E.coli* strain "top 10 one shot". LB agar plates containing kanamycin were used for selection.

The following clonase reaction was done with 50 - 150 ng of the pENTR™/D-TOPO® vector, which was mixed with 1.5 µl of TE buffer. 150 ng of the respective Gateway® destination vector was added and reaction started with 1 µl of clonase. Incubation took place for 60 min at 25°C and inactivation of the reaction was achieved by adding 0.5 µl of Proteinase K for 10 min at 37°C. Transformation was done into *E.coli* DH5α or XL-1 blue. Constructs which were generated in this work are listed in Table 8 below.

Table 8: Constructs generated in this work

name	property
CG43427-PM pENTR	pENTR™/D-TOPO® vector containing the coding sequence of *CG43427-RM*
CG43427-PM pUASpGW	N-terminal tagged *GFP-CG43427-RM* under control of UASp promotor; contains attp site for site directed injection
CG43427-PM pTGW	N-terminal tagged *GFP-CG43427-RM* under control of UASt promotor
CG43427-PN pENTR	pENTR™/D-TOPO® vector containing the coding sequence of *CG43427-RN*
CG43427-PN pUASpGW	N-terminal tagged *GFP-CG43427-RN* under control of UASp promotor; contains attp site for site directed injection
CG43427-PE pENTR	pENTR™/D-TOPO® vector containing the coding sequence of *CG43427-RE*
CG43427-PE pUASpGW	N-terminal tagged *GFP-CG43427-RE* under control of UASp promotor; contains attp site for site directed injection
CG31534-PA Y64F pENTR	pENTR™/D-TOPO® vector containing the coding sequence of *CG31534-RA* carrying a pointmutation for Y64 to F
CG31534-PA Y64F pPGW	N-terminal tagged *GFP-CG31534-RA* with mutation for Y64 to F under control of UASp promotor
CG31534-PA Y152F pENTR	pENTR™/D-TOPO® vector containing the coding sequence of *CG31534-RA* carrying a pointmutation for Y152 to F
CG31534-PA Y152F pPGW	N-terminal tagged *GFP-CG31534-RA* with mutation for Y152 to F under control of UASp promotor
CG31534-PA Y162F pENTR	pENTR™/D-TOPO® vector containing the coding sequence of *CG31534-RA* carrying a pointmutation for Y162 to F
CG31534-PA Y162F pPGW	N-terminal tagged *GFP-CG31534-RA* with mutation for Y162 to F under control of UASp promotor

CG31534-PA Y244F pENTR	pENTR™/D-TOPO® vector containing the coding sequence of *CG31534-RA* carrying a pointmutation for Y244 to F
CG31534-PA Y244F pPGW	N-terminal tagged *GFP-CG31534-RA* with mutation for Y244 to F under control of UASp promotor
CG31534-PA Y601F pENTR	pENTR™/D-TOPO® vector containing the coding sequence of *CG31534-RA* carrying a pointmutation for Y601 to F
CG31534-PA Y601F pPGW	N-terminal tagged *GFP-CG31534-RA* with mutation for Y601 to F under control of UASp promotor
CG31534-PA Y685F pENTR	pENTR™/D-TOPO® vector containing the coding sequence of *CG31534-RA* carrying a pointmutation for Y685 to F
CG31534-PA Y685F pPGW	N-terminal tagged *GFP-CG31534-RA* with mutation for Y685 to F under control of UASp promotor
CG31534-PA YmultiF pENTR	pENTR™/D-TOPO® vector containing the coding sequence of *CG31534-RA* carrying pointmutations for Y64, 152, 162, 244, 601 and 685 to F
CG31534-PA YmultiF pPGW	N-terminal tagged *GFP-CG31534-RA* with mutations for Y64, 152, 162, 244, 601 and 685 to F under control of UASp promotor
CG31534-PA Δprr1/2 pENTR	pENTR™/D-TOPO® vector containing the coding sequence of *CG31534-RA* were the two prolin rich regions were mutated
CG31534-PA Δprr1/2 pPGW	N-terminal tagged *GFP-CG31534-RA* with mutated proline rich regions 1 and 2 under control of UASp promotor
Src42A ΔSH3 pENTR	pENTR™/D-TOPO® vector containing the coding sequence *Src42A* where the SH3 domain was deleted
Src42A ΔSH3 pPWH	C-terminal tagged *Src42A-HA* where the SH3 domain was deleted, under control of UASp promotor
Src42A ΔSH2 pENTR	pENTR™/D-TOPO® vector containing the coding sequence *Src42A* where the SH2 domain was deleted
Src42A ΔSH2 pPWH	C-terminal tagged *Src42A-HA* where the SH2 domain was deleted, under control of UASp promotor
Src42A ΔKin pENTR	pENTR™/D-TOPO® vector containing the coding sequence *Src42A* where the tyrosine kinase domain was deleted
Src42A ΔKin pPWH	C-terminal tagged *Src42A-HA* where the tyrosine kinase domain was deleted, under control of UASp promotor
Src42A YF pENTR	pENTR™/D-TOPO® vector containing the coding sequence *Src42A* where Y411 was mutated to F
Src42A YF pPWH	C-terminal tagged *Src42A-HA* where Y411 was mutated to F, under control of UASp promotor

2.2.8 Isolation of DNA from bacteria

2 ml of LB medium containing the respective antibiotic were inoculated with a single *E.coli* colony and grown over night at 37°C while shaking. 1.5 ml of the culture was transferred into a microtube and bacteria were centrifuged for 1 min at 14.000 rpm. After discarding the supernatant, the cell pellet was resuspended with 200 µl S1 resuspension buffer. 200 µl of S2 lysis buffer were added and the mix vortexed. After this step cells were incubated for 5 min on ice. Neutralization is achieved by adding 200 µl of S3 neutralization buffer. After this step the microtube was inverted 5 – 6 times and subsequently centrifuged for 20 min at 14.000 rpm at 4°C. The supernatant, containing the plasmid DNA, was transferred to a new tube. Precipitation of the DNA was achieved by adding 400µl of isopropanol and centrifugation at 14.000 rpm at 4°C for 30 min. The supernatant was discarded and the DNA precipitate washed with 200 µl of ice cold 70% ethanol and centrifuged for 5 min at 14.000 rpm at 4°C. Supernatant was discarded and the DNA precipitate dried at room temperature. 25 µl of dH_2O were given to the DNA for dissolving and stored at -20°C.

2.2.9 Restriction digestion

By using restriction enzymes it is possible to cut DNA into fragments. These restriction endonucleases can specifically cut DNA at the sequence motif they recognize, e.g. EcoRV is a type II restriction endonuclease cutting GAT ↓ ATC into blunt ends (Pingoud and Jeltsch, 2001).

For a control digestion (e.g. after clonase reaction) 1-2 µg of DNA are digested in a volume of 10 µl, which contains 0.2 µl of the restriction enzyme and 1 µl of its respective 10x digestion buffer. The restriction digestion takes place for 60 min at 37°C and DNA is afterwards separated by agarose gel electrophoresis.

2.2.10 Determining DNA concentration

DNA concentration was determined with a photometer at OD_{260} (Eppendorf Biophotometer). The dsDNA program was used with a dilution factor of 1:99. A small cuvette was filled with 99 µl dH_2O

to define the blank value and then DNA concentration was obtained by adding 1 µl of the DNA solution and a second measurement.

2.2.11 Sequencing of DNA

For the sequencing of plasmids 300 ng of DNA were used as template. For one reaction 1.5 µl of SeqMix, 1.5 µl of SeqBuffer were set up with 8 pmol of a respective primer and the template. Table 9 shows the PCR program, which was used for this reaction.

Table 9: Sequencing program

step	time	temperature [°C]
I denaturation	2 min	96
II denaturation	20 sec	96
III annealing	30 sec	55
IV elongation	4 min	60
V	*repeat from step II for 25 times*	
VI end of reaction		12

After the reaction the PCR product was transferred into a new microtube. Solution was mixed with 1 µl 125 mM EDTA, 1 µl 3M sodium acetate (pH 5.2) as well as with 50 µl 100% Ethanol. After incubation for 5 min at room temperature the microtube was centrifuged at 14.000 rpm for 15 min. The supernatant was discarded and the precipitate washed with 70 µl of 70% ethanol. After centrifugation at 14.000 rpm for 5 min the supernatant was discarded, the precipitate air dried for at least 2 min and resolved in 15 µl HiDi (formamide). Sequencing was performed by the department of Prof. Dr. Pieler.

2.2.12 Isolation of genomic DNA from flies

Isolation of genomic DNA out of a single fly

By use of this method the isolation of genomic DNA out of a single fly is possible. For this purpose a fly is put into a microtube and shock frozen in liquid nitrogen. Afterwards the fly was homogenized with a biovortexer in 50 µl squishing buffer containing 0.5 µl Proteinase K.

Incubation for 30 min at 37°C was followed and inactivation of the Proteinase K was achieved by a heat shock for 5 min at 94°C. Before PCRs have been set up, the lysate was centrifuged for 2 min at 14.000 rpm to sediment the remaining cuticle of the fly. For a PCR of 25 µl volume 2.5 µl of the supernatant were used as template.

Isolation of genomic DNA out of several flies (Quick fly genomic DNA prep)

30 flies were collected in a microtube and shock frozen in liquid nitrogen. Using a biovortexer flies were homogenized in 200 µl buffer A, another 200 µl buffer A were added and further homogenized till just cuticles were left over. The lysate was incubated for 30 min at 65°C and subsequently mixed with 800 µl LiCl/KAc (575 µl 6 M LiCl + 230 µl 5 M KAc) solution. After centrifuging at 13.000 rpm for 15 min the supernatant was mixed with 600 µl isopropanol in a new miocrotube. Precipitation of the DNA was achieved after centrifuging for 15 min at 13.000 rpm. The supernatant was discarded and the DNA precipitate was washed with 200 µl of 70% ethanol for 10 min at 13.000 rpm. DNA was resolved in 150 µl dH_2O or TE buffer. This step was done for 60 min at room temperature or at 4°C over night. The DNA was stored at -20°C.

2.2.13 UAS/Gal4 system

The UAS/Gal4 system is binary and was isolated from the yeast (*Saccharomyces cerevisiae*). The Gal4 protein is the transcription factor and UAS (=upstream activating sequence) its binding site. This system is used in *Drosophila* to mediate targeted expression of transgenes, which were hooked up to an UAS element (Brand and Perrimon, 1993).

For this purpose a driver line, carrying the sequence for the Gal4 protein hooked up to a promoter of a *Drosophila* gene (e.g. *engrailed*, *en*), is crossed against an UAS line. Hereby, expression is controlled in temporal and spatial manner. *en* for example is a segment polarity gene, expressed in stripes to the posterior compartment of segments. Therefore an *en Gal4* driver line allows expressing an UAS transgene in stripes, like the endogenous expression pattern of *en*. Fig.11 shows a schematic of the UAS/Gal4 system.

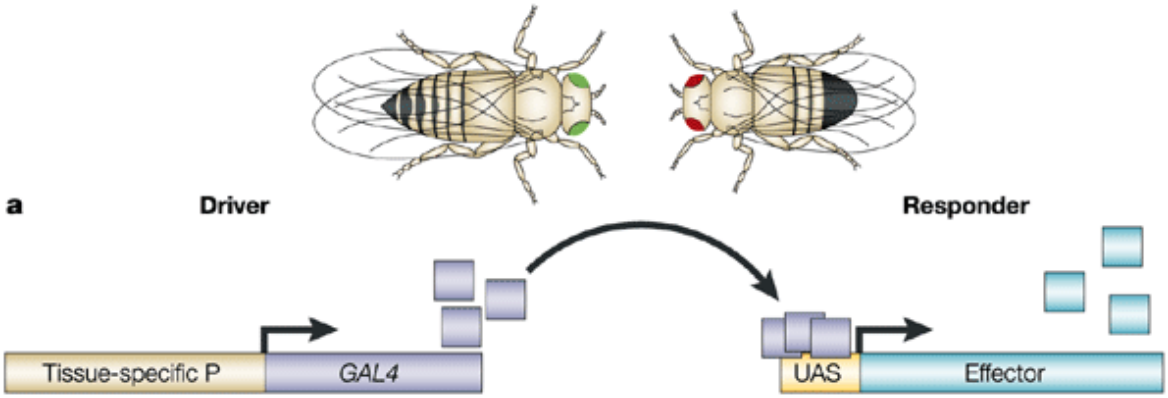

Fig.11: UAS/Gal4 system

The UAS/Gal4 system is used for the expression of transgenes in *Drosophila*. A driver line, expressing Gal4 under the control of any promoter, is crossed to a responder line, carrying a transgene fused to a the UAS sequence. Adapted from Wimmer, 2003.

2.2.14 Generation of transgenic flies

By the use of P-elements and transposons it is possible to inject DNA into *Drosophila* embryos for insertion into its genome (Bachmann and Knust, 2008).

The destination vectors of the Gateway® system are constructed with a P-element cassette and a promoter (e.g. UASp or UASt) upstream of the coding sequence, as well as a *mini white* gene. It is therefore suitable for the generation of transgenic fly lines. For the insertion it is necessary to co-inject a helper plasmid (Δ2,3), encoding for a transposase, which recognizes the P-element and mobilizes it and leads to its random insertion into the *Drosophila* genome.

For injection 20 µg of the respective DNA were mixed with 5 µg of Δ2,3 helper plasmid DNA. 5 µl of 10x injection buffer (1 mM trisodium phosphate, 50 mM KCl, pH 6.8) were added and the solution filled up with dH_2O to a volume of 50 µl. Centrifugation for 10 min at 14.000 rpm at 4°C was performed to get rid of particles, which could block the injection needle later on.

Injection was done into w^{1118} mutant embryos (these flies exhibit white eyes), which were laid for 20 min at 18°C. Embryos were transferred on a mesh with dH_2O and dechorionized with sodium hypochlorite for 1-2 min and subsequently aligned (to their anterior-posterior axis) on a piece of apple juice agar. Afterwards embryos were transferred on a coverslip, which was coated with embryo glue and dried at room temperature for 14 min (dependent on actual temperature and

humidity). During this step embryos lost their inner turgor, which prevents them from bursting during the injection step. Right before injection embryos were covered with 10S oil and injected into their posterior end where the pole cells will form later (the precursors of the germline). After 36-48 hours hatched larvae were collected and transferred into fly food. Emerging flies were crossed against *w^{1118}; gla /CyO [ftz::lacZ]* flies. In the second generation red eyed flies can appear, which indicated the insertion of the transgene into their genome.

For the identification of the chromosome of insertion, a red eyed male fly either carrying the *gla* marker or the *CyO [ftz::lacZ]* balancer chromosome has to be crossed against virgins of the *w^{1118}; gla /CyO [ftz::lacZ]* fly line. Table 10 shows the phenotypical markers for the identification of the chromosome carrying the insertion (adapted and modified from Bachmann and Knust, 2008).

Table 10: Phenotypical markers for identification of the chromosome carrying the transgene

F2 *w^+ / gla*		F2 *w^-; gla /CyO*		F2 *w^+; gla /CyO*		F2*w^-; CyO*		F2*w^-; gla*		Chr.
male	female	male	female	male	female	male	female	male	female	
	+	+			+	+		+		**I**
+	+	+	+							**II**
+	+	+	+	+	+	+	+	+	+	**III**

Another injection system used is based on the phi C31 integrase, allowing the insertion specifically on landing positions (attp sites) in the genome (Groth et al., 2004). Here embryos were used for injections which exhibit an attp site on position 22A on the second chromosome. Transgenes were inserted by the phi C31 integrase, which is under control of the *vasa* promoter. An advantage of this method is that established UAS lines display the same expression levels, thereby allowing better comparison between the expression of different transgenes. The injection was performed as described above, only the helper plasmid was not added to the injection mix. Furthermore, emerging flies were crossed to *w^{1118}; gla /CyO [ftz::lacZ]* and transformants were directly balanced with *CyO [ftz::lacZ]*.

2.3 Biochemical methods

2.3.1 SDS-PAGE

The SDS-PAGE (sodium dodecyl sulfate polyacrylamide gel electrophoresis) is a method which is used to separate proteins according to their molecular weight. Hereby proteins are denaturated and packed with SDS, giving them a total negative charge. In an electric field, these proteins will migrate to the positively charged anode. The density of the gel can be controlled by the amount of acrylamide which is used. For example, bigger proteins can be better separated by gels with lower concentration of acrylamide, as in contrast smaller proteins by gels with higher concentration. Table 11 lists the amount of contents for different gels.

Table 11: Examples of contents for different molecular SDS-PAGE gels

	separation gel		stacking gel
	7.5%	**10%**	
30% acrylamide	1.9 ml	2.5 ml	620 µl
Tris-HCl pH 8.8	2.8 ml	2.8 ml	
Tris-HCl pH 6.8			470 µl
20% SDS	38 µl	38 µl	20 µl
dH_2O	2.7 ml	2.1 ml	2.6 ml
10% APS	30 µl	30 µl	20 µl
TEMED	8 µl	8 µl	10 µl

SDS gels were made by using the BioRad system. Here two glass plates were fixed into a retaining clip. The separation gel was poured in between the glass plates and covered with isopropanol. After polymerization of the acrylamide the isopropanol layer was removed. Stacking gel was poured on top of the separating gel and a comb, maintaining the space for the pockets, was pushed between the two glass plates.

After polymerization of the stacking gel, the SDS gel was put into a BioRad electrophoresis chamber (either two gels or one gel and one plastic dummy) and both chambers were filled with 1x SDS running buffer. Protein samples were loaded into the pockets with a syringe (Hamilton). One pocket was filled with a protein mass ruler and protein separation took place for approximately 60 min at 200V (depending on the concentration of polyacrylamide).

2.3.2 Western blot

For a Western blot, proteins are first separated via SDS-PAGE and afterwards transferred to a nitrocellulose membrane. Detection of a specific protein occurs with an antibody and concomitant signal development (e.g. chemiluminescence).

Horizontal transfer of the proteins from the SDS gel onto the nitrocellulose membrane occurs at 4°C for 60 min in transfer buffer using the BioRad system. Hereby a supplied blotting chamber is assembled as follows: plastic mat – two whatman papers – SDS polyacrylamide gel – nitrocellulose membrane – two whatman papers – plastic mat. After transfer the nitrocellulose membrane can be stained with Ponceau red, which stains proteins and thereby indicates the quality of the transfer. Subsequent incubation in blocking buffer is necessary to saturate unspecific binding sites, which might cross react with antibodies. The nitrocellulose membrane had to be incubated in blocking buffer containing a primary antibody in an appropriate dilution. This incubation was done over night at 4°C.

After washing the nitrocellulose membrane 3 times for 5 min with TBST a secondary antibody (conjugated with HRP) is added in blocking buffer at a dilution of 1:10.000. This incubation is done for 2 hours at room temperature. Another 3 washes for 5 min followed with the subsequent development of the chemiluminescence signal after incubating the nitrocellulose membrane for 1 min in POD solution (1ml solution A mixed with 10 µl solution B and 15 min incubation in the dark before use, Roche). Detection of the signal was monitored using X-Ray developing films (Fuji).

2.3.3 Lysis of *Drosophila* embryos

For an embryonic protein extraction an overnight egg laying collection is usually used. Embryos were washed with dH_2O, dechorionized with sodium hypochlorite and transferred into a microtube. Lysis was achieved by homogenizing the embryos in 200 µl lysis buffer (containing proteinase inhibitors or additionally phosphatase inhibitors) with a biovortexer. The lysate was filled up to a volume of 1000 µl and incubation on ice followed for 20 min. After a centrifugation at 14.000 rpm at 4°C the supernatant was transferred into a new microtube and protein concentration was determined. If protein lysates were not used directly, they were stored at -20°C. Co-IPs were always continued without freezing to avoid disassembly of protein complexes.

2.3.4 Lysis of *Drosophila* S2 cells

S2 cells were harvested and centrifuged for 10 min at 1000 rpm. Culture medium was discarded and cells were washed with 3 ml PBS. Another centrifugation at 1000 rpm for 5 min was done and PBS removed. S2 cells were lysed by pipetting them up and down with 500 µl of lysis buffer (containing proteinase inhibitors or additionally phosphatase inhibitors) and incubation on ice for 20 min. After centrifugation at 14.000 rpm at 4°C the supernatant was transferred into a new microtube and protein concentration was determined. If protein lysates were not used directly, they were stored at -20°C. Co-IPs were continued without freezing as mentioned above.

2.3.5 Determination of protein concentration

Protein concentration was determined with a photometer. 800 µl of dH_2O were mixed with 200 µl of Bradford reagent (Roth) and 2 µl of the used lysis buffer. This solution was incubated for 3 min at room temperature. The blank value was set at OD_{600}. Protein samples were also mixed in 800 µl dH_2O and 200 µl Bradford in the same way and the OD_{600} was measured. The value was multiplied by 10 which then reflected the protein concentration in µg / µl.

2.3.6 Co-Immunoprecipitation (Co-IP)

An Immunoprecipitation (IP) is a method, where a specific protein is precipitated out of a protein lysate. This is achieved by adding an antibody, which binds its antigen within this lysate. Under physiological conditions (e.g. pH of lysis buffer) protein-protein interactions remain intact. It is thereby possible to detect binding partners in Western blots after a Co-Immunoprecipitation (Co-IP) (Wodarz, 2008).

For an IP it is important in which species the antibody was raised. The reason for this is that the immunoglobulin domains of the antibodies show different affinities for the protein A/G agarose/sepharose beads (see Table 12 for different affinities). Furthermore it is important that the possible protein binding partner is bigger than 60 kDa in size or smaller than 50 kDa, if the antibody against this protein is raised in the same animal species. The secondary antibody used

for Western blotting is targeted against the immunoglobulin domains of the animal species, which does not allow to detect a protein of about 55 kDa, if the antibody used in the IP was from the same animal species. In this case a possible interaction would not be detectable, because the signal of the immunoglobulin domains would interfere.

Table 12: Affinities of protein A/G agarose for different immunoglobulins

species	protein A	protein B
rat	+ / -	++
mouse	++	++
rabbit	++++	+++
guinea pig	++++	++

For a Co-IP 1000 – 2000 µg of total protein were used in a volume of 500 – 1000 µl. An input sample of 25 µg was taken for control. The lysate was preincubated with 20 µl of the respective protein A or G agarose beads to get rid of unspecific binding proteins within the lysate. After incubation at 4°C for 2 hours beads were centrifuged down for 1 min at 14.000 rpm at 4°C. The supernatant was transferred into a new microtube and the respective antibody was added. As a general rule 2 µl of serum antibodies were added or 1 µl of commercial ones (in the case of using hybridoma supernatant antibodies, 15 µl of beads were preincubated in 300 µl of the respective lysis buffer and 200 µl of the hybridoma antibody at 4°C for 2 hours; after centrifugation the preincubated beads with the bound antibody were given to the lysate) and incubated over night at 4°C.

15 µl of protein agarose beads were added and incubation at 4°C for 2 hours was carried out. Beads were subsequently centrifuged down at 6.000 rpm for 30 sec at 4°C and washed three times with the respective lysis buffer. The immunoprecipitated protein is coupled to the beads via its bound antibody and interaction partners are also remaining bound to the precipitated protein, if the physiological conditions were good. After denaturation of the protein agarose beads with 15 µl of 2x SDS loading buffer and concomitant separation via SDS-PAGE interaction partners can be detected in Western Blot.

2.4 Cellculture

2.4.1 Transfection of S2 Schneider cells with FuGENE HD transfection reagent

Transfection for Co-IP experiments were done always with 2 wells for each (co-) transfection. Two million cells were given into one well of a six well plate in 2 ml of S2 medium. Transfection mix for one well was prepared as followed: 96 µl of dH_2O containing 2 µg of the respective DNA construct(s) were mixed with 4 µl of FuGENE HD transfection reagent. The mixture was vortexed shortly and incubated for 15 min at room temperature. Transfection mix was given to the cells, the six well plate carefully swung to achieve equal distribution of the solution within the well. S2 cells were incubated at 25°C for 48 hours and transferred to a cell culture flask, containing 5 ml of fresh S2 medium. Cells were grown another 48 – 72 hours at 25°C before S2 cells were harvested.

2.5 Histology

2.5.1 Formaldehyde fixation of embryos

An overnight egg collection was transferred into a 15 mm Netwell (Corning Life Sciences, USA; 74 µm mesh size) and washed with dH_2O. Netwell was placed into a supplied 12 well plate and embryos were dechorionated in sodium hypochlorite for 1 – 2 min. After washing the embryos with dH_2O Netwell was held on top of a glass vial containing 4 ml heptane and was vigorously inverted. After embryos were transferred into the glass vials, 3 ml of fixing solution (4% formaldehyde in PBS) were added and fixation was performed for 18 min at room temperature while rotating. The fixing solution (lower phase) was removed, 3 ml of methanol added and embryos vortexed for 30 sec to remove the vitellin membrane. Embryos were transferred into a microtube and washed with methanol twice. Storage could be done at -20°C or staining was performed directly.

2.5.2 Formaldehyde fixation of larval tissue

L3 wandering stage larvae were selected and anaesthetized in PBS on ice. The posterior end was cut off by using a micro scissor and the larva subsequently inverted on a needle. Larvae were transferred into a microtube containing 885 µl PBS and 5 µl PBT. Fixation was started by adding 110 µl of 37% formaldehyde solution and was performed for 25 min on a rocking platform. Fixing solution was removed and staining was continued (see 2.5.4).

2.5.3 Heat fixation of embryos

An overnight egg collection was washed with dH_2O and dechorionized with 50% sodium hypochlorite solution for 5 min. Embryos were washed on a mesh with dH_2O and transferred with a brush into a glass vial containing boiling 1x Triton salt. The vial was subsequently shaken for 5 times and put into ice and filled up with cold 1x Triton salt solution. Buffer was removed using a plastic pipette and 3 ml of heptane and 3 ml of methanol were added. The glass vial was vortexed for 30 sec to remove the vitelline membrane. Embryos were transferred into a microtube and washed with methanol twice and were stored at -20°C for at least 2 hours before proceeding with the staining.

2.5.4 Immunofluorescence staining

Fixed embryos were washed 3 times with PBT for 20 min at room temperature on a rocking platform. PBT containing 5% NHS was given to the embryos for 30 min to block unspecific binding sites. The primary antibodies were given to the embryos in PBT containing 5% NHS and incubation took place at 4°C over night.

Embryos were washed 3 times with PBT for 20 min on a rocking platform. Secondary antibodies coupled with fluorescence markers were given to the embryos in a concentration of 1:200 in PBT containing 5% NHS. Incubation took place for 2 hours at room temperature. Afterwards embryos were washed another 3 times for 20 min in PBT. During the first washing step DAPI was added in a

concentration of 1:1000 for marking the DNA. Embryos were mounted in a drop of Mowiol and stored at 4°C.

Immunofluorescence staining of larval tissue was performed according to the protocol of embryo staining. F-actin staining was achieved by use of fluorochrome conjugated phalloidin, which was given to the secondary antibody solution in a dilution of 1:100. Phalloidin was placed into a fresh microtube to evaporate the methanol in which it is dissolved. PBT containing 5% NHS and the secondary antibodies were subsequently added.

2.5.5 Cuticle preparation

An overnight egg laying collection was taken and aged for another 24 hours to allow completion of embryonic development. Hatched larvae were removed from the apple juice agar plate, as well as embryos which did not possessed the respective genotype of interest (e.g. *CyO [twist::GFP]/ CyO [twist::GFP]*). Embryos were dechorionated in sodium hypochlorite, washed with dH_2O on a mesh and mounted with a drop of hoyers mountant. Incubation at 65°C was done overnight and the coverslip was fixed afterwards with nail polish on the slide.

2.5.6 Wing preparation

Flies of the respective genotype were put into 100% isopropanol, wings dissected and laid on top of a glass slide. After the isopropanol had evaporated, wings were mounted with a drop of Roti®-Histokitt (Carl Roth) and a coverslip.

2.5.7 Eye preparation

Flies of the respective genotype were collected and placed into 100% ethanol in a glass dish. Pictures of the eyes were taken from female flies with a Leica MZ 16 FA microscope and size

measurements were performed using the supplied scale bar from anterior to posterior as well as from dorsal to ventral. Data were examined using Microsoft Excel.

3 Results

3.1 Baz binds to Smash *in vivo*

A yeast two-hybrid screen conducted by Ramrath, 2002 revealed that Baz might be a potential interactor of the gene product of *smash.* To follow up on this finding, baits were used encoding for either the region containing all three PDZ domains or for the regions containing PDZ 1 and 2 or PDZ 2 and 3 of Baz, respectively. The C-terminal part of Smash, exhibiting a LIM domain and a class I PDZ binding motif (S/T $X^{\ddagger}\Phi^{\S}$ -COOH) (Harris and Lim, 2001) was identified as prey (Fig.12).

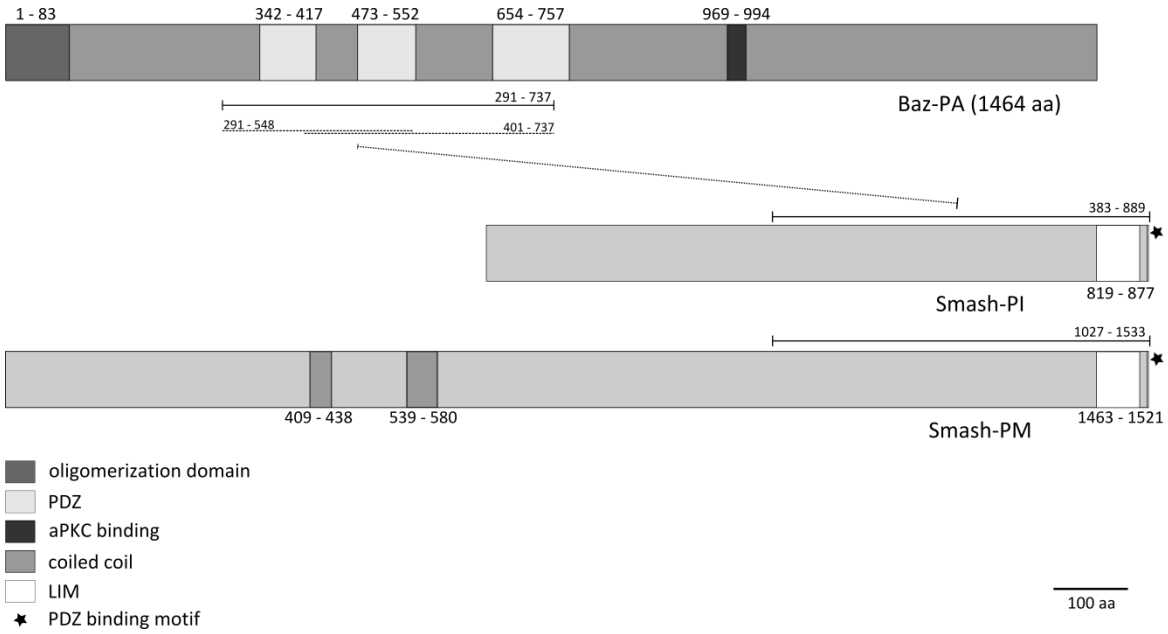

Fig.12: Yeast two-hybrid screen with PDZ domains of Baz as bait

The gene product of *smash* was identified in a yeast two-hybrid screen as a potential interactor of Baz. Bars and dashed bars indicate the region of the proteins, which were used in this screen. The PDZ containing bait constructs were generated based upon the predicted PDZ domains at this time. In this scheme, a current domain prediction by the smart server (http://smart.embl-heidelberg.de/) was used for the PDZ domains. The oligomerization domain and the aPKC binding site are adapted from Benton and Johnston, 2003. Furthermore, the short isoform Smash-PI as well as the larger isoform Smash-PM are indicated.

The subcellular localization shown in (Fig.13 A) shows colocalization of Smash and Baz in the region of the AJs in embryonic ectodermal epithelium. A physical interaction was already shown (Beati, 2009) but has been repeated in this work. Embryonic lysate was used for Co-IP experiments, which expressed an N-terminally GFP tagged version of Smash-PI under control of an UASt promotor with *daughterless* (*da*) *Gal4*. Baz was immunoprecipitated and GFP-Smash-PI detected in Western blot (Fig.13 B). These results show that Baz and Smash are showing the same subcellular localization in ectodermal epithelia and that they form a complex *in vivo*.

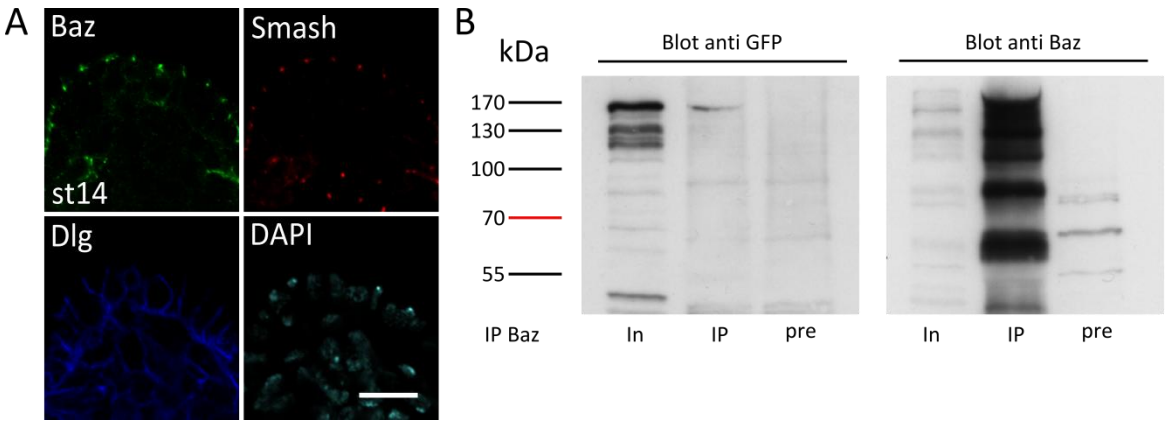

Fig.13: Smash colocalizes with Baz and binds to *in vivo*

(A) Staining for endogenous Smash protein (red) shows clear colocalization with Baz (green) in the region of the AJs. The lateral membrane domain is marked with staining for Dlg (blue). DNA is stained with DAPI. Scalebar = 10 µm. (B) *da* > GFP-Smash-PI. Co-IP experiments show that GFP-Smash-PI protein is detectable by Western blot after IP of Baz from embryonic lysates. Co-IP experiment represents result of three independent experiments.

3.2 Expression pattern of *smash*

To examine the expression of *smash*, two different antibodies were generated against recombinant GST fusion proteins. One antibody was raised against an intramolecular region of the short isoform Smash-PI (amino acids 328 – 634 of Smash-PI; 972 – 1278 of Smash-PM respectively) in rabbit. This anti-Smash intra antibody showed apical staining of ectodermal epithelia (Neugebauer, 2007), as well as expression in the trachea, where it strongly marks the

dorsal trunk and the dorsal branches (see Fig.14 B). However, this antibody does not work well and harsh fixation methods are necessary (e.g. heat fixation).

While this work was in progress the gene annotation release 5.40 indicated that the neighboring gene *CG31531* located upstream of the *CG31534* gene locus represents a single gene together with *CG31534*, now annotated as *CG43427* (see 1.5 and Fig.17 B). By PCR, using embryonic cDNA as template, it was possible to amplify an overlapping fragment of both coding sequences, confirming the reannotation of these two invidual genetic loci into a single molecular unit (data not shown).

We therefore raised another antibody in guinea pigs against the first 300 amino acids of the very N-terminus of the full length protein (see Fig.14 A).The anti-Smash N-term antibody works with standard formaldehyde fixation and shows that Smash protein is detectable after cellularization of the embryo present from stage 5 onwards throughout embryogenesis (see Fig.14 B). It is localized cortically at the membrane in a honey comb pattern, similar to Baz. Cross section images of the epithelium clearly show subcellular colocalization with Baz in the region were the AJs are located (see Fig.15). The same subcellular localization was also observed when an N-terminally HA tagged version of Smash-PI was expressed (Beati, 2009).

It was also apparent that Smash protein is strongly expressed in the amnioserosa in contrast to Baz which is barely detectable there. Furthermore, Smash accumulated at the dorsal side of the leading edge cells in a planar polarized fashion, where Baz is excluded from the cortex (see Fig.15 C and E and Laplante and Nilson, 2011). These results may indicate that membrane localization of Smash is independent of Baz. Furthermore high levels of Smash were detected in the developing hindgut, which was shown previously by RNA *in situ* hybridization (Ramrath, 2002).

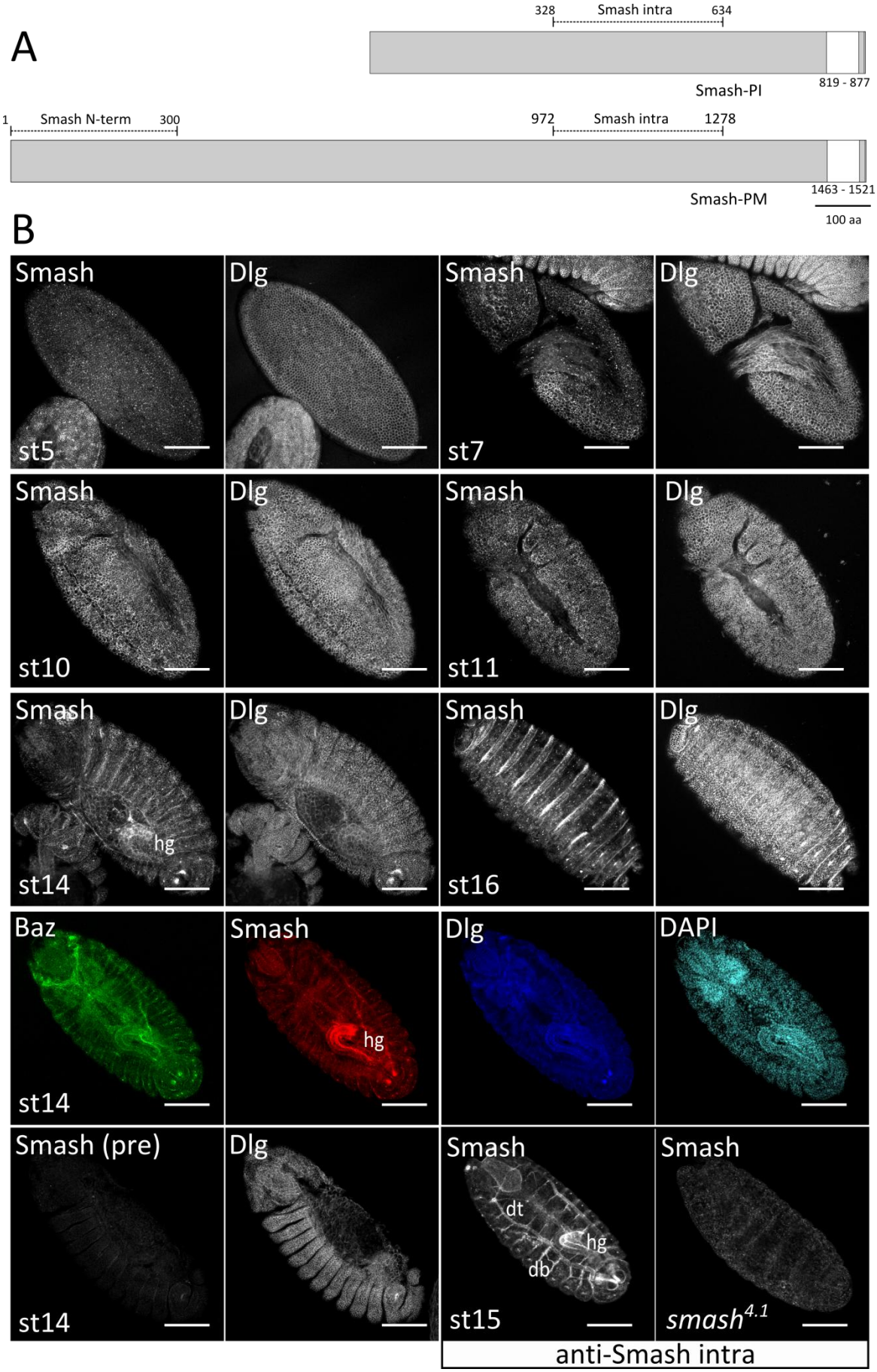
A
328
Smash intra
634
819 - 877
Smash-PI
1
Smash N-term
300
972
Smash intra
1278
1463 - 1521
Smash-PM
100 aa
B
Smash
Dlg
st5
st7
st10
st11
hg
st14
st16
Baz
DAPI
Smash (pre)
dt
db
st15
smash4.1
anti-Smash intra

Fig.14: Embryonic expression pattern of *smash*

(A) Scheme indicates regions of Smash which were used for antibody production. (B) Expression pattern analysis using anti-Smash N-term antibody revealed that Smash is detectable throughout embryogenesis after cellularization is completed. Note that from stage 14 onwards Smash protein accumulates in a stripe like pattern, which reflects the structure of the denticle belts. The staining against Smash is specific, as preimmune serum does not show signal (pre). Denticle belt staining is also observed with the anti-Smash intra antibody. This antibody shows that Smash is present in the tracheal system, where it strongly marks the dorsal trunk (dt) and the dorsal branches (db). Staining with this antibody is lost in the mutant *smash*$^{4.1}$. Scalebar = 100 µm, embryos are positioned from anterior to posterior.

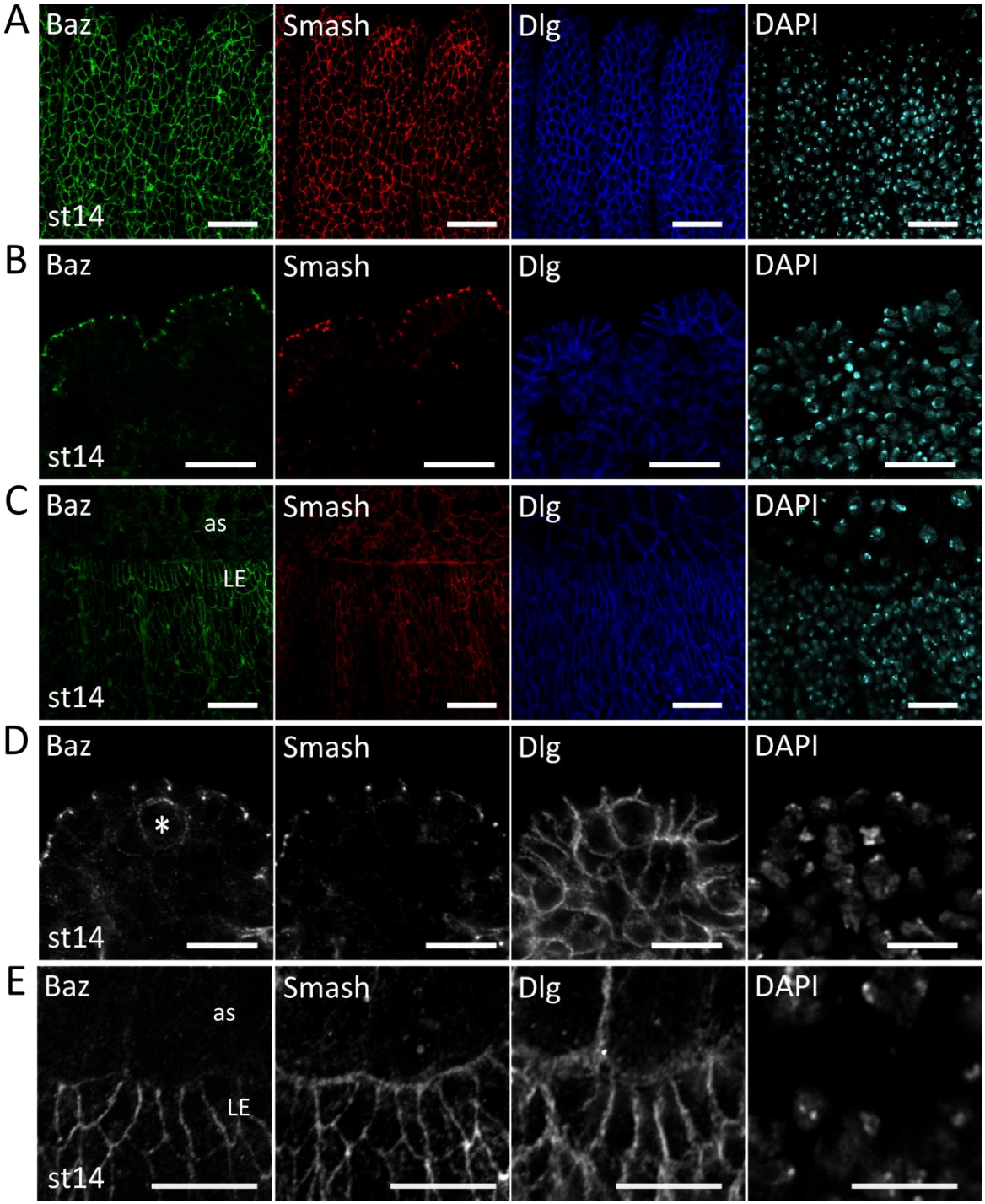
A
Baz
Smash
Dlg
DAPI
st14
B
Baz
Smash
Dlg
DAPI
st14
C
Baz
as
LE
Smash
Dlg
DAPI
st14
D
Baz
*
Smash
Dlg
DAPI
st14
E
Baz
as
LE
Smash
Dlg
DAPI
st14

Fig.15: Subcellular localization of Smash

(A) Surface projection of embryonic epithelium showing membrane localization of Smash (red). (B) In a cross section through the epithelium it is obvious that Smash is localized at the apical tip of the lateral membrane, where the AJs are located and shows colocalization with Baz (green). Dlg was used as a marker for the lateral membrane (blue). (C) High levels of Smash protein can be detected at the dorsal side of leading edge cells (LE). Baz was barely detectable in the amnioserosa cells (as), whereas Smash shows higher expression levels. (D) Smash localization at the AJs shown at a higher magnification. Smash is not expressed in embryonic NBs (marked with asterisk). (E) Higher magnification of leading edge cells shows that Baz is excluded from the dorsal membrane, whereas Smash accumulates dorsally in these cells. Scalebars represent 20 µm in (A - C) and 10 µm in (D and E) respectively.

Using the UAS/Gal4 system, an N-terminal GFP tagged version of isoform Smash-PM, encoding two additional coiled coil domains in its N-terminal part compared to the shorter isoform Smash-PI (see 1.5 and Fig.12), could be shown to localize to the region of the AJs like the shorter fragment. This shorter isoform also showed a comparatively stronger cytosolic localization compared to the larger isoform (see Fig.16 A). Additionally, using an *actin > CD2 > Gal4* flip out line, GFP-Smash-PI was found in the nucleus of fat body cells, and the larger isoform GFP-Smash-PM localized cortically as well as to a region adjacent to the nuclear envelope (see Fig.16 B). However, the latter localization could not be shown with the antibodies raised against endogenous Smash protein (data not shown).

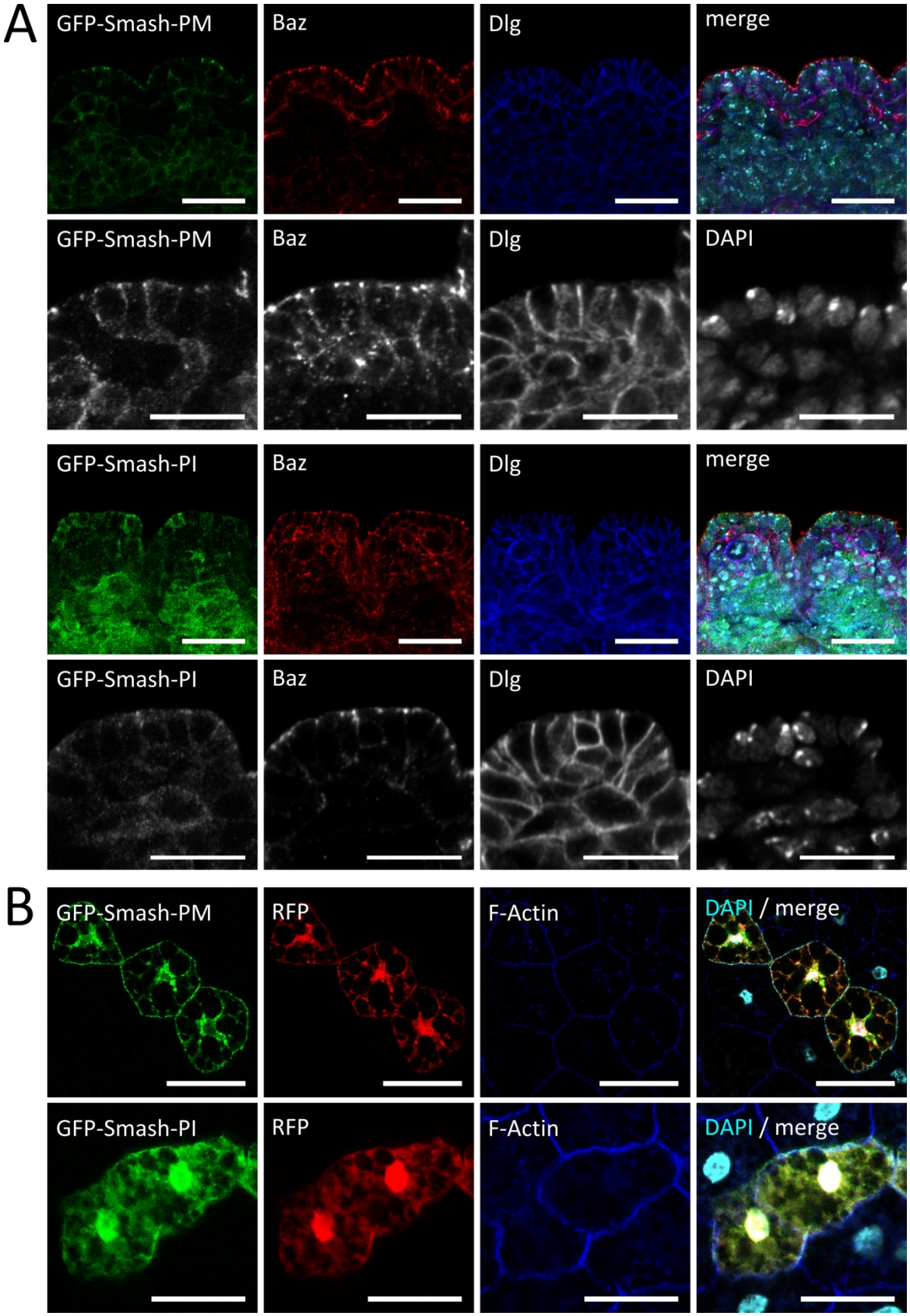
A
GFP-Smash-PM
Baz
Dlg
merge
GFP-Smash-PM
Baz
Dlg
DAPI
GFP-Smash-PI
Baz
Dlg
merge
GFP-Smash-PI
Baz
Dlg
DAPI
B
GFP-Smash-PM
RFP
F-Actin
DAPI / merge
GFP-Smash-PI
RFP
F-Actin
DAPI / merge

Fig.16: Subcellular localization of Smash transgenes

Localization of N-terminally GFP tagged versions of Smash-PM and -PI. (A) Transgenes, carrying UASp promoters inserted on the 2nd Chromosome at position 22A, expressed with *da Gal4*. Both proteins had been detected at the AJs, although GFP-Smash-PM showed much stronger apical localization compared to the short isoform GFP-Smash-PI. Lower panels show higher magnification of subcellular localizations. Scalebars represent 20 µm and 10 µm respectively. (B) Expression clones of N-terminally GFP tagged versions of Smash-PM and -PI in fat body cells with an *actin > CD2 > Gal4*, *UAS RFP* flip out line. GFP-Smash-PM was found at the cell cortex but showed localization to a region surrounding the nucleus as well. However, the short isoform was strongly localized to the nucleus. Scalebar = 50 µm.

3.3 *smallish* knockout

In order to study the *in vivo* function of *smash*, a knockout allele was generated for the former annotated gene *CG31534* by transdeletion. Two FRT site containing piggyBac elements in *trans* were recombined upon activation of a Flipase (Thibault et al., 2004). This led to deletion of the genomic region present between both FRT sites. According to the reannotated genetic model, this allele reflects a C-terminal truncation and therefore cannot be considered a classical null allele, because it may still expresses the upstream region of the gene (see Fig.17 A). It therefore could retain some function or furthermore cause dominant negative effects.

A full knockout allele was generated by a second transdeletion using two FRT-containing piggyBac elements flanking the whole genomic region of *smash* (see Fig.17 B). Successful deletions were confirmed by PCR (see Fig.18 B and C) and loss of antibody staining (see Fig.14 and Fig.20 A). Both mutations $smash^{4.1}$ as well as the new allele $smash^{35}$ are homozygous viable, fertile and can be kept as homozygous stocks.

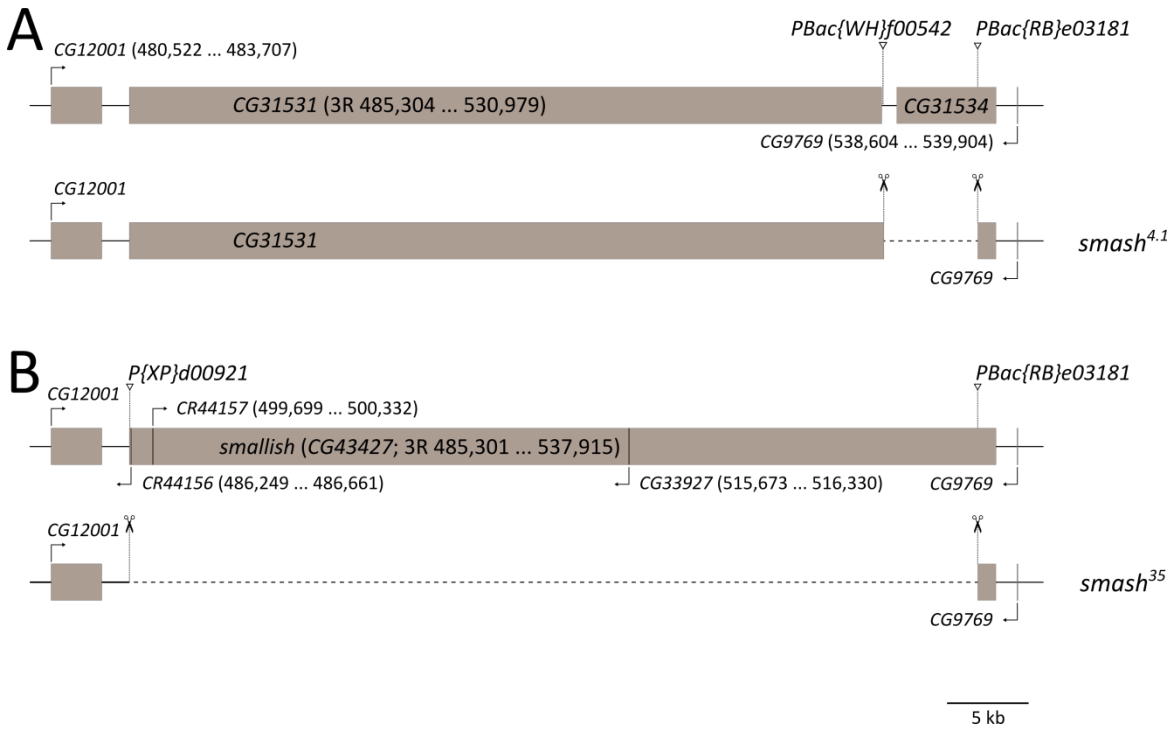

Fig.17: Transdeletion of the genomic locus of *smallish*

By using two different FRT containing piggyBac lines in *trans* it was possible to delete genomic DNA, which was lying in between these FRT sites. (A) Genomic locus of the gene annotation releases 3.0 (2002) and 3.1 (2003). *CG31531* is located upstream of the gene *CG31534* (531,867 - 537,915). Position of piggyBac elements is indicated (see Fig.18 for structure of piggyBac elements). Transdeletion led to a precise knockout of *CG31534*. (B) Genomic locus according to the gene annotation release 5.40. *smallish (CG43427)* reflects the genomic locus of the fusion between *CG31531* and *CG31534*. Three new genes were annotated, *CR44156* and *CR44157*, as well as *CG33927*, which were also deleted by the new knockout. P{XP} and piggyBac positions are indicated in the upper panel.

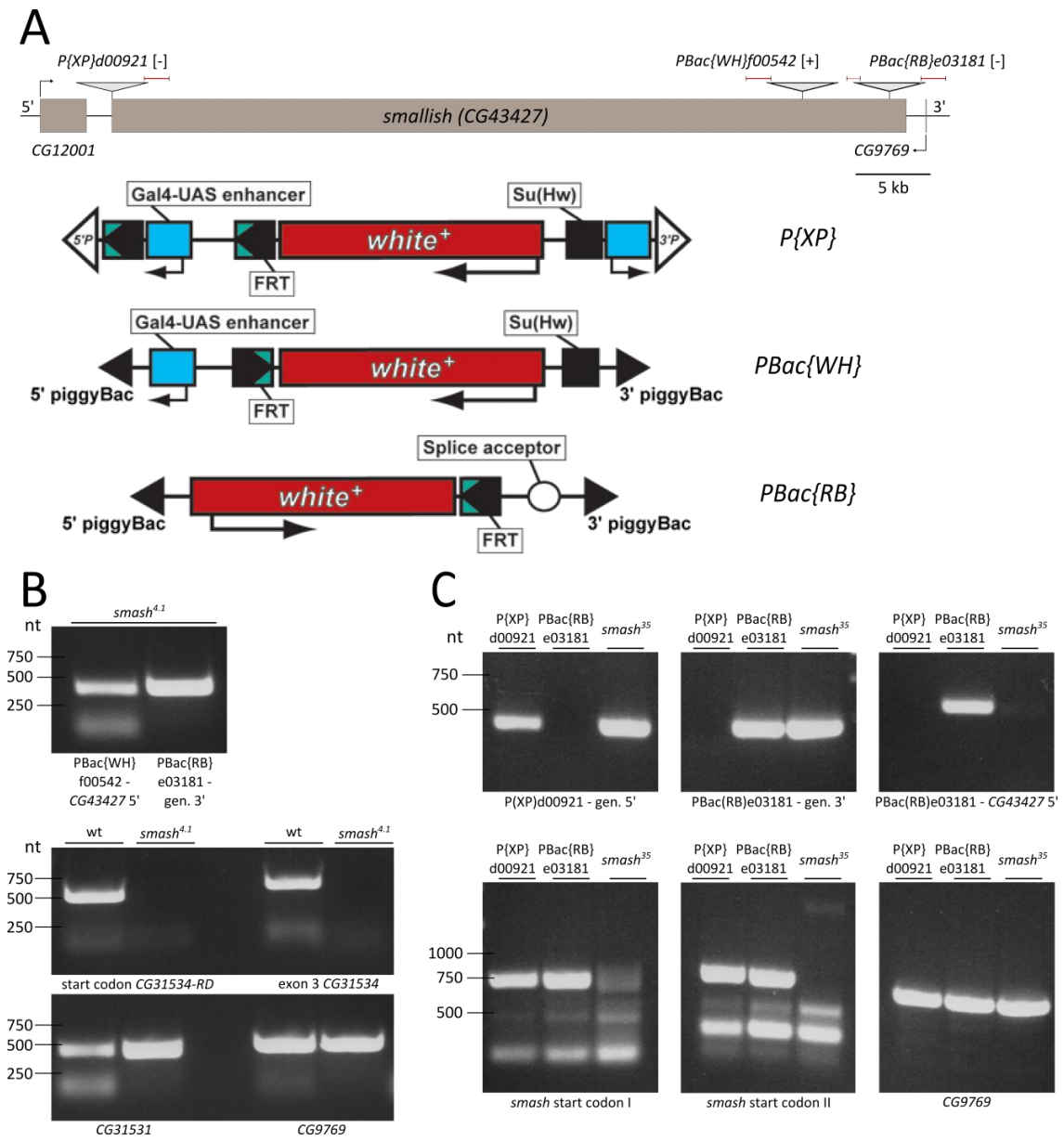

Fig.18: Verification of *smash* knockout

Mutant alleles for *smash* were verified by PCR on genomic DNA isolated from homozygous flies. (B) *smash*$^{4.1}$ and (C) *smash*^{35}. After transdeletion both alleles were screened for their ability to amplify DNA corresponding to overlapping fragments from the piggyBac elements into the respective genomic regions. (A) Scheme indicates overlapping PCR fragments with regard to the piggyBac elements (PCR fragments are marked in red; size of piggyBac elements and PCR products does not reflect real length). Amplification of both fragments corresponding to the overlapping fragments indicated successful transdeletion. This could be shown for both mutant alleles. PCRs on genomic DNA of the deleted regions showed a loss of the respective fragments (regions are not marked in the scheme). Structure of the piggyBac elements used is shown in (A) and was taken from http://flypush.imgen.bcm.tmc.edu/pscreen/transposons.html. Direction of insertion is indicated in the scheme with a [+] or [-] respectively.

Lethality was examined for F1 and F2 generations, as well as after shifting the temperature to 29°C from 25°C. One observation was that approximately 40% of mutant embryos die during embryogenesis, either in the F1 or F2 generation. However, lethality after embryogenesis was slightly increased in the F2 generation where about 25% of flies eclosed in contrast to approximately 40% in F1. Shifting the temperature to 29°C increased lethality strongly. For the individual lethality tests see Fig.19.

A

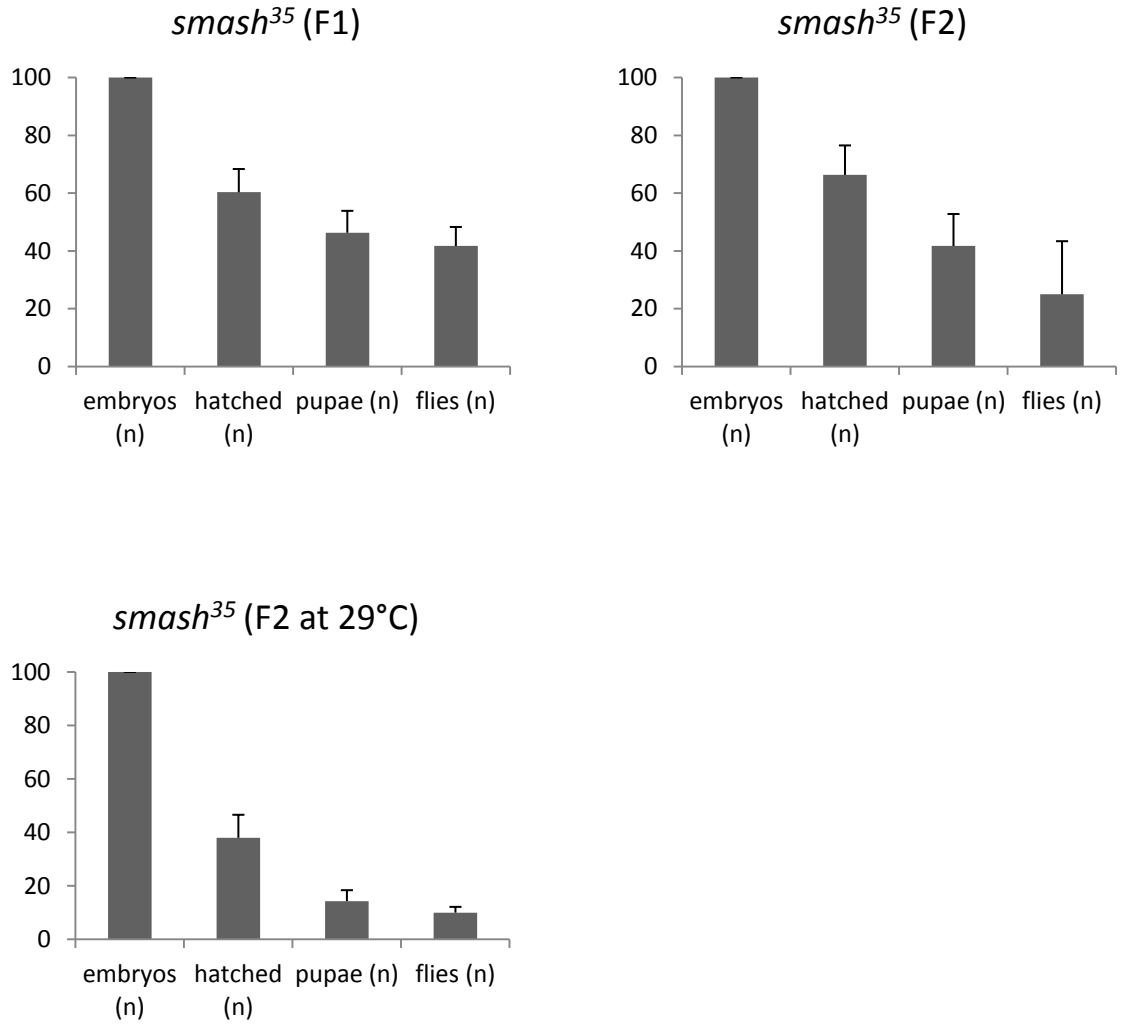

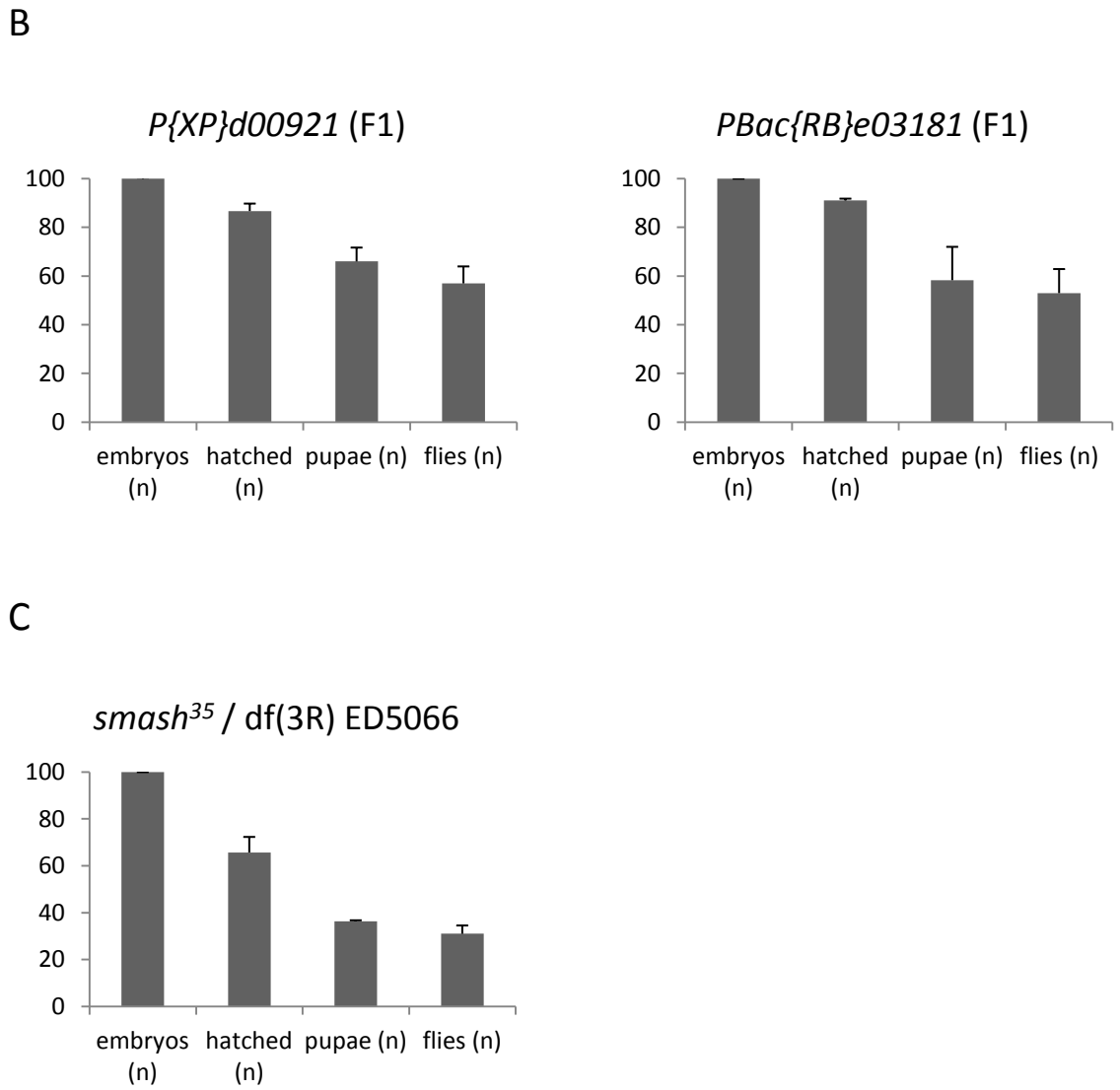

Fig.19: Lethalities shown for *smallish* knockout

Lethality scores obtained for *smash*^{35}. (A) Lethality score for *smash*^{35} homozygous mutant embryos either in the F1 or F2 generation and after temperature shift to 29°C. (B) Lethality score for the P-element lines used for the transdeletion. (C) Complementation test of *smash*^{35} with deficiency line df(3R) ED5066 showing nearly the same lethality score as *smash*^{35} in (A). Data were obtained repeating the experiment three times, error bars indicate standard error.

Due to the fact that both mutant alleles generated for *smash* are homozygous viable, mislocalization of its binding partner Baz was not excpected. Mutations in the *baz* gene reported so far are lethal (see 1.1 and 1.5). Staining for Baz in embryos mutant for either *smash*^{35} or *smash*$^{4.1}$ showed that Baz is localized to the apical membrane. Furthermore, DE-Cad, an integral component of the AJs, also showed normal localization (see Fig.20).

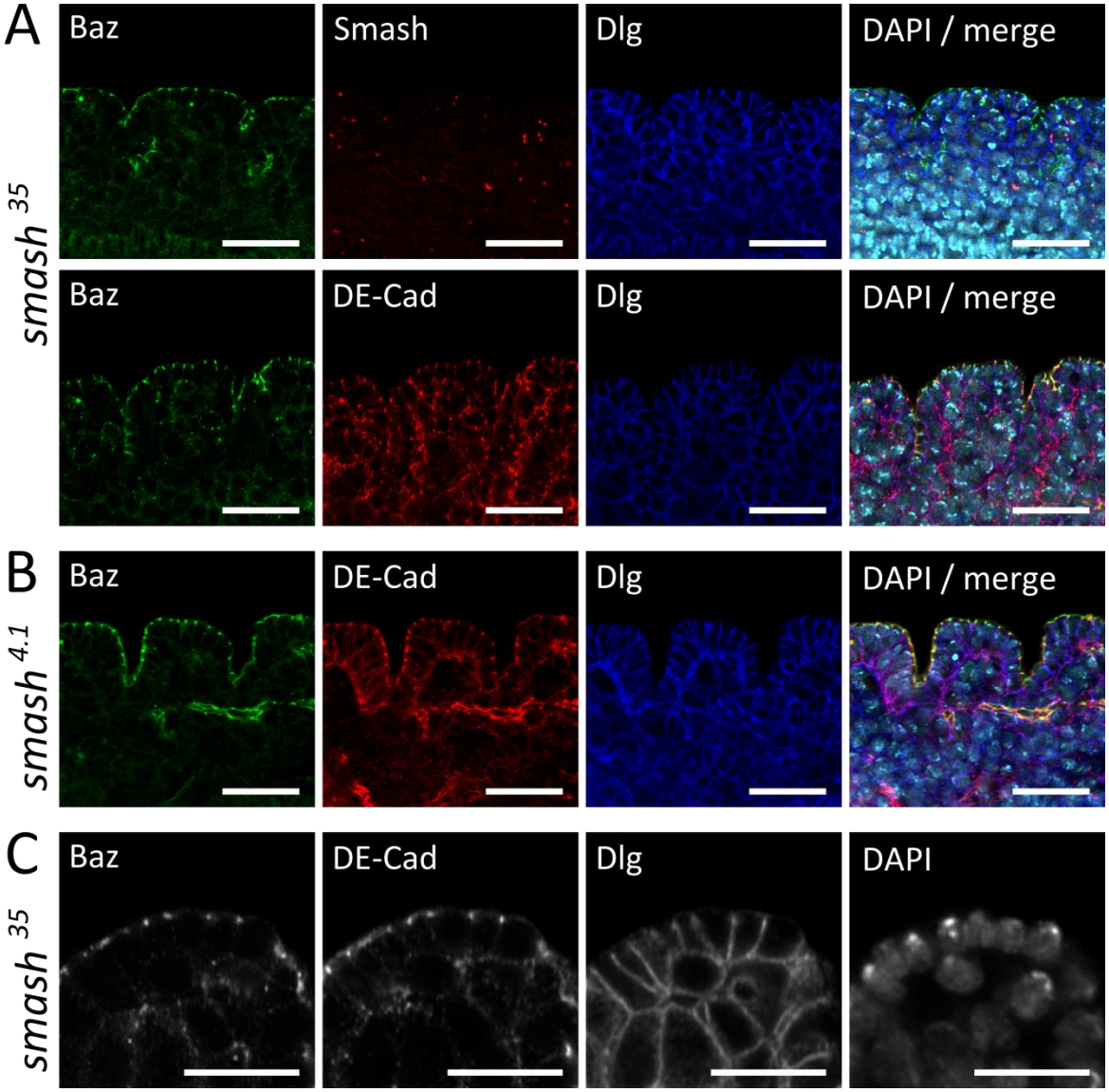

Fig.20: Epithelial integrity is not lost upon *smash* knockout

(A) Staining for Smash (anti-Smash N-term) is lost in the full knockout allele *smash*^{35} (shown in upper panel in red), compare with Fig.13 A and Fig.15 B. Baz localization is not affected (green), lateral membrane is marked by staining against Dlg (blue). DE-Cad protein localizes apically to the AJs (shown in lower panel in red). (B) Staining for Baz (green) and DE-Cad (red) in the truncated knockout shows correct localization of both proteins. Lateral membrane was marked with staining against Dlg (blue). (C) Higher magnification of Baz and DE-Cad localization in *smash*^{35} mutant embryos. Scalebars represent 20 µm in (A and B) and 10 µm in (C) respectively.

Examining protein levels of Baz, DE-Cad and Arm by Western Blot using embryonic lysates of *smash*^{35} mutants could not show any change in their expression (see Fig.21). It was also tested whether a change in protein levels could be observed when the N-terminal GFP tagged isoform GFP-Smash-PM was overexpressed. No change in the expression levels of the respective protein markers was detectable in Western blot.

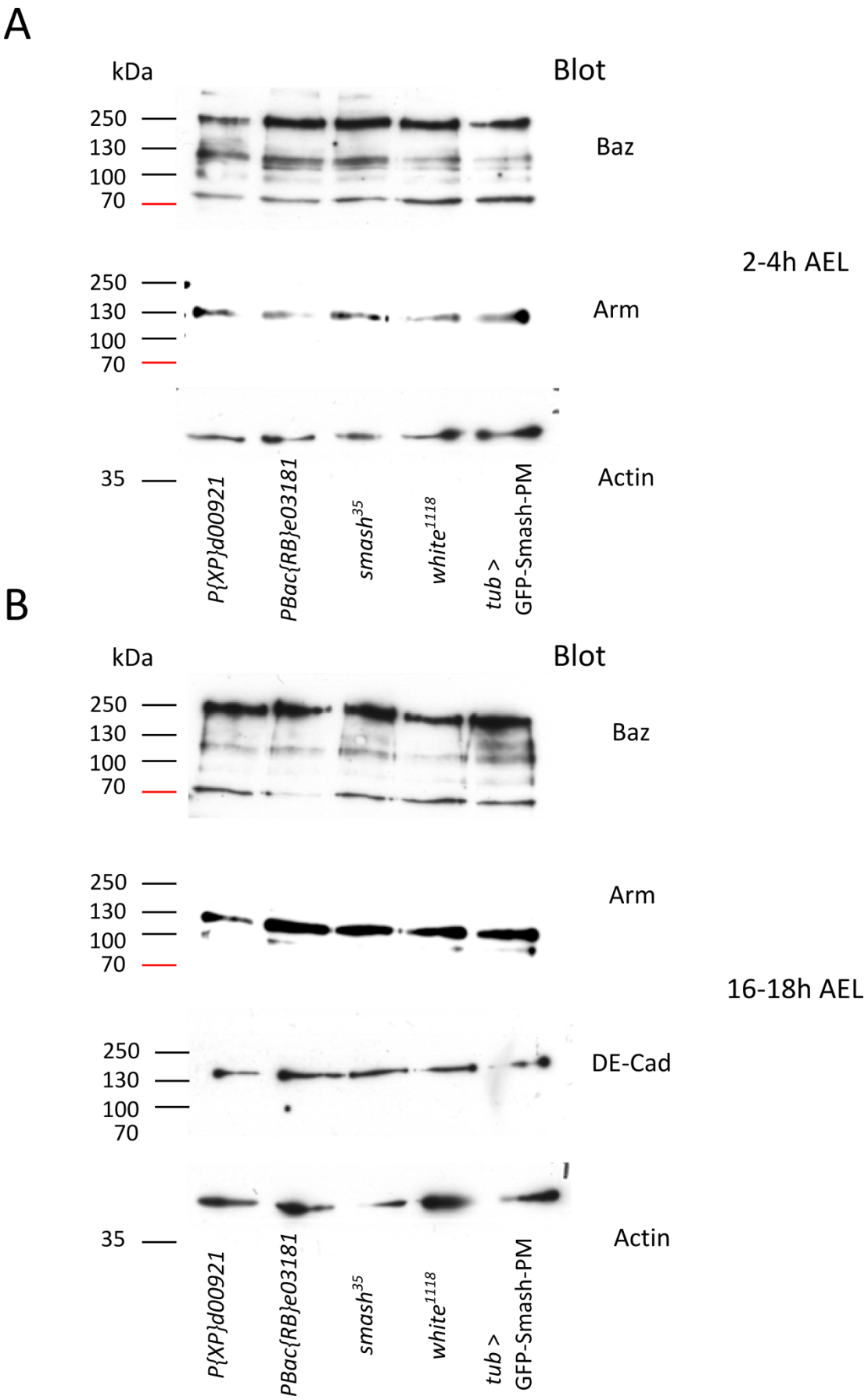
A
kDa
Blot
250
130
100
70
Baz
2-4h AEL
250
130
100
70
Arm
35
Actin
P{XP}d00921
PBac{RB}e03181
smash35
white1118
tub > GFP-Smash-PM
B
kDa
Blot
250
130
100
70
Baz
250
130
100
70
Arm
16-18h AEL
250
130
100
70
DE-Cad
35
Actin
P{XP}d00921
PBac{RB}e03181
smash35
white1118
tub > GFP-Smash-PM

Fig.21: Protein levels of AJ and polarity markers in *smash* mutants

To examine expression levels of AJ and polarity markers in *smash* mutants, protein lysates from *smash*^{35} homozygous mutant embryos were Western blotted and Baz, DE-Cad and Arm protein levels examined using respective antibodies. (A) Embryo collection staged 2-4h AEL and (B) embryo collection staged 16-18h AEL. As controls, piggyBac lines used for the transdeletion as well as *white*^{1118} embryos were taken for comparison. Protein lysate from embryos overexpressing an N-terminal GFP tagged version of Smash-PM using *tub Gal4* was tested as well. No changes in protein levels were detectable. Anti-Smash N-term antibody was not used, due to its background. This experiment was repeated three times, Actin is shown as a loading control.

3.4 Overexpression of Smash

As shown in the previous chapter, *smash* gene function is not crucial for embryonic development, nor for the survival of the adult fly (see Fig.19). In contrast to this finding, overexpression using *tub Gal4* (a strong driver line) and transgenic flies carrying transgenes for N-terminal GFP tagged versions of Smash-PI or Smash-PM under control of UASt promotors respectively, resulted in almost complete lethality. Overexpression of the short isoform GFP-Smash-PI did not lead to embryonic lethality, but increased larval and pupal lethality (see Fig.22 A). Rare escaper flies that hatched were strongly reduced in size (see Fig.23 A and B), a result also observed using *da Gal4,* but in a milder form (data not shown). In comparison, overexpression of the larger isoform GFP-Smash-PM resulted in high embryonic lethality, where almost 50% of embryos died before hatching (see Fig.22 B). Almost 25% of embryonic cuticles displayed anterior holes, up to 5% dorsal holes and approximately 5% showed both anterior and dorsal holes (see Fig.24). Hatched larvae died before pupation (see Fig.22 B). No adult flies expressing GFP-Smash-PM under the control of *tub Gal4* could be recovered. It was also tested whether adult flies expressing GFP-Smash-PM under the control of *tub Gal4* could be recovered at 18°C, where the efficiency of the UAS/Gal4 system is reduced compared to 25°C, however no escapers could be observed.

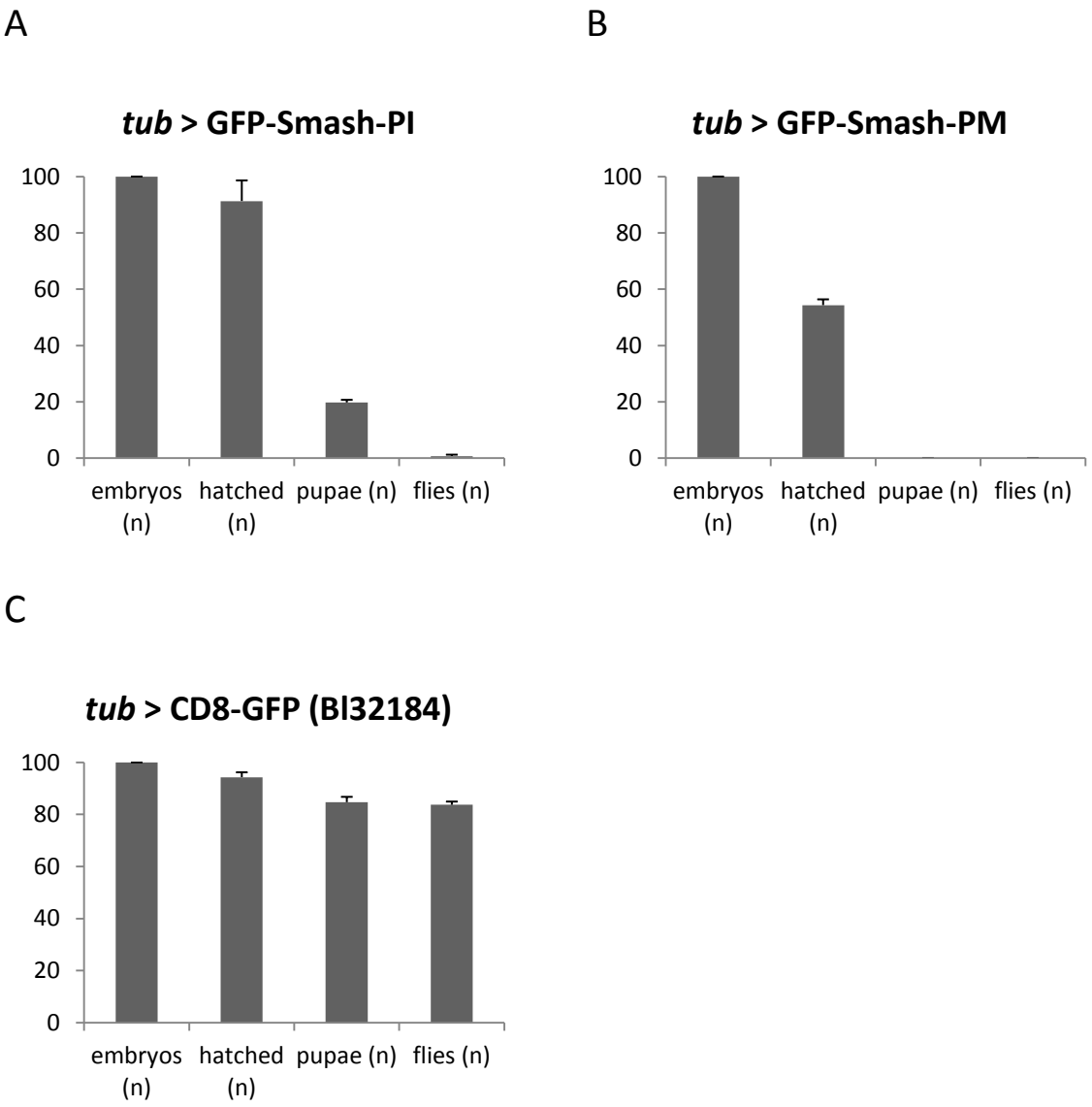

Fig.22: Lethality after overexpression of GFP-Smash epitopes

Lethality tests were conducted as mentioned before. *tub Gal4* was used as a driver line and GFP positive embryos were assayed. (A) Expression of an N-terminal GFP tagged short isoform Smash-PI leads to high larval and pupal lethality. Rare escapers are observed that are reduced in size. (B) Expression of the respective larger isoform Smash-PM, N-terminally tagged with GFP, leads to high levels of embryonic lethality. Hatched larvae died before pupation. (C) CD8-GFP expression was used as control. All experiments were repeated three times, error bars indicate the standard error.

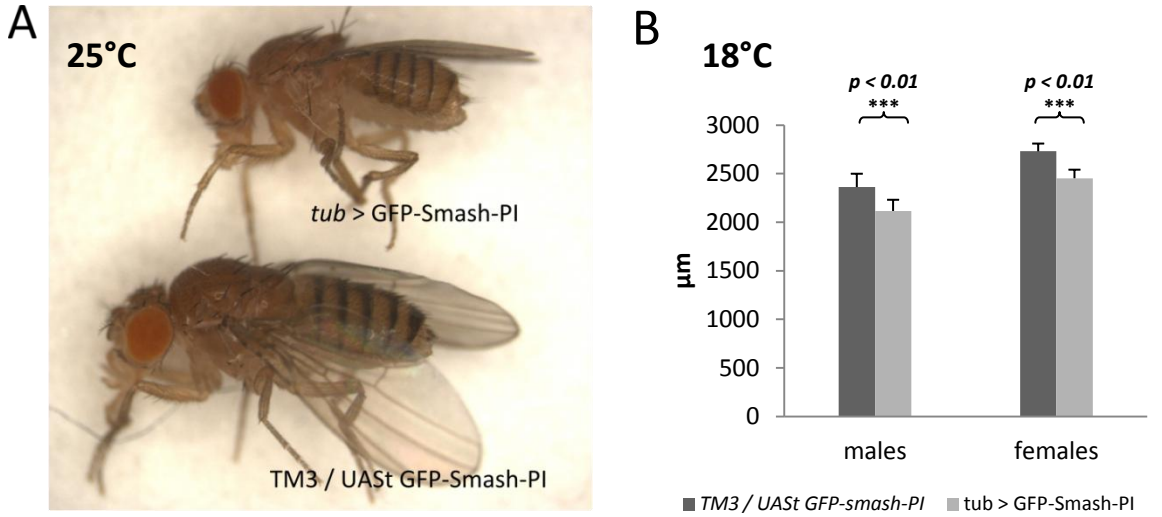

Fig.23: Size decrease upon GFP-Smash-PI expression

(A) Rare eclosing escaper flies strongly expressing GFP-Smash-PI under the control of *tub Gal4* show a strong reduction in their size (upper female fly in comparison with a sibling carrying TM3 balancer chromosome instead of *tub Gal4*). (B) Diagram showing the expression dependent size reduction of *tub* > GFP-Smash-PI flies. The data represents measurements of flies from anterior to posterior which had been raised at 18°C to obtain a sample size that was large enough to make a statistically relevant statement. Too few escaper flies emerged at 25°C to make a statistically significant conclusion. Size was measured with the supplied scale bar from Leica, error bars indicate standard error.

A

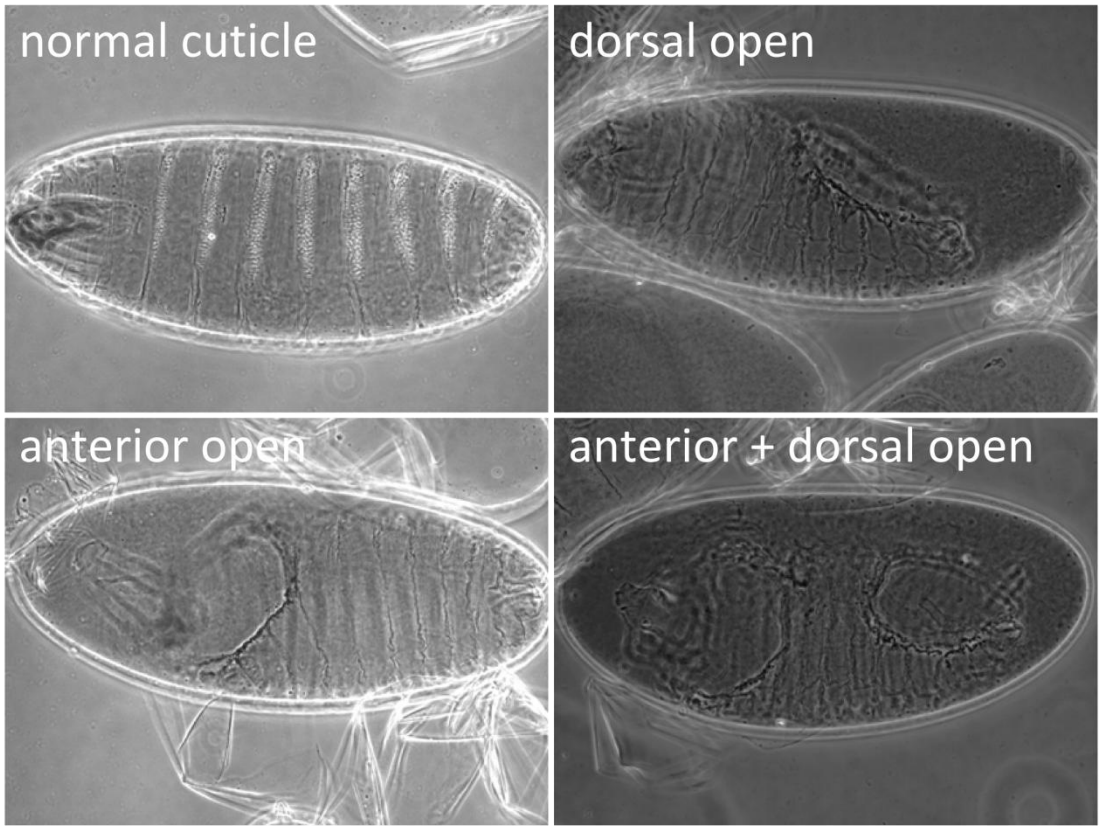
normal cuticle
dorsal open
anterior open
anterior + dorsal open

B

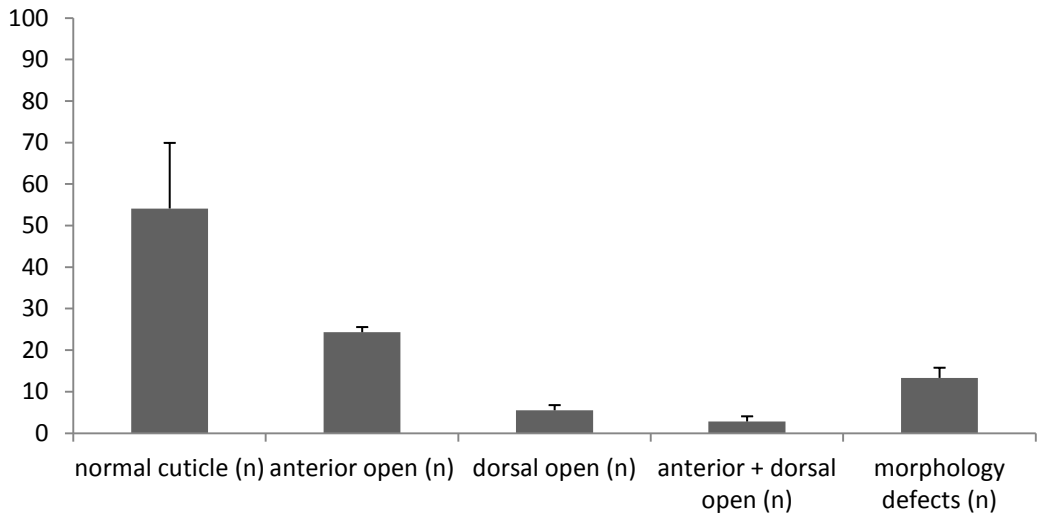
100
90
80
70
60
50
40
30
20
10
0
normal cuticle (n)
anterior open (n)
dorsal open (n)
anterior + dorsal open (n)
morphology defects (n)

Fig.24: Cuticle phenotypes observed after overexpression of GFP-Smash-PM

(A) Embryos overexpressing GFP-Smash-PM under the control of *tub Gal4* show variable cuticle phenotypes. Approximately 50% of cuticles examined displayed no obvious defects. A subset of approximately 25% showed an anterior hole phenotype, whereas 5% showed dorsal hole phenotypes. Moreover, another 5% showed both anterior and dorsal hole phenotypes. In total, approximately 35% of examined cultices showed combinations of these holes within the cuticle. Cuticles with other defects were also observed which could not be classified and were summarized as morphology defects. (B) Diagram showing statistical significance of phenotypes, which had been observed. Data were generated by repeating the cuticle preparation three times, error bars indicate standard error.

Overexpression of the large isoform Smash-PM in a striped pattern using *en Gal4* (see 2.2.13) showed that these cells remained smaller in their size. The total length of AJs and the apical surface area was significantly reduced (see Fig.26 B). Neighboring cells of GFP-Smash-PM expression stripes were reduced in size compared to non-expressing cells of control embryos. Smash might functions non cell autonomously and thereby shows an effect on neighboring cells as well. Furthermore staining for DE-Cad showed that there is a slight accumulation of the protein compared to non expressing cells (see Fig.25 A). This result indicates that Smash is probably involved in pathways controlling apical constriction, which is a common feature of epithelia undergoing morphogenesis (see 1.2). However, embryonic lysates from embryos expressing GFP-Smash-PM under the control of *tub Gal4* did not show any changes in total DE-Cad levels (see Fig.21 B).

Expressing the same transgene in imaginal wing discs did not lead to malformed wings. Here, *en Gal4* was used to drive expression in the posterior half of the wing, or *patched* (*ptc*) *Gal4*, which drives expression in an proximal/distal stripe (see Fig.27). *dpp Gal4* was also tested, which exhibits basically the same expression pattern as *ptc Gal4* which also did not show any effect on the wing shape (data not shown). Only wings from *tub Gal4* driven overexpression showed an overall size reduction which was expected given that the whole flies were reduced in size (see Fig.23 A).

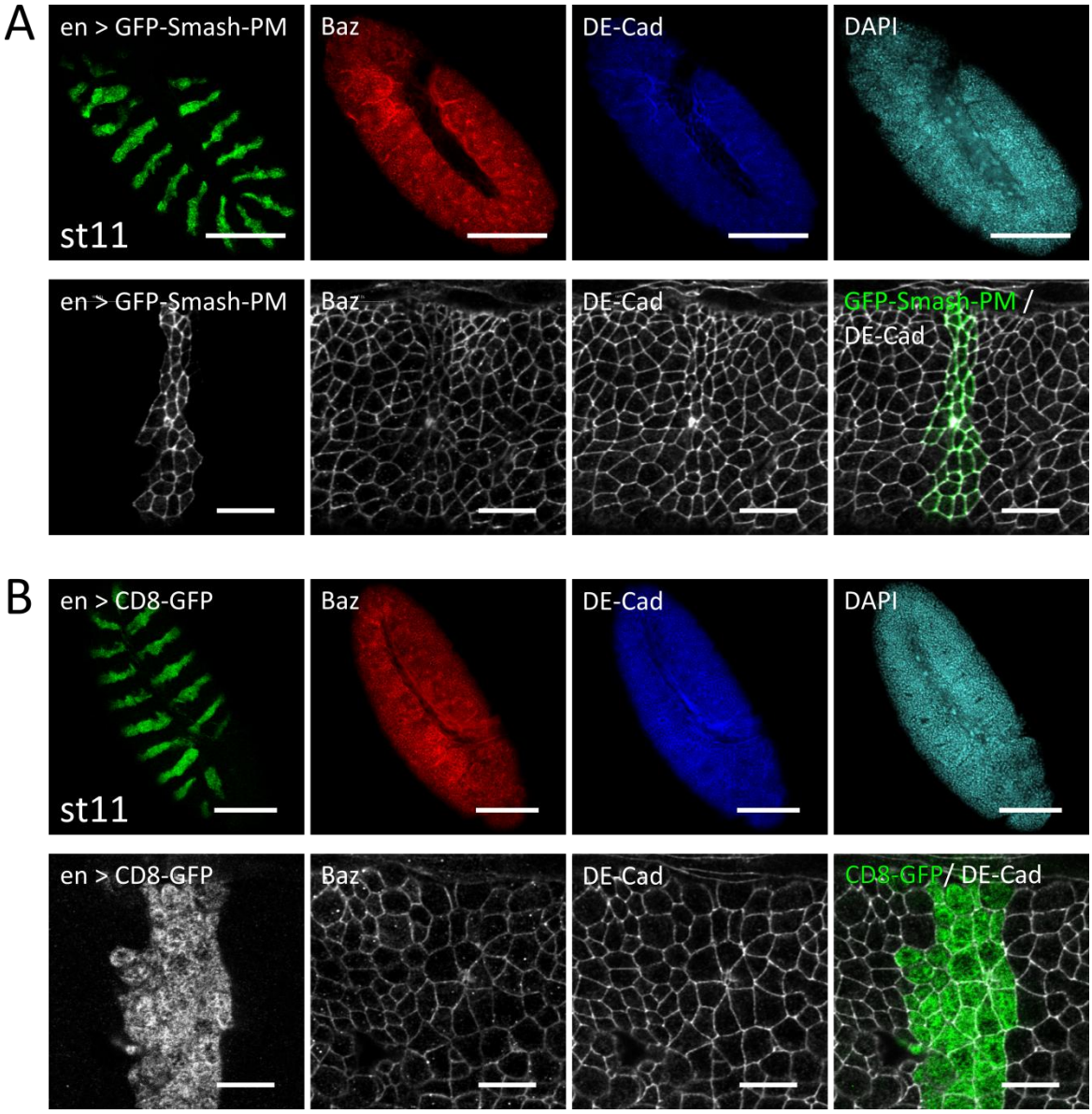

Fig.25: Overexpression of GFP-Smash-PM leads to cells smaller in size

Segmental expression of a *UASt GFP-smash-PM* transgene with *en Gal4* leads to a decrease in cell size. Expression of CD8-GFP in a striped pattern did not show any effect on cell size nor changes in protein levels of DE-Cad or Baz in stage 11 embryos (B). However, expression of an N-terminally GFP tagged version of Smash-PM caused those cells to remain smaller in size as compared to neighboring cells which did not express the transgene. Interestingly DE-Cad levels at the membrane appeared to be slightly increased (A). Scalebars =100 µm in the overviews and 10 µm in the respective magnification.

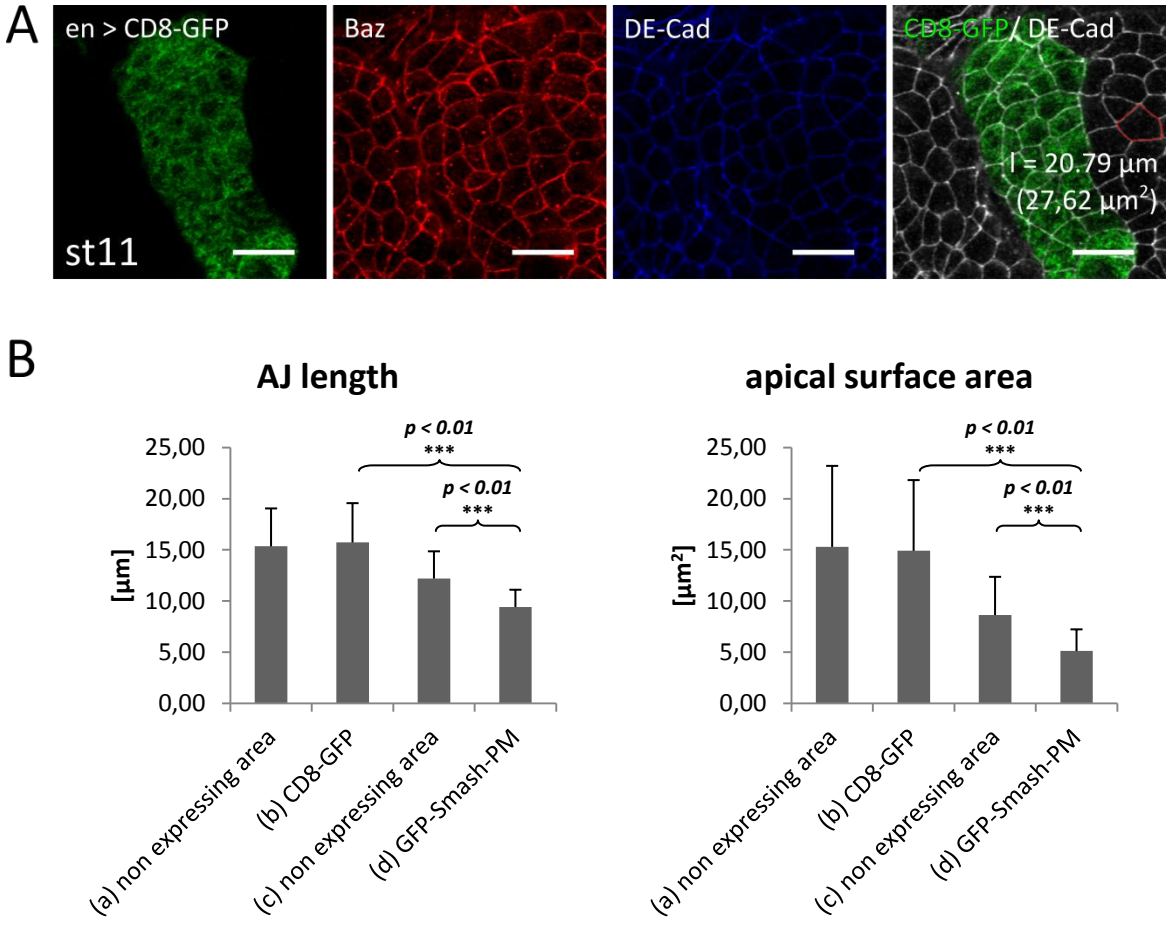

Fig.26: AJ length and apical surface area is reduced upon GFP-Smash-PM expression

Total length of AJs and apical membrane area was analyzed in *en Gal4* expression stripes. Area close to the end of the elongated germband of stage 11 embryos was chosen for analysis. (A) Example of how the length of AJs and the apical membrane area was determined. DE-Cad staining (blue and white in merge) was used to mark the AJs (red marked cell). LSM software provided respective AJs length in µm and apical surface area in μm^2. Scalebar = 10 µm. (B) AJs length and apical surface area is comparable in non expressing cells and *en Gal4* expressing CD8-GFP stripes. A significant reduction in AJs length was observed upon expression of GFP-Smash-PM. Apical surface area was strongly reduced compared to non expressing neighboring cells. However, non expressing cells of control embryos showed that AJs were longer as compared to non expressing cells of GFP-Smash-PM expressing embryos. Comparable observation was also made with regards to the apical surface area. This might indicate that Smash is functioning non cell autonomously. Error bars indicate standard error.

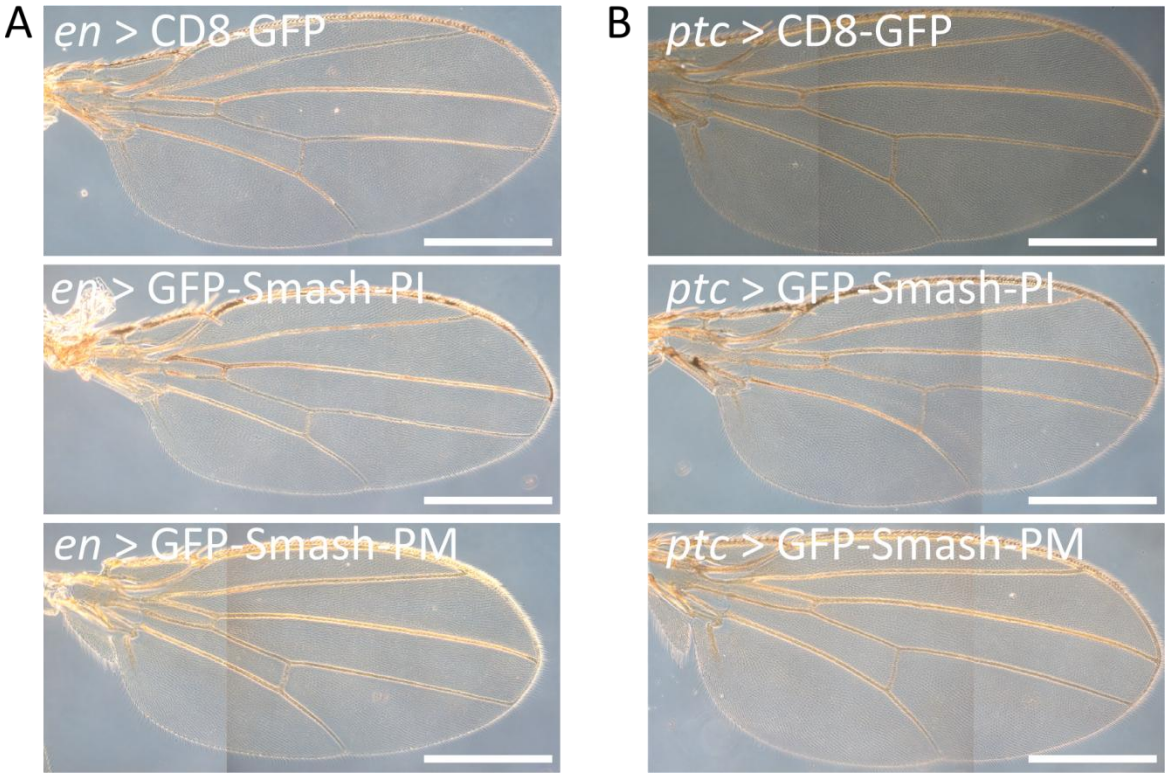

Fig.27: Expression of GFP-Smash-PM does not show an effect on wing shape

Using *en Gal4* as a driver allows specific expression of transgenes in the posterior compartment of the developing wing. (A) Expression of the N-terminal GFP tagged short isoform Smash-PI or the larger protein Smash-PM do not show effects on the wing shape. As control *UAS CD8-GFP* (Bl 32184) was used. (B) *ptc Gal4* used as a driver line, which expresses in a stripe from proximal to distal in the developing wing. No wing malformation had been observed. Scalebars = 500 µm.

Overexpression of these transgenes in the eye using *pGMR Gal4* as a driver resulted in a rough eye phenotype (see Fig.28 A). Eyes were furthermore reduced in their size in comparison to the transgenic lines without expression (see Fig.28 B). The rough eye phenotype was slightly enhanced by expressing two copies of the large isoform GFP-Smash-PM. The rough eye phenotype observed for Smash overexpression was also slightly apparent in the rare escapers using *tub Gal4* (data not shown).

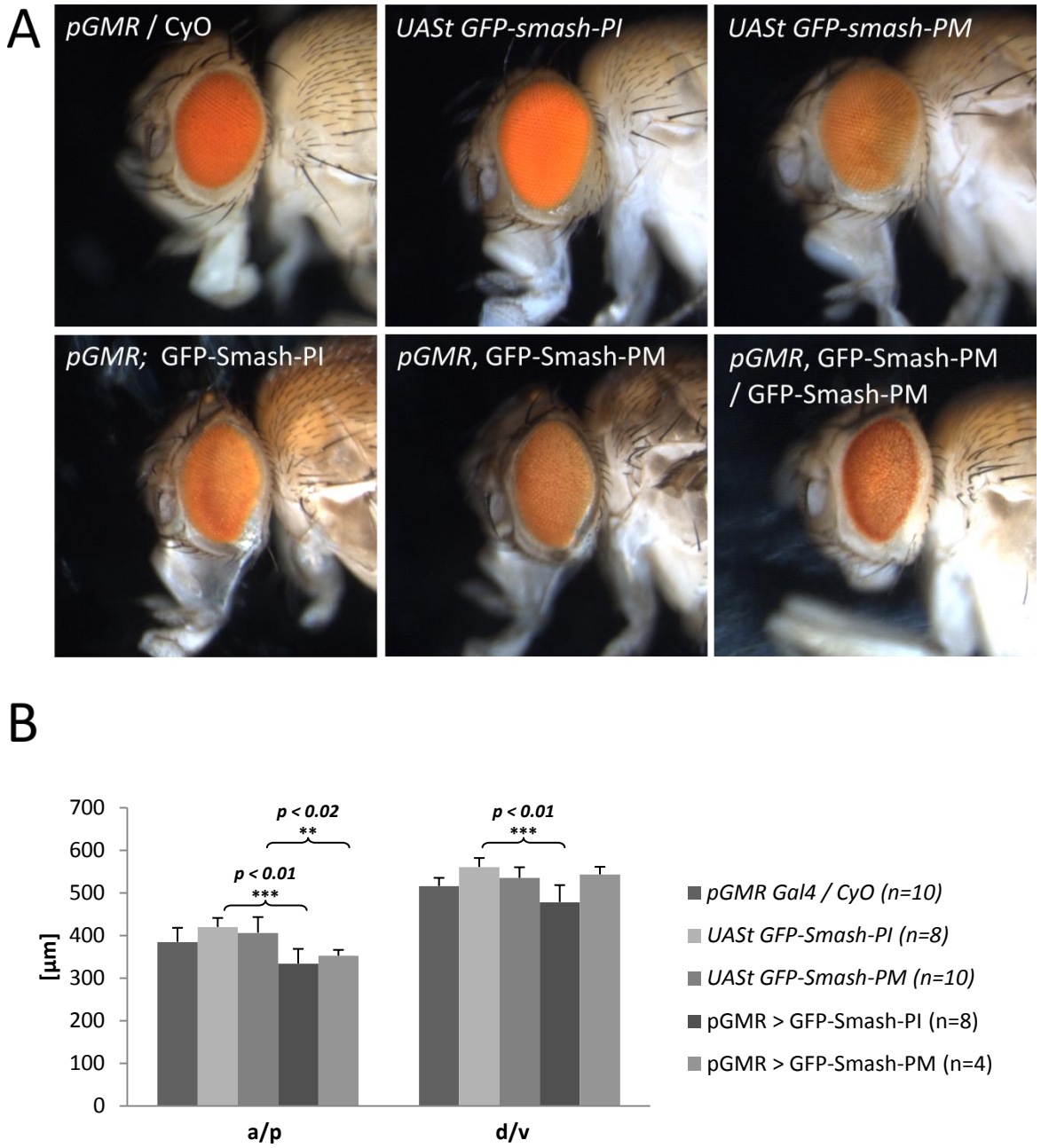

Fig.28: Eye restricted expression of Smash leads to rough eyes and size reduction

pGMR Gal4 driven expression of N-terminal GFP tagged versions of Smash. (A) Figures show results of expression of GFP-Smash-PI as well as GFP-Smash-PM in the eye. Upper panel shows respective transgenic lines and *pGMR Gal4*. *UASt GFP-smash-PM* line was recombined with *pGMR Gal4* and crossed against the *UASt GFP-smash-PM* line for expression of two copies of the transgene, which led to a slightly enhanced phenotype. (B) Diagram summarizes results of eye sizes. Measurements were performed for the anterior/posterior axis (a/p) as well as for the dorso/ventral axis (d/v) by using the supplied scalebar from Leica. Expression of either GFP-Smash-PI or GFP-Smash-PM led to a size reduction in the a/p axis, compared to *pGMR Gal4* and the transgenic lines. Error bars indicate standard error.

3.5 Smash binds Src42A and Src64B *in vivo*

In order to get more insight into the gene function of *smash*, other potential binding partners of Smash were examined. A yeast two-hybrid screen which was designed for an interaction map of *Drosophila* proteins (Giot et al., 2003), indicated that the non-receptor tyrosine kinase Src42A is a potential binding partner of Smash-PI and Smash-PJ, the latter representing a slightly shorter isoform lacking the LIM domain by an alternatively spliced exon containing a stop signal (see 1.5 and Fig.32, prior annotation CG31534-PB). It was previously shown that Src42A and Src64B have the abilities to bind Smash-PI (Beati, 2009), but additional effort was investigated in this work.

Antibody staining against endogenous Src42A protein showed that it is localizing along the basolateral membrane of epithelial cells but showing slightly higher accumulation in the region of the AJs (see Fig.29 A and 1.3). Furthermore a phosphospecific antibody directed against tyrosine phosphorylated Src42A, which represents an activated form, is localizing specifically at the AJs (see Fig.29 B and 1.3) and at places where morphogenetic processes like the invagination of the cephalic furrow happen (Shindo et al., 2008). As it has been proposed and supported by antibody stainings that the region of AJs are rich in phosphotyrosines (see Fig.29 C and 1.3) Src42A was a good candidate for further studies.

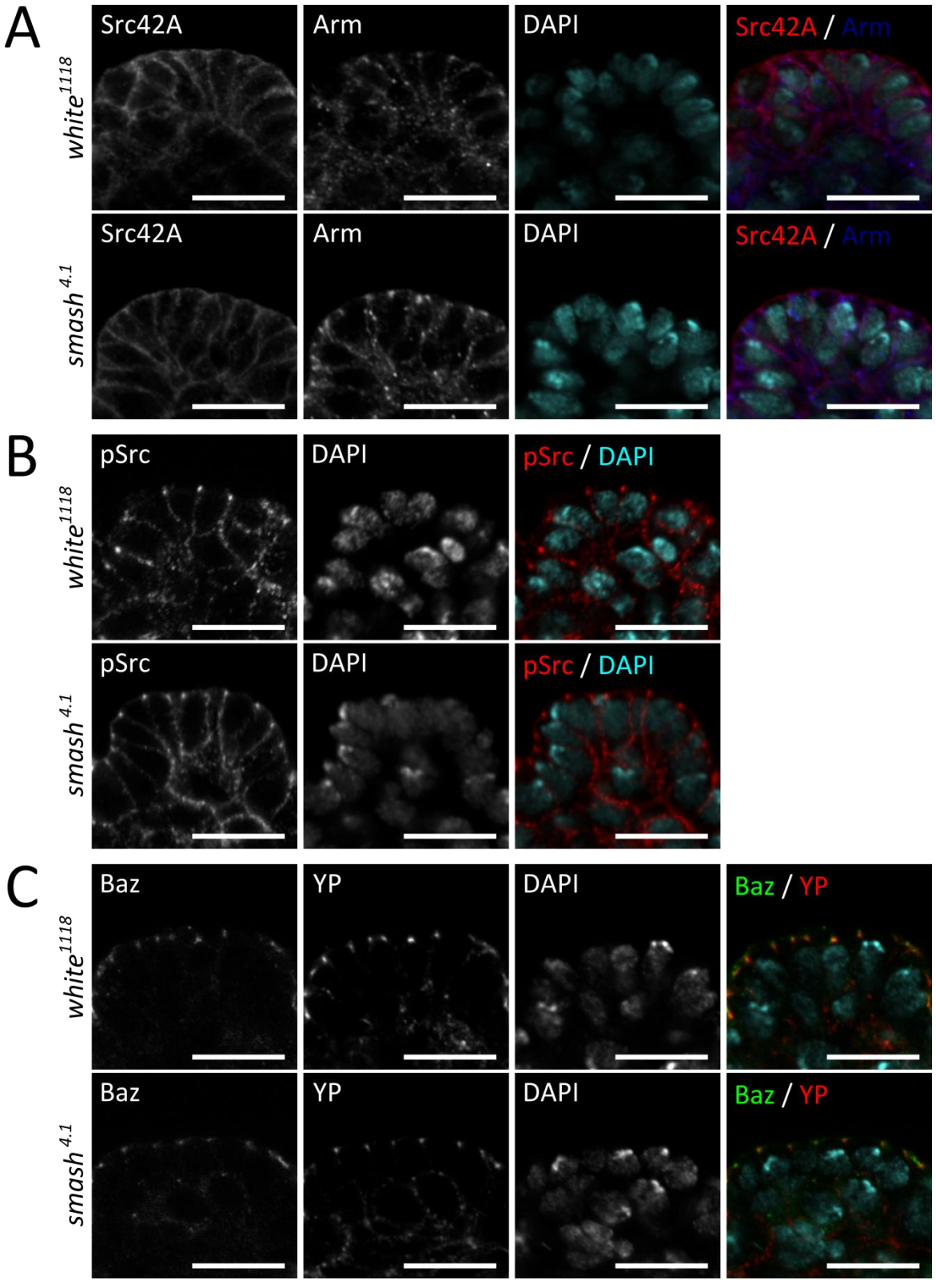
A
white1118
Src42A
Arm
DAPI
Src42A / Arm
smash4.1
Src42A
Arm
DAPI
Src42A / Arm
B
white1118
pSrc
DAPI
pSrc / DAPI
smash4.1
pSrc
DAPI
pSrc / DAPI
C
white1118
Baz
YP
DAPI
Baz / YP
smash4.1
Baz
YP
DAPI
Baz / YP

Fig.29: Subcellular localization of Src42A and the activated form pSrc

Stainings show subcellular localization of Src42A and pSrc in *white*^{1118} embryos, as well as in mutants for *smash*$^{4.1}$. (A) Src42A was detected along the basolateral membrane with slightly higher accumulation at the apical membrane. Arm is shown as an AJs marker. Merged image shows Src42A in red and Arm in blue. Lower panel shows subcellular localization of Src42A and Arm in *smash*$^{4.1}$ mutant embryos. (B) Staining for the activated form of Src42A, labeled as pSrc (Shindo et al., 2008), showed strong localization in the region of the AJs. Lower panel shows no apparent mislocalization of pSrc in *smash*$^{4.1}$ mutants. (C) Staining for phosphotyrosine (YP) shows that AJs are rich in proteins with phosphorylated tyrosines. Baz was stained as an AJs marker. Phosphotyrosine levels were not affected in *smash*$^{4.1}$ mutant embryos. Scalebars = 10 µm.

To test whether both proteins interact physically, N-terminally GFP tagged Smash-PI was co-expressed in S2 cells either with C-terminally HA tagged Src42A or Src64B, respectively. After immunoprecipitation of GFP, HA was detected by Western blot, indicating that GFP-Smash-PI binds to both Src kinases *in vitro* in this cell culture system. Furthermore, using an antibody against phosphotyrosine, a strong phosphorylation signal was detected at the respective molecular weight of GFP-Smash-PI, which was not observed after expression of GFP-Smash-PI without Src42A (see Fig.30 A). This finding strongly indicates that Smash-PI is phosphorylated by Src42A *in vitro*.

Smash was also shown to be tyrosine phosphorylated *in vivo*. Embryonic lysates were prepared from *white*^{1118} and *smash*$^{4.1}$ mutants using phosphatase inhibitors in the lysis buffers. Smash was immunoprecipitated using the anti-Smash intra antibody and phosphotyrosine antibody was used for Western blot. A phosphorylation signal could be observed for *white*^{1118} but not for *smash*$^{4.1}$ mutants (see Fig.30 B). This gives additional evidence to the identified interaction.

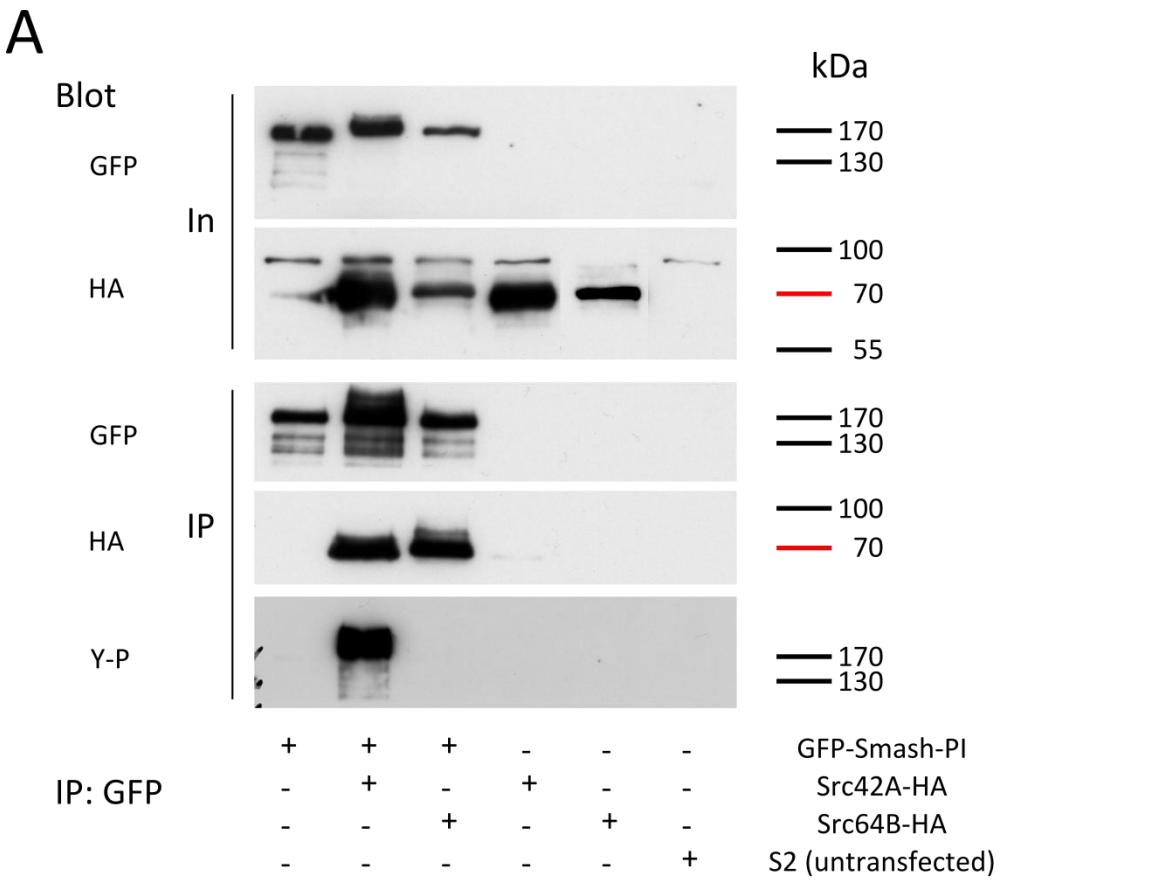
A
Blot
kDa
GFP
In
HA
170
130
100
70
55
GFP
IP
HA
Y-P
170
130
100
70
170
130
IP: GFP
+ + + - - - GFP-Smash-PI
- + - + - - Src42A-HA
- - + - + - Src64B-HA
- - - - - + S2 (untransfected)

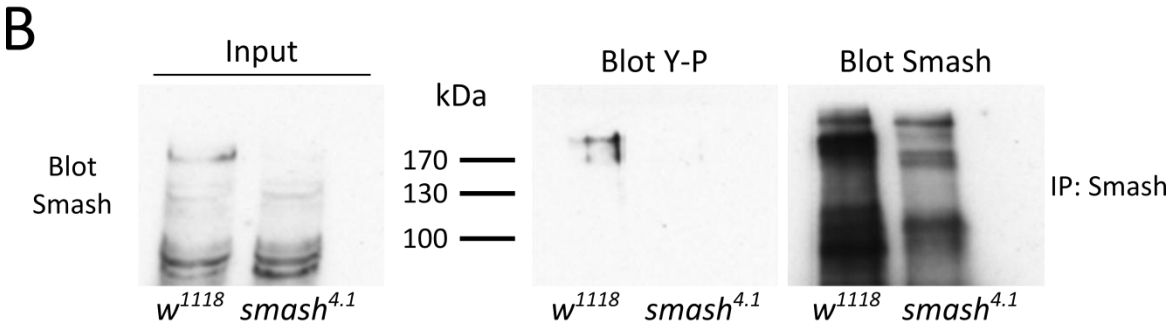
B
Input
Blot Y-P
Blot Smash
Blot
Smash
kDa
170
130
100
IP: Smash
w1118 smash4.1
w1118 smash4.1
w1118 smash4.1

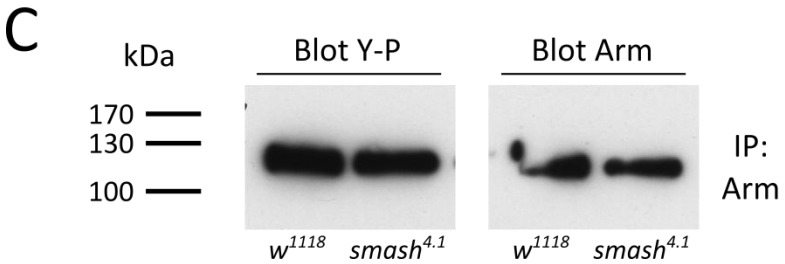
C
kDa
Blot Y-P
Blot Arm
170
130
100
IP:
Arm
w1118 smash4.1
w1118 smash4.1

Fig.30: GFP-Smash binds to Srcs and is tyrosine phosphorylated *in vivo*

(A) Expressing an N-terminal GFP tagged version of Smash-PI together with C-terminal HA tagged versions of Src42A or Src64B respectively, showed that both non-receptor tyrosine kinases were detectable in Western Blot after immunoprecipitation of GFP-Smash-PI. Furthermore, using an antibody directed against phosphotyrosine, a corresponding signal was observed at a molecular size of GFP-Smash-PI upon co-expression with Src42A-HA. This phosphorylation event appeared to specifically require Src42A-HA as co-expression with Src64B-HA resulted in very little phosphorylation. (B) The tyrosine phosphorylation of Smash was also shown *in vivo*. *white*^{1118} embryonic protein lysates were compared with lysates from homozygous *smash*$^{4.1}$ mutants for phosphotyrosine levels. Smash was immunoprecipitated with anti-Smash intra antibody and concomitant Western blotting for phosphotyrosine showed a phosphorylation signal, which was lost in the mutant. (C) Phosphotyrosine levels of Arm were unaffected in mutants for *smash*$^{4.1}$ in comparison to *white*^{1118} embryos.

It has been suggested that LIM domain containing scaffolding proteins could act as adapters between kinases and their respective targets (Khurana et al., 2002). Due to the fact that Arm is a phosphorylation target of Src42A and Src64B (Takahashi et al., 2005), its tyrosine phosphorylation state was analyzed in mutants for *smash*$^{4.1}$. Embryonic lysates of the C-terminal truncated allele *smash*$^{4.1}$ were used, Arm was immunoprecipitated and phosphotyrosine signal was analyzed in Western blot. A change in phosphorylation was not observed in mutants for *smash*$^{4.1}$ (see Fig.30 C).

In an attempt to uncover protein domains required for the interaction between Smash-PI and Src42A a set of domain deletions were generated. Either the N-terminal SH3 domain, the SH2 domain or the C-terminal tyrosine kinase domain were deleted (see Fig.31 A). However, none of these deletions showed complete abolishment of the interaction with GFP-Smash-PI (see Fig.31 B). Furthermore, deletion mutants lacking the SH3 or SH2 domain were still able to phosphorylate GFP-Smash-PI. Only deletion of the tyrosine kinase domain showed loss of phosphorylation, as expected. However, Src42A ΔSH2-HA showed a reduced ability to immunoprecipiate with GFP-Smash-PI, possibly indicating a special role for this domain in the context of this interaction.

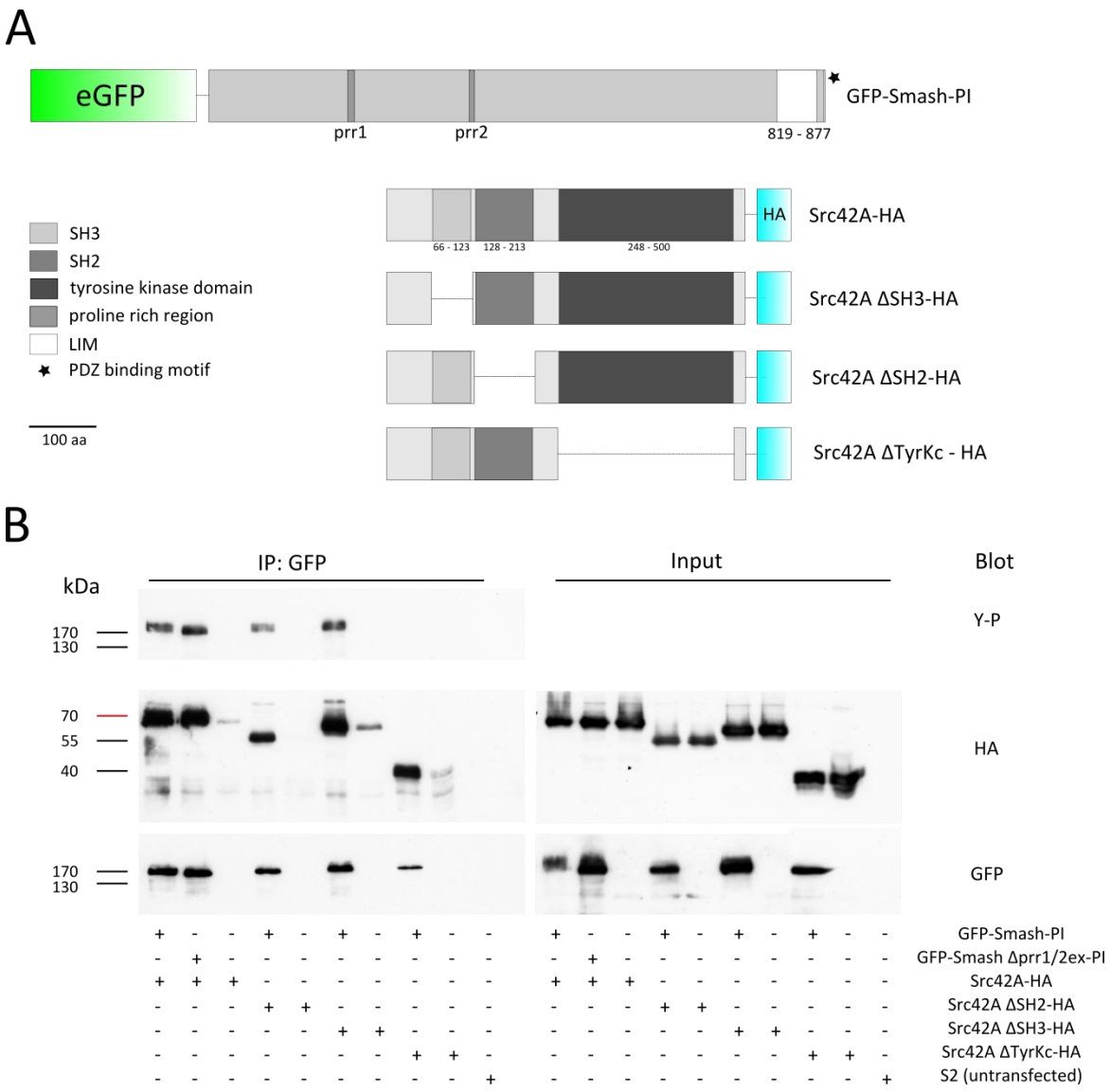

Fig.31: Src deletion Co-IPs

(A) Different Src42A domain deletions generated with the C-terminal HA tag shown in turquoise. Upper panel shows the N-terminal GFP tagged version of the short isoform Smash-PI. Both proline rich regions (prr) are indicated. (B) Co-IP experiments showed that all Src42A deletions generated can still bind to GFP-Smash-PI. Phosphorylation of GFP-Smash-PI was still detected after SH3 or SH2 deletion. A slight decrease in binding was observed upon SH2 deletion. Vice versa mutations in both proline rich regions of Smash-PI did not show any decrease in the binding ability between both proteins. Mutations in the proline rich regions of Smash-PI showed no effect on Src42A binding.

The tyrosine phosphorylation shown in cell culture experiments (see Fig.30 A and Fig.31 B) as well as *in vivo* in embryos (see Fig.30 B) raised interest in the phosphorylation target sites. Phosphorylation of the protein by Src42A may have functions such as activation or inactivation and overexpression of respective point mutated forms of the protein could have shed light on its biological function.

The NetphosK software from the technical university of Denmark (http://www.cbs.dtu.dk/services/NetPhosK/) was used to identify Src specific phosphorylation motifs within the amino acid sequence of Smash-PI. Five tyrosine residues were detected as Src phosphorylation target sites (Y64/708, Y152/796, Y162/806, Y244/888 and Y601/1245, red numbers indicate respective sites in Smash-PM). An additional residue (Y685/1329) was identified by PhosphoPep, a phosphoproteome resource of *Drosophila* proteins based on mass spectrometry (Bodenmiller et al., 2007). Due to the change in the gene annotation release a further tyrosine residue was detected in the N-terminal region of Smash-PM by the NetphosK software as a Src motif, which is Y295. This residue has not been investigated yet.

The identified tyrosine residues were mutated to phenylalanine and co-expressed with Src42A-HA in S2 cells to monitor the phosphorylation state of each respective point mutated protein. Y64/708 as well as Y162/806 showed decreased phoyphorylation signal, which was supported by loss of one band (a double band was usually detectable after separation with lower percentage SDS-gels) detected by Western blotting and probing against phosphotyrosine (see Fig.32). Furthermore a mutant form carrying mutations in all of the identified tyrosine residues showed strongly reduced phosphorylation but not a complete abolishment. These results indicate that the tyrosine residues, Y64/708 and Y162/806, most likely represent two phosphorylation sites for Src42A. However, there must be at least one more target site, which was not detected by the NetphosK prediction software.

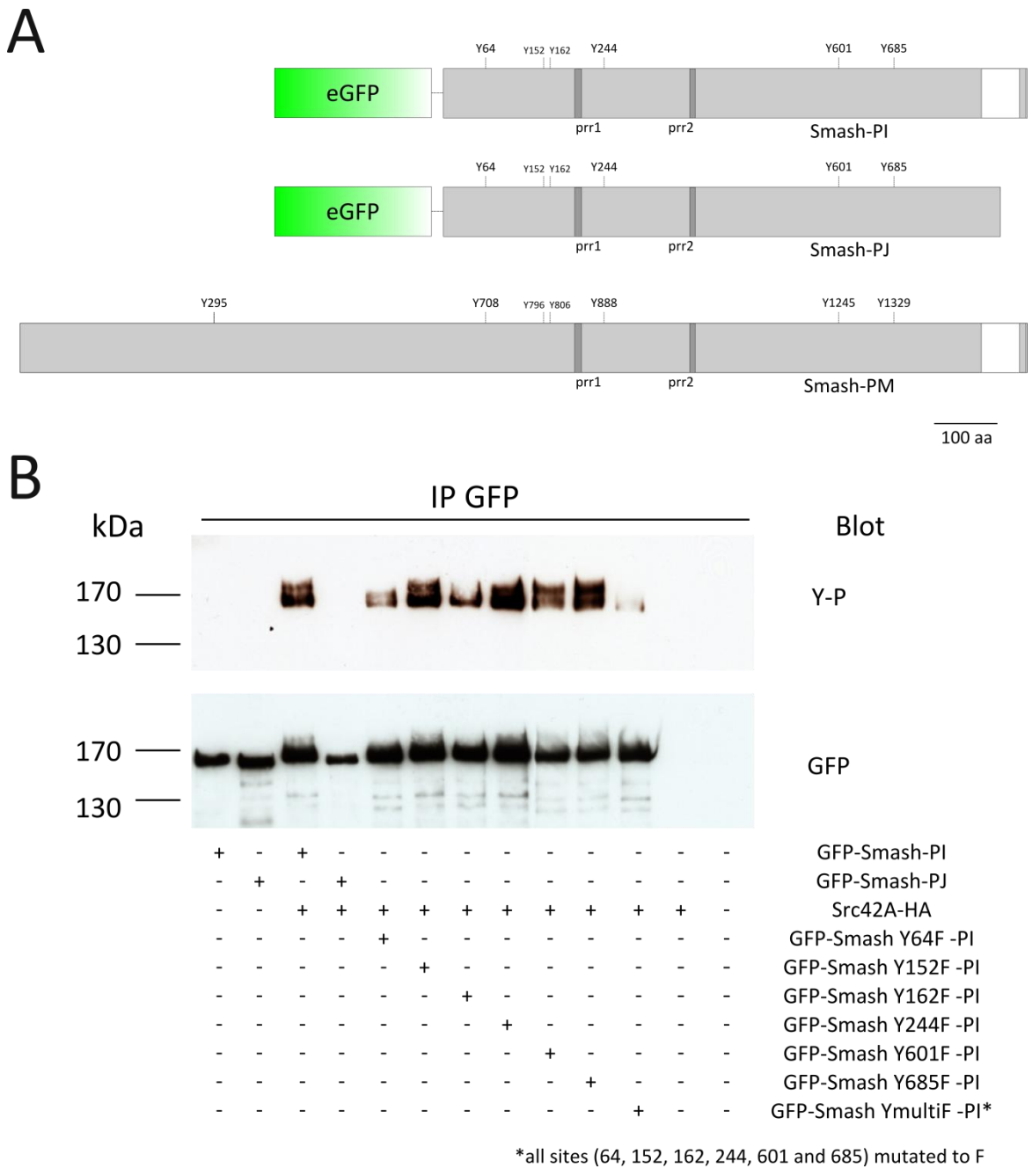

Fig.32: Analysis of Smash-PI phosphomutants

In order to unravel the Src phosphorylation target sites, a set of point mutations were generated for Smash-PI. (A) Scheme indicates the Src phosphorylation motifs by the NetphosK prediction server of the Technical University of Denmark and the single tyrosine residue 685 predicted by the PhosphoPep analysis (Bodenmiller et al., 2007). Upper panel shows the respective sites in the short isoform Smash-PI and Smash-PJ, which lacks the LIM domain due to alternative splicing. The corresponding sites are indicated for the larger isoform Smash-PM. An additional tyrosine was predicted by NetphosK in the N-terminal region. (B) Co-IP experiments between Src42A-HA and different point mutated forms of N-terminal GFP tagged Smash-PI. Predicted tyrosines were exchanged to phenylalanine. Western blot and probing for

phosphotyrosine implicated Y64 and Y162 as phosphorylation targets because the phosphorylation signal is strongly decreased. Moreover a respective mutant form, carrying mutations to phenylalanine in all predicted sites, showed almost complete abolition of the phosphorylation signal.

3.6 Overexpression of Src42A in the eye

It was previously reported that overexpression of SFK transgenes in the *Drosophila* eye, as well as their constitutively active forms, causes interruption of normal development (Pedraza et al., 2004). Based on this assay different transgenic fly lines were generated with constructs encoding C-terminally HA tagged forms of Src42A, Src64B and two different alleles for constitutively active forms of Src42A (Y511 to F mutation). These cannot be phosphorylated by Csk anymore (see 1.3). Expression of these transgenes with *pGMR Gal4* reproduced the reported phenotypes, although they were milder here (see Fig.33 A). Since SFKs are involved in cell proliferation control another observation was a change in eye size. As expected, the expression of the constitutively active forms showed slightly stronger phenotypes.

It has been published that the vertebrate homolog of *smash*, *LMO7* (see 1.4) has tumor suppressor functions in mice (Tanaka-Okamoto et al., 2009). To check whether *smash* could also have tumor suppressor functions especially with regard to its interaction with Src42A, expression of the above mentioned Src transgenes were performed together with GFP-Smash-PM. As already shown in Fig.28 A, expression of an *UASt GFP-smash-PM* transgene causes a rough eye phenotype as well as size reduction along the a/p axis (see Fig.28 B). However, co-expression with Src42A YF-HA led to an enhancement of the rough eye phenotype and a reduction in size. Vice versa, expressing these Src transgenes in eyes mutant for *smash* would be of great interest.

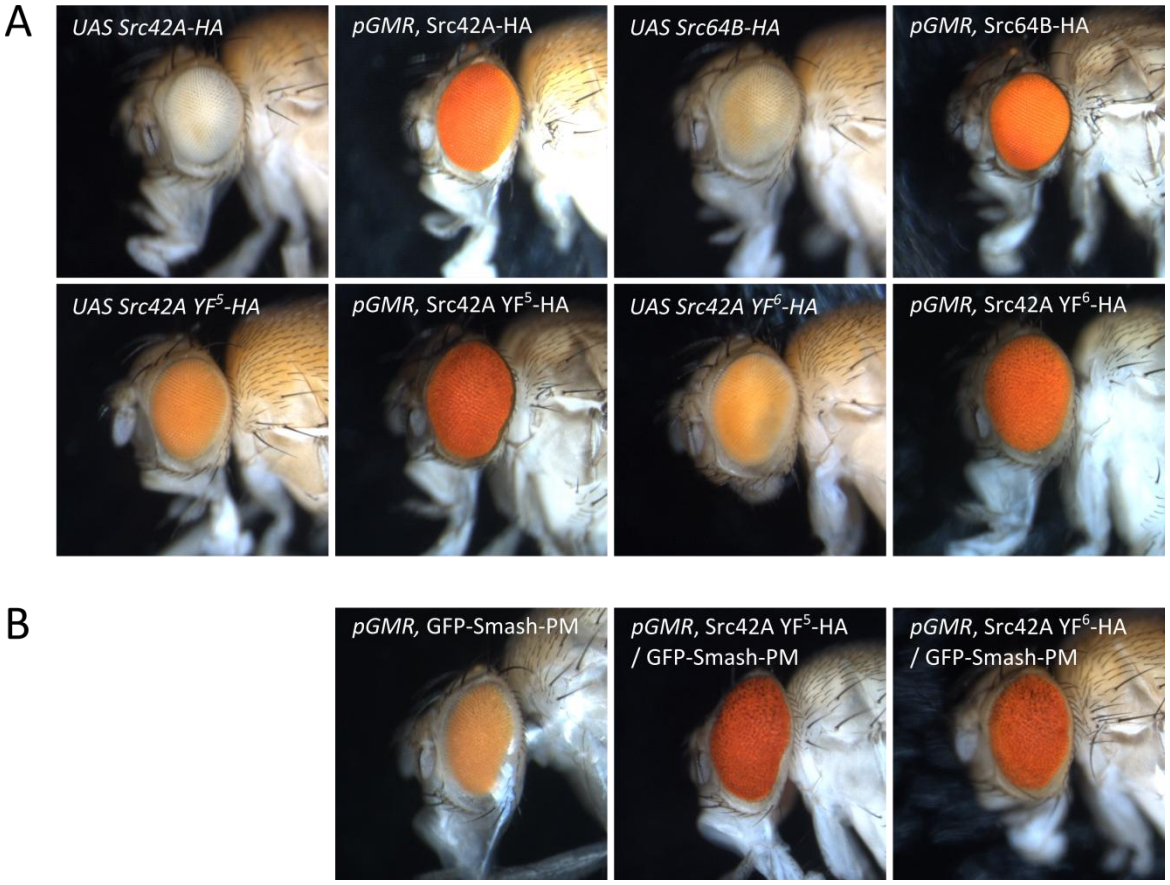
A
UAS Src42A-HA
pGMR, Src42A-HA
UAS Src64B-HA
pGMR, Src64B-HA
UAS Src42A YF5-HA
pGMR, Src42A YF5-HA
UAS Src42A YF6-HA
pGMR, Src42A YF6-HA
B
pGMR, GFP-Smash-PM
pGMR, Src42A YF5-HA / GFP-Smash-PM
pGMR, Src42A YF6-HA / GFP-Smash-PM

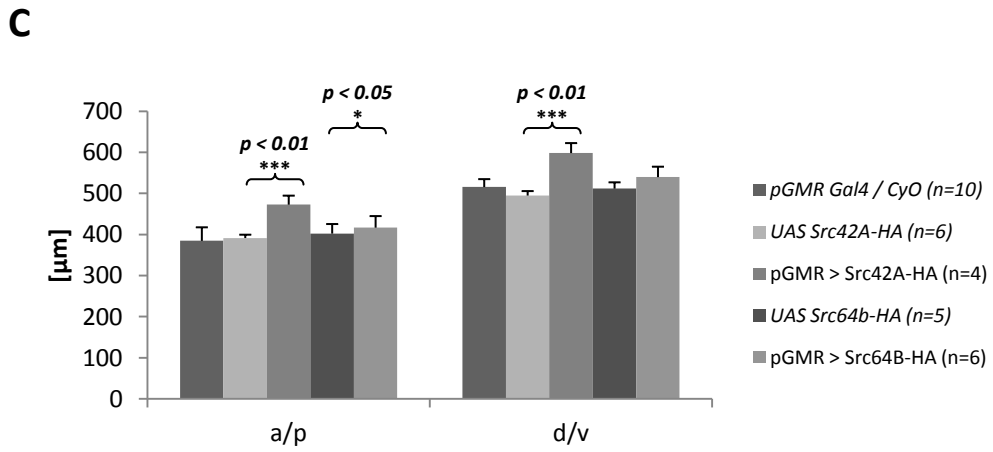
C
p < 0.05
*
p < 0.01
***
p < 0.01
***
700
600
500
400
300
200
100
0
[µm]
a/p
d/v
pGMR Gal4 / CyO (n=10)
UAS Src42A-HA (n=6)
pGMR > Src42A-HA (n=4)
UAS Src64b-HA (n=5)
pGMR > Src64B-HA (n=6)

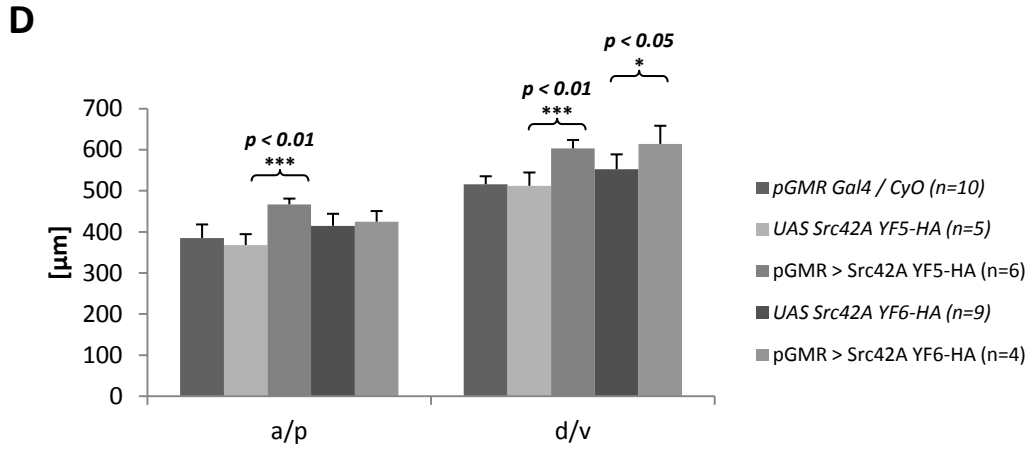
D
p < 0.05
*
p < 0.01
***
p < 0.01
***
700
600
500
400
300
200
100
0
[µm]
a/p
d/v
pGMR Gal4 / CyO (n=10)
UAS Src42A YF5-HA (n=5)
pGMR > Src42A YF5-HA (n=6)
UAS Src42A YF6-HA (n=9)
pGMR > Src42A YF6-HA (n=4)

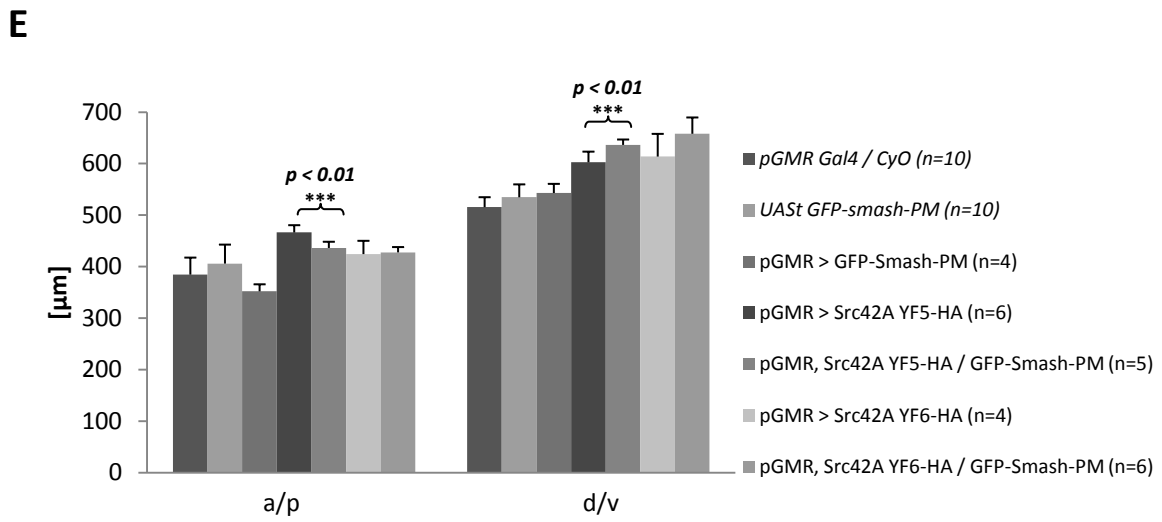

Fig.33: Expression of Src in the eye

pGMR Gal4 driven expression of different Src transgenes. (A) Rough eye phenotypes caused by expression of Srcs. Slight rough eye phenotypes have been observed upon expression of either Src42A-HA or Src64B-HA. Size measurements revealed a slight increase along the a/p as well as the d/v axis (C). Phenotypes were enhanced by expressing constitutively active forms of Src42A (carrying Y511F mutation). The eye size was increased as well compared to the non mutated form of Src42A (D). (B) The rough eye phenotype was slightly enhanced by co-expressing the constitutively active forms of Src42A together with GFP-Smash-PM. Furthermore, the enlarged eye phenotype was suppressed slightly in the a/p axis but not in the d/v axis (E). Error bars indicate standard error.

3.7 *smallish* genetically interacts with *Src64B*

Single mutants for *Src42A* as well as *Src64B* do not show strong defects with regards to morphogenetic processes like dorsal closure. However double mutants for both kinases exhibit severe defects in dorsal closure and head involution (see 1.3). To examine whether *smash* has redundant functionality in these pathways, double mutants for both kinases were generated. *Src42A* single mutants are homozygous lethal but *Src64B* mutants are homozygous viable. The $Src42A^{26\text{-}1}$ mutation, the strongest reported mutant allele for *Src42A* (Takahashi et al., 2005), can still be kept in the homozygous mutant background of $smash^{4.1}$. This observation indicates that both proteins act in the same pathway, as one copy of *Src42A* is still enough for survival in the *smash* mutant background.

Interestingly a double mutant for *smash*$^{4.1}$ and *Src64B*^{KO} shows high embryonic lethality (see Fig.34 A and B and Fig.19 A for *smash*^{35} lethality scores). Approximately 70% die during embryogenesis and larvae furthermore die immediately after hatching. However, some eclosing escapers were observed. Embryonic cuticles do not exhibit dorsal closure defects (see Fig.35 A), which were reported for *Src42A* and *Src64B* double mutants (see 1.3). Stainings for Baz and DE-Cad did not show mislocalization, indicating that cell polarity and the formation of AJs remains intact, which supports the finding that some escapers were observed. However, a *da Gal4* driven transgene of GFP-Smash-PM could not significantly rescue the lethality of this double mutation, although a few homozygous flies were recovered. *smash* may exhibit more isoform specific functions (10 isoforms are annotated on flybase), which may explain this finding. Unfortunately a resuce using transgenic flies carrying the genomic locus of *smash* could not be performed because the injected genomic clone did not give rise to any transformant flies. A rescue experiment using a transgene for Src64B has not been tested so far. These results may indicate a new redundant pathway for *smash* in regard to *Src64B* which is not important for dorsal closure.

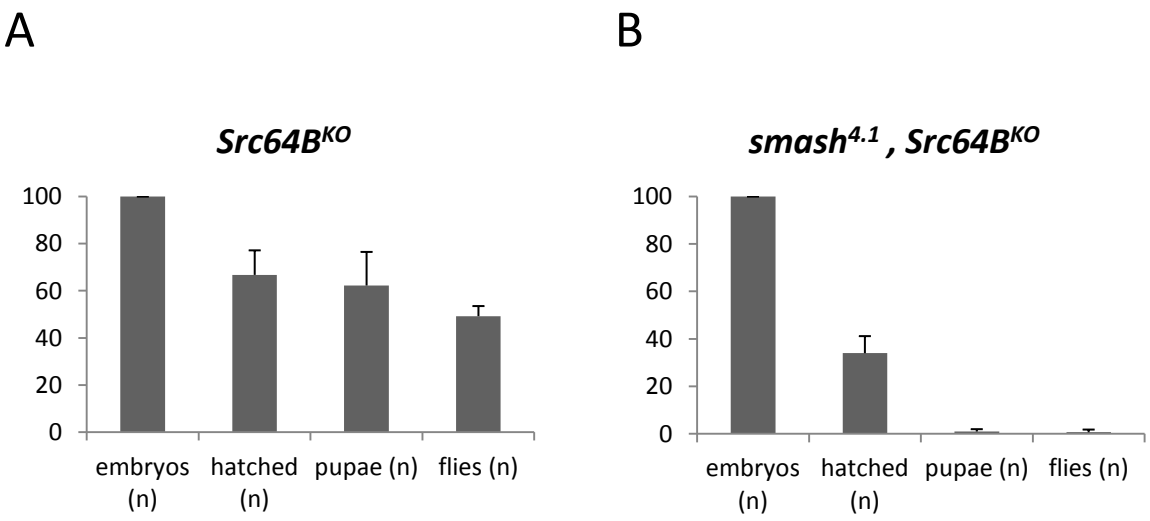

Fig.34: Lethality of *smash* and *Src64B* double knockout

Double-knockout of *Src64B* and *smash* showed significantly increased lethality. (A) The null allele *Src64B*^{KO} is homozygous viable and can be kept as a homozygous stock. The same observation was made for both *smash* alleles (see Fig.19 A for lethality scores of *smash*^{35}). (B) A double-knockout of *smash*$^{4.1}$ and *Src64B*^{KO} showed high embryonic lethality. Almost 70% died during embryogenesis, hatched larvae usually died immediately. Very few eclosing escapers were observed. Lethality scores represent data from three experiments, error bars indicate standard error.

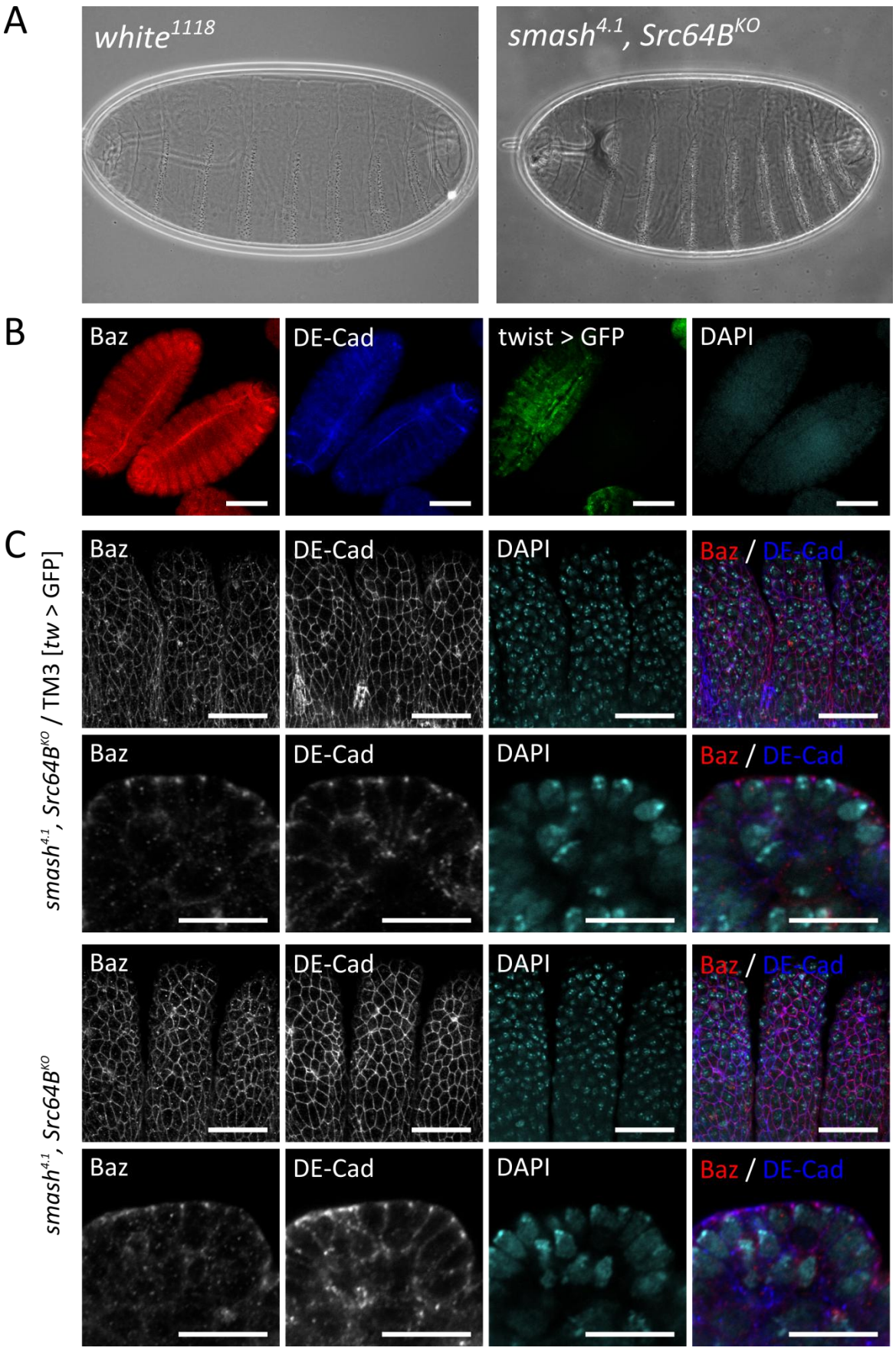
A
white1118
smash4.1, Src64BKO
B
Baz
DE-Cad
twist > GFP
DAPI
C
smash4.1, Src64BKO / TM3 [tw > GFP]
Baz
DE-Cad
DAPI
Baz / DE-Cad
smash4.1, Src64BKO

Fig.35: Double-knockout of *smash* and *Src64B* shows no dorsal closure defects and normal epithelial integrity

(A) A double-knockout for *smash* and *Src64B* does not show cuticular defects. (B) Heterozygous embryo compared to a homozygous double mutant for *smash* and *Src64B*, marked by GFP expression of the TM3 balancer chromosome. Difference in Baz and DE-Cad levels were not detectable. Dorsal closure was completed in the homozygous mutant. Scalebar = 100 µm. (C) Epithelia showed normal organization. Staining for Baz showed correct apical localization, DE-Cad was found to be localized at the AJs. These findings indicate that lethality of the double mutant is probably not caused by defects in epithelial cell polarity. Scalebars represent 20 µm in the surface projections and 10 µm in the cross sections respectively.

4 Discussion

In this study we investigated the function of the so far undescribed gene *CG43427*, which we named *smallish* (*smash*) due to its reduced size phenotype caused by overexpression. The gene product of *smash* was identified in a yeast two-hybrid screen as a potential interactor of Baz (Ramrath, 2002), a keyplayer in regard to cell polarity and AJs formation (Johnson and Wodarz, 2003; McGill et al., 2009). In this screen the three PDZ domains of Baz were selected as bait. These domains are known to be protein-protein-interacting modules (Sheng and Sala, 2001; Te Velthuis and Bagowski, 2007). The C-terminus of Smash possesses a PDZ binding motif of class I (S/T $X^{\ddagger}\Phi^{\S}$ -COOH) (Harris and Lim, 2001), a motif binding to PDZ domains. Furthermore, a vertebrate homolog of *smash*, *LMO7*, had already been shown to function at AJs (Ooshio et al., 2004). We confirmed the *in vivo* binding of Baz and Smash and continued studying the developmental relevance of this interaction. Furthermore we showed that the non-receptor tyrosine kinase Src42A is a binding partner of Smash *in vitro* (Beati, 2009). We further investigated this interaction and found that Src42A phosphorylates Smash and that *smash* genetically interacts with the second *Src* kinase encoded by the *Drosophila* genome, *Src64B*.

4.1 Baz binds to Smash *in vivo*

As we have shown previously (Beati, 2009), Baz forms a complex with Smash *in vivo* in embryos. At this time we did not have access to antibodies against Smash that worked well in Western blots. The anti-Smash intra antibody showed many unspecific bands. In this work we used embryonic lysates expressing an N-terminally GFP tagged version of Smash-PI, which showed an ability to co-immunoprecipitate with Baz. However, it would be interesting to test whether endogenous Smash can be detected as well, when Baz is precipitated from embryonic lysates, as we do not know anything about the stoichiometry of this binding. Furthermore it was only tested whether Baz forms a complex with Smash during embryogenesis. It would be interesting to test whether Baz and Smash can be still detected in a complex *in vivo* in larval as well as in adult tissues. Since Smash was identified as a potential binding partner of Baz by a yeast two-hybrid screen, the likelihood is high that both proteins can bind directly to each other, which we have not tested so far. Further evidence for direct binding of Baz to Smash is given by additional yeast

two-hybrid analyses, where only PDZ 1 and PDZ 2, or PDZ 2 and PDZ 3 were used as baits respectively (Ramrath, 2002; see Fig.12). In both cases, the C-terminus of Smash still bound to the bait proteins. GST pulldown assays could show whether both proteins can interact directly, and if so, which of those three PDZ domains is of importance by using PDZ deletion versions of Baz.

As we found that Baz is colocalizing with Smash in the region of AJs, it would be important to analyze whether Smash mislocalizes in mutants for *baz*. So far we have not investigated whether Smash is expressed in the follicular epithelium, which is derived from the mesoderm. An easy test would be to induce *baz* mutant clones in this tissue and co-stain for Smash. However, a *baz* deletion allele is not available and respective mutants may still express defective fragments of Baz (Shahab, unpublished data). However, some alleles are supposed to lack the region carrying the PDZ domains and thus could be used for the respective experiment (Krahn et al., 2010b). It was reported that Baz is excluded dorsally in leading edge cells in a planar polarized fashion (Laplante and Nilson, 2011). As we detected that Smash shows strong accumulation dorsally in leading edge cells (see Fig.15) it may indicate that Smash can localize to the plasma membrane in a Baz independent way. Furthermore staining for Baz showed low protein levels in the amnioserosa, whereas Smash was clearly detectable in this tissue. Furthermore, Smash transgenes lacking C-terminal parts still localized to the membrane (Beati, 2009). Currently, all generated transgenic fly lines were created with the old injection system. It would be important to test the localization of respective deletion mutants with site directed insertion of the respective transgenes. This would guarantee comparable expression levels via the UAS/Gal4 system. Another mechanism for Smash localization could be via Src42A. However, Smash localizes to regions containing AJs, whereas Src42A localizes along the whole plasma membrane (see Fig.29). It would therefore be interesting to analyze this interaction with regards to pSrc, which was shown to exclusively localize at AJs (Shindo et al., 2008). It is possible that Smash may only bind to pSrc, however, we could not discuss this specific interaction using our experimental setup.

4.2 Expression of *smallish*

As the anti-Smash intra antibody did not work well with standard fixation methods (e.g. formaldehyde fixation) and staining required harsh fixation methods (e.g. heat fixation), co-stainings with other proteins were not easy. Due to the change in the current gene annotation release 5.40 and the fact that *smash* consists of both transcription units of *CG31534* and *CG31531* we decided to generate a second antibody. As shown in Fig.14 we could show ubiquitous expression of Smash in ectodermal epithelia throughout embryogenesis. Staining is apparent after cellularization of the embryo, when the first epithelium is established (Knust and Bossinger, 2002). Currently it is not clear if Smash is maternally deposited into the egg in the form of proteins or mRNAs. To determine when zygotic expression begins, female mutants for *smash* could be crossed to wildtype males. Staining for Smash would indicate the start of zygotic expression, since any maternal supply would be depleted in those eggs.

We found that Smash protein shows similar subcellular localization as Baz. It localizes at the membrane in a honey comb fashion and was found to localize at AJs (see Fig.15). Immuno electron microscopy could reveal the subcellular localization in greater detail. The vertebrate homolog LMO7 was shown to localize specifically at AJs (see 1.4) and at the free apical membrane (Ooshio et al., 2004).

We further detected Smash in the tracheal tubes using the anti-Smash intra antibody. This staining was shown after heat fixation and was lost in the $smash^{4.1}$ mutant allele, supporting the specifity of the staining. However, the anti-Smash N-term antibody only showed non specific tracheal staining, which did not disappear in mutant embryos (data not shown). Both antibodies showed high accumulation of Smash in the embryonic hindgut, which was also confirmed by RNA *in situ* hybridization (Ramrath, 2002), and the denticle belts. However, expressing N-terminally GFP tagged versions of Smash-PI and Smash-PM in clones in fat body cells, showed clear localization of GFP-Smash-PI in the nucleus (see Fig.16 B), whereas the large isoform GFP-Smash-PM showed strong cortical localization and accumulation in a region adjacent to the nuclear envelope. These localizations could not be shown for endogenous Smash (data not shown). If there is an *in vivo* function of Smash in the nucleus, the amount of protein entering the nucleus is probably below the detection limit. Use of drugs inhibiting nuclear export may lead to accumulation of endogenous Smash in the nucleus, which would probably be detectable using anti-Smash antibody. Nuclear localization of Smash would show homology to LMO7 nuclear function. LMO7 enters the nucleus and regulates expression of muscle-relevant genes, among

them the LEM domain protein Emerin. Emerin in turn binds to LMO7 inhibiting *emerin* expression, indicating a negative feedback mechanism. Mutations in *emerin* cause Emery-Dreifuss muscular dystrophy (Nagano et al., 1996; Emery, 2000; Bengtsson and Wilson, 2004). *emerin* has homologs in *Drosophila* as well, the closest one being *otefin*. Otefin has been shown to be essential for germline stem cell maintenance (Jiang et al., 2008). Co-IP experiments between Smash and Otefin could show whether a function in this pathway may be conserved.

4.3 Knockout of *smallish*

We found that *smash* gene function is not essential. Homozygous flies are viable and fertile, although they seem weaker than heterozygous siblings. However, temperature shift to 29°C increased the lethality score, indicating that stress may influences death rate. So far we have not tested whether nutritional stress can also change their viability. Differences in the lethality scores of the two generated alleles $smash^{4.1}$ and $smash^{35}$ have not been detected (data not shown). The latter allele was generated recently, as the gene annotation release 5.40 in 2011 indicated that the gene annotation was not correct (see 1.5). The $smash^{4.1}$ allele represents a C-terminal truncation and therefore cannot be considered a classical null allele. So far we do not know whether the N-terminal part is expressed in $smash^{4.1}$. In this regard, by use of the newly produced anti-Smash N-term antibody we can likely answer this question. Here it would be also interesting to examine the subcellular localization of the N-terminus. If it is expressed and localized at the membrane it would clearly show localization independent of Baz.

As the knockout of *smash* did not lead to lethality, mislocalization of polarity markers was not expected. Staining for markers such as Baz or DE-Cad showed that cell polarity is intact and AJs are formed. Examining protein levels did not reveal any change in accumulation of Baz, DE-Cad and Arm (Fig.21).

The observed lethality scores are comparable with those reported for a knockout of *LMO7*, where homozygous mice show up to 40% lethality between birth and weaning. Surviving mice normally give rise to progeny (Tanaka-Okamoto et al., 2009). In this allele the PDZ domain was precisely excised, which may disrupt the functionality of the protein. Another *LMO7* allele was reported carrying an 800 kb deletion. Parts of the neighboring gene *Uchl3* were taken out as well. Only 40% of mice were born alive carrying this deletion. Homozygous mice showed growth retardation and

muscular as well as retinal degeneration. However, latter observation is most likely caused by the *Uchl3* mutation, as single mutants for this gene showed a comparable phenotype (Semenova et al., 2003). Our *smash* knockouts do not exhibit obvious defects, but respective electron microscopy analysis of muscle fibers and the ommatidia has not been performed so far. Subtle morphological defects are probably not detectable by conventional light and confocal microscopy.

4.4 Overexpression of Smash

We found that in contrast to the *smash* knockout, overexpression of N-terminally GFP tagged versions of Smash dramatically increased the lethality score (using *tub Gal4* as a strong driver line). The short isoform, GFP-Smash-PI caused no embryonic lethality but many individuals died during larval and pupal development. Expression of the larger isoform GFP-Smash-PM led to embryonic lethality for approximately 50% of individuals, and no hatched larvae developed to pupation. Since the activity of the UAS/Gal4 system is temperature-dependent, a shift to 18°C reduces transgene expression. Even at this temperature not a single fly eclosed, emphasizing the high lethality caused by expression of GFP-Smash-PM. We found that eclosing flies expressing GFP-Smash-PI were strongly reduced in size (see Fig.23 A). With regards to this, expression of GFP-Smash-PM by *en Gal4* showed that cells overexpressing GFP-Smash-PM were smaller in comparison to their neighboring non expressing cells. The apical surface area of expressing cells was significantly decreased. These observations indicate a potential function of *smash* in apical constriction, which is a process important for an epithelium undergoing morphogenetic changes (e.g. invagination, see 1.2). Cuticles of embryos which expressed GFP-Smash-PM under the control of *tub Gal4* showed anterior holes, dorsal holes, or both. It would be interesting to test whether Smash transgenes lacking the LIM domain or the PDZ binding motif show the same phenotypes upon overexpression. This could clarify the functional relevance of the C-terminal part of Smash with regards to the observations.

It would be of big interest whether *smash* mutant clones would show the opposing effect, i.e. a widening of the apical surface. However genetic methods are restricted. FRT recombination is the method of choice for clone induction. Recombination of *smash* alleles with a FRT is not easy, as the relevant FRT chromosome used for this chromosome arm is FRT82B. The genomic locus of *smash* (3R 82D-E) is very close to this FRT and we were not able to obtain a single recombinant so far. Another possibility would be the generation of clones with a translocated genomic locus of

smash (e.g. on the second chromosome) in the *smash* mutant background. However, only a single genomic clone is available carrying the entire *smash* gene locus and generation of respective transformants did not work so far.

4.5 Smash forms a complex with Src42A *in vivo* and interacts genetically with *Src64B*

In a *Drosophila* wide yeast two-hybrid screen it was previously shown that the non-receptor tyrosine kinase Src42A is a potential binding partner of Smash-PI and Smash-PJ respectively (Giot et al., 2003). Src42A was shown to be expressed in epithelia (Takahashi et al., 2005) and its activated form, pSrc is restricted to AJs and sites of morphogenetic rearrangements (Shindo et al., 2008). Due to this we were interested in investigating the possible binding of Smash and Src42A. We previously showed that Src42A as well as Src64B can bind to Smash-PI *in vitro* in S2 cells (Beati, 2009). Furthermore, results presented in this thesis indicate that Src42A phosphorylates Smash-PI *in vitro* in cell culture, which is specific for Src42A, as Src64B mediated phosphorylation was barely detectable (see Fig.30). This finding was strongly supported by the fact that endogeneous Smash protein showed tyrosine phosphorylation *in vivo* in embryos as well (see Fig.30 B). We have not tested whether Smash is still phosphorylated in *Src42A* mutants. As described in the introduction SFKs have many overlapping functions. Therefore it would be interesting to check the tyrosine phosphorylation state of Smash in these respective mutations.

We found that deletion mutants of Src42A can still bind to Smash. As Smash is likely phosphorylated at three residues, the following mechanism is imaginable: Src42A could bind Smash via its SH3 domain and thereby phosphorylate Smash on an initial residue. Concomitant binding to this phosphorylated tyrosine, likely mediated via the SH2 domain could cause intense phosphorylation of Smash. This would suggest a positive feedback loop and would fit into a proposed model for phosphotyrosine signaling (Lim and Pawson, 2010). This hypothesis is supported by the fact that deletion of the SH2 domain showed reduction in binding and phosphorylation of Smash (see Fig.31 B). However, the developmental relevance of this interaction is not clear so far.

It was shown that Abelson, another tyrosine kinase, is able to phosphorylate Arm Y667, which is also phosphorylated by Src42A (Takahashi et al., 2005; Tamada et al., 2012). However, Abelson

can also induce activation of Src42A, as expression of *abelson* transgenes with *dpp Gal4* in the wing discs led to specific activation of Src42A in the expression stripe (Singh et al., 2010). We performed comparable experiments using anti-pSrc antibody (Shindo et al., 2008) but could not detect changes in pSrc levels upon overexpression of Smash (data not shown). From these results we conclude that *smash* is probably not involved in activation of Src42A. *smash* could also have functions in inhibiting Src42A activity, as *LMO7* was implicated in functioning as a tumor suppressor. Here 90 week old *LMO7* deficient mice showed development of adenocarcinomas in the lung (Tanaka-Okamoto et al., 2009). To address this possibility we expressed Src and Smash in the eye by *pGMR Gal4*. We found contradictory phenotypes: Src42A-HA and Src64B-HA expression resulted in rough eyes which were slighty enlarged, stronger phenotypes were observed upon expression of constitutively active forms of Src42A (carrying Y to F mutation, thereby losing the ability to be phosphorylated by Csk, see 1.3). However, expression of GFP-Smash-PM resulted in rough eyes as well, which were smaller in size. The same observation was made upon expression of GFP-Smash-PI. The size decrease was observable most strongly in the a/p axis of the eye (see Fig.28). However, co-expression of Src42A-HA and GFP-Smash-PM could reduce the enlarged eye phenotype caused by Src42A-HA expression, which is likely caused by additive effects. If Smash has the potential to inhibit Src42A function it would be interesting to test whether the Src42A-HA mediated overexpression phenotype is enhanced in eyes mutant for *smash*. Unfortunately we have not performed this experiment yet.

Src42A and *Src64B* function redundantly in several morphogenetic processes like dorsal closure or germband retraction (Tateno et al., 2000; Takahashi et al., 2005). Single mutants do not exhibit strong defects, whereas double mutants do. We generated double mutants of *smash* with *Src42A* and *Src64B*. Reported mutations in *Src42A* are lethal (Takahashi et al., 2005) and one copy of *Src42A* gene function is still sufficient for survival in the *smash* mutant background. If both proteins are acting in the same pathway, this would explain this observation. In contrast, a double mutant for $smash^{4.1}$ and $Src64B^{KO}$ resulted in a high lethality score. Only 30% of larvae hatched, which usually died immediately. However, some eclosing escaper flies were observed. Epithelial polarization and integrity was not affected. We cannot exclude that the observed lethality is caused by disruption of cell polarity, as we only analyzed zygotic mutants. Homozygous escaper flies could not be kept as a stock and did not give rise to any progeny. Maternal supply of either *Src64B* or *smash* is probably important and rescues epithelial polarity in embryos of the first generation of heterozygous parents. As escaper flies were extremely rare, we could not analyze embryos in the second generation, lacking maternal supply. Currently we also do not know

whether the C-terminal truncated allele *smash*$^{4.1}$ retains part of its function. Another double mutant with the full knockout allele *smash*^{35} could increase embryonic lethality and possible defects. As discussed above, we were unable to generate a recombinant for the FRT82B with *smash*$^{4.1}$ for clone induction. As the *Src64B* gene locus is on the left arm of the 3rd chromosome, clones mutant for both mutations are not inducible easily.

We tried to rescue the lethality of *Src64B smash* double mutants by ubiquitous expression of GFP-Smash-PM under the control of *da Gal4*, which could not rescue the observed lethality. As the gene annotation release 5.40 lists 10 isoforms, we cannot exclude isoform specific functions of *smash*. Furthermore, overexpression of Smash might have a negative effect on survival, as we found that strong overexpression led to 50% lethality during embryogenesis (see Fig.22 B). Flies were viable expressing the N-terminally tagged version of GFP-Smash-PM with *da Gal4*, although they were slightly reduced in size (data not shown). However the genomic background could be sensitized due to the *Src64B* mutation. A rescue could be performed with a transgene carrying the genomic *smash* locus on a different chromosome as well, but as mentioned above we currently do not have these flies. However, in this way we would circumvent the problem of functions of different isoforms, and expression levels of *smash* would better reflect endogenous levels. A rescue with *Src64B* transgenes has not been tested yet.

5 Conclusion and future perspectives

We showed that *smash* gene function only plays minor roles during *Drosophila* development and is not important for survival of the fly. We generated two different mutant alleles, one representing a classical null allele due to deletion of the genomic locus of *smash* and a second allele truncated at the C-terminus by deletion of the 3' genomic region. Both mutant alleles do not result in lethality or obvious epithelial defects. However, it cannot be ruled out that minor defects have been overlooked. Since we showed that Src42A phosphorylates Smash *in vitro*, and Smash is tyrosine phosphorylated *in vivo* as well, it would be helpful to identify the missing phosphorylation target sites by mass spectrometry. By our approach we were able to identify Y64 and Y162 as potential phosphorylation sites of the short isoform Smash-PI. Antibodies raised against phosphorylated Smash could shed light on its subcellular site of function, although we do not know whether phosphorylation correlates with activation of Smash. In this regard it would be very interesting to test whether transgenic flies encoding for the *smash* gene locus have the ability to rescue *smash Src64B* double mutants. A respective transgene mutated in the phosphorylation sites would clearly show the importance of the Smash Src42A interaction and its phosphorylation. In the context of the interaction with Src42A it was shown that the vertebrate homolog of Baz, Par3, is phosphorylated by c-Src, which is the closest homolog of Src42A. Par3 tyrosine phosphorylation results in the dissociation of LIM kinase 2, which in turn regulates phosphorylation of cofilin and thereby delays TJ assembly (Wang et al., 2006). We could not find a link between Smash function and Baz in this regard. Baz co-immunoprecipitates with Src42A as well and showed tyrosine phosphorylation *in vitro* in cell culture, likely independent of Smash (data not shown). This observation was made after co-expressing Baz and Src42A in S2 cells and analyzed in a similar manner to the Smash and Src42A interaction. Since we did not downregulate Smash protein levels in this system we cannot exclude a function for Smash in the complex formation of Baz and Src42A. So far we have not tested whether Baz can associate with Src42A in the absence of Smash. The easiest way would be to test Baz association with Src42A, as well as phosphorylation of Baz *in vivo* in embryos compared to *smash* mutants.

Contradictory to loss of *smash*, overexpression resulted in a dramatic increase in embryonic lethality. Overexpression of GFP-Smash-PM using *en Gal4* as a driver line resulted in cells that are smaller and decreased in their apical surface area, which likely represents an apical constriction

phenotype. Apical constriction is a process that depends on the Actin/Myosin network, which lies beneath the AJs (see 1.2). This process is of importance for morphogenetic rearrangements, as contraction exerts force on AJs and their relocation results in cell shape changes. Apical constriction is regulated by Rho-associated kinase (ROCK) activity, which is involved in the phosphorylation of Myosin light chain, thereby enhancing the Actin/Myosin contractility (Riento and Ridley, 2003; Vicente-Manzanares et al., 2009). For example, expression of Spaghetti-squash the *Drosophila* homolog of Myosin light chain, mutated in its phosphorylation sites results in apical expansion if mutated to non phosphorylatable alanine, whereas glutamate exchange results in apical constriction (Zimmerman et al., 2010). Recently it was shown that aPKC is negatively involved in apical constriction, as it is recruited to the apical membrane not only by Par3 but also by Willin. Simultaneous depletion of Willin and Par3 resulted in loss of aPKC at the apical membrane and induced apical constriction. aPKC had been shown to phosphorylate ROCK, thereby reducing the junctional localization of ROCK explaining these findings (Ishiuchi and Takeichi, 2011). If the observed phenotype caused by Smash represents apical constriction it is still elusive how Smash might function in this pathway. So far we have not focused on potential interacting proteins of the Actin/Myosin network. Candidates would be Canoe, the *Drosophila* homolog of Afadin and α-Actinin. Both proteins were shown to bind LMO7 (Ooshio et al., 2004). Furthermore, Canoe supports a link between the Actin cytoskeleton and AJs during apical constriction and mutants for *canoe* show dorsal closure defects (Takahashi et al., 1998; Sawyer et al., 2009). Whether Src42A plays a part in this pathway as well could be tested by expressing Smash-PM mutated at its phosphorylation sites. Loss of the smaller cell phenotype would clearly place Src42A in this context.

The classical model of cell-cell adhesion was thought to be mediated by a stable connection between AJs and the cytoskeleton through α-Cat (see 1.2). However, it was shown that a quaternary complex of E-Cad-β-Cat-α-Cat-Actin does not exist and that the link between AJs and the cytoskeleton is likely mediated by several different interacting modules (e.g. Afadin) resulting in a highly dynamic connection (Drees et al., 2005; Yamada et al., 2005). The cortical Actin based cytoskeleton was also reported to be more dynamic than the AJs by FRAP (fluorescene recovery after photobleaching) (Gates and Peifer, 2005; Yamada et al., 2005). Smash might represent a so far undescribed link between AJs and the cytoskeleton. It would be interesting to perform FRAP analysis of the cortical Actin cytoskeleton upon overexpression of Smash and record its activity.

We provide evidence that *smash* gene function is not essential but cannot exclude whether *smash* functions redundantly with other genes. The vertebrate homolog *LMO7* was duplicated and shows a paralog *LIMCH1* (Friedberg, 2009, 2010). It is possible that a double knockout of *LMO7* and *LIMCH1* results in lethality and severe defects, if both genes function redundantly. However, a *LIMCH1* mutant is not reported. It would be important to search for similar proteins encoded by the *Drosophila* genome, although *smash* appears not to be duplicated. Generation of different double mutants with *smash* might exhibit specific defects. However, blast search does not show genes similar to *smash*. In this context proteins with related domain composition would be of interest as well.

6 References

Atwood, S.X., Chabu, C., Penkert, R.R., Doe, C.Q., and Prehoda, K.E. (2007). Cdc42 acts downstream of Bazooka to regulate neuroblast polarity through Par-6 aPKC. Journal of Cell Science *120*, 3200–3206.

Bach, I. (2000). The LIM domain: regulation by association. Mechanisms of Development *91*, 5–17.

Bachmann, A. and Knust, E. (2008). The use of P-element transposons to generate transgenic flies. Methods in Molecular Biology *420*, 61-77.

Beati, H. (2009). Die Rolle der Bazooka-CG31534 Interaktion bei der Etablierung der Zellpolarität in *Drosophila melanogaster*. Diplomarbeit an der Georg-August-Universität Göttingen, Göttingen.

Behrens, J., Vakaet, L., Friis, R., Winterhager, E., Van Roy, F., Mareel, M.M., and Birchmeier, W. (1993). Loss of epithelial differentiation and gain of invasiveness correlates with tyrosine phosphorylation of the E-cadherin/beta-catenin complex in cells transformed with a temperature-sensitive v-SRC gene. The Journal of Cell Biology *120*, 757–766.

Bengtsson, L., and Wilson, K.L. (2004). Multiple and surprising new functions for emerin, a nuclear membrane protein. Current Opinion in Cell Biology *16*, 73–79.

Benton, R., and Johnston, D.S. (2003). A conserved oligomerization domain in *drosophila* Bazooka/PAR-3 is important for apical localization and epithelial polarity. Current Biology *13*, 1330–1334.

Betschinger, J., Mechtler, K., and Knoblich, J.A. (2003). The Par complex directs asymmetric cell division by phosphorylating the cytoskeletal protein Lgl. Nature *422*, 326–330.

Bilder, D., Li, M., and Perrimon, N. (2000). Cooperative regulation of cell polarity and growth by *Drosophila* tumor suppressors. Science *289*, 113–116.

Bilder, D., and Perrimon, N. (2000). Localization of apical epithelial determinants by the basolateral PDZ protein Scribble. Nature *403*, 676–680.

Bilder, D., Schober, M., and Perrimon, N. (2003). Integrated activity of PDZ protein complexes regulates epithelial polarity. Nature Cell Biology *5*, 53–58.

Bloor, J.W., and Brown, N.H. (1998). Genetic analysis of the *Drosophila* alphaPS2 integrin subunit reveals discrete adhesive, morphogenetic and sarcomeric functions. Genetics *148*, 1127–1142.

Bodenmiller, B., Malmstrom, J., Gerrits, B., Campbell, D., Lam, H., Schmidt, A., Rinner, O., Mueller, L.N., Shannon, P.T., Pedrioli, P.G., et al. (2007). PhosphoPep--a phosphoproteome resource for systems biology research in *Drosophila* Kc167 cells. Molecular Systems Biology *3*.

Boschek, C.B., Jockusch, B.M., Friis, R.R., Back, R., Grundmann, E., and Bauer, H. (1981). Early changes in the distribution and organization of microfilament proteins during cell transformation. Cell *24*, 175–184.

Boyer, B., Roche, S., Denoyelle, M., and Thiery, J.P. (1997). Src and Ras are involved in separate pathways in epithelial cell scattering. The EMBO Journal *16*, 5904–5913.

Brand, A.H., and Perrimon, N. (1993). Targeted gene expression as a means of altering cell fates and generating dominant phenotypes. Development *118*, 401–415.

Brown, M.T., and Cooper, J.A. (1996). Regulation, substrates and functions of src. Biochimica Et Biophysica Acta. *1287*, 121–149.

Cenciarelli, C., Chiaur, D.S., Guardavaccaro, D., Parks, W., Vidal, M., and Pagano, M. (1999). Identification of a family of human F-box proteins. Current Biology *9*, 1177–1179.

Chen, J., Shi, X., Padmanabhan, R., Wang, Q., Wu, Z., Stevenson, S.C., Hild, M., Garza, D., and Li, H. (2008). Identification of novel modulators of mitochondrial function by a genome-wide RNAi screen in *Drosophila melanogaster*. Genome Research *18*, 123–136.

Cherret, C., Furutani-Seiki, M., and Bagby, S. (2012). The Hippo pathway: key interaction and catalytic domains in organ growth control, stem cell self-renewal and tissue regeneration. Essays in Biochemistry *53*, 111-127.

Chihara, T., and Hayashi, S. (2000). Control of tracheal tubulogenesis by Wingless signaling. Development *127*, 4433–4442.

Cizkova, M., Cizeron-Clairac, G., Vacher, S., Susini, A., Andrieu, C., Lidereau, R., and Bièche, I. (2010). Gene expression profiling reveals new aspects of PIK3CA mutation in ERalpha-positive breast cancer: major implication of the Wnt signaling pathway. PLoS Genetics *5*, e15647.

Dawes-Hoang, R.E., Parmar, K.M., Christiansen, A.E., Phelps, C.B., Brand, A.H., and Wieschaus, E.F. (2005). *folded gastrulation*, cell shape change and the control of myosin localization. Development *132*, 4165–4178.

Dedeic, Z., Cetera, M., Cohen, T. V, and Holaska, J.M. (2011). Emerin inhibits Lmo7 binding to the Pax3 and MyoD promoters and expression of myoblast proliferation genes. Journal of Cell Science *124*, 1691–1702.

Desprat, N., Supatto, W., Pouille, P.-A., Beaurepaire, E., and Farge, E. (2008). Tissue deformation modulates twist expression to determine anterior midgut differentiation in *Drosophila* embryos. Developmental Cell *15*, 470–477.

Dodson, G.S., Guarnieri, D.J., and Simon, M.A. (1998). *Src64* is required for ovarian ring canal morphogenesis during *Drosophila* oogenesis. Development *125*, 2883–2892.

Doe, C.Q. (2008). Neural stem cells: balancing self-renewal with differentiation. Development *135*, 1575–1587.

Drees, F., Pokutta, S., Yamada, S., Nelson, W.J., and Weis, W.I. (2005). Alpha-catenin is a molecular switch that binds E-Cadherin-beta-catenin and regulates actin-filament assembly. Cell *123*, 903–915.

Emery, A.E.H. (2000). Emery-Dreifuss muscular dystrophy - a 40 year retrospective. Neuromuscular Disorders *10*, 228–232.

Engen, J.R., Wales, T.E., Hochrein, J.M., Meyn, M.A. 3rd, Banu Ozkan, S., Bahar, I., and Smithgall, T.E. (2008). Structure and dynamic regulation of Src-family kinases. Cellular and Molecular Life Sciences *65*, 3058–3073.

Fanning, A.S., and Anderson, J.M. (1999). PDZ domains: fundamental building blocks in the organization of protein complexes at the plasma membrane. The Journal of Clinical Investigation *103*, 767–772.

Freyd, G., Kim, S.K., and Horvitz, H.R. (1990). Novel cysteine-rich motif and homeodomain in the product of the *Caenorhabditis elegans* cell lineage gene *lin-11*. Nature *344*, 876–879.

Friedberg, F. (2009). Alternative splicing for members of human mosaic domain superfamilies. I. The CH and LIM domains containing group of proteins. Molecular Biology Reports *36*, 1059–1081.

Friedberg, F. (2010). Singlet CH domain containing human multidomain proteins: an inventory. Molecular Biology Reports *37*, 1531–1539.

Förster, D., and Luschnig, S. (2012). Src42A-dependent polarized cell shape changes mediate epithelial tube elongation in *Drosophila*. Nature Cell Biology *14*, 526–534.

Gates, J., and Peifer, M. (2005). Can 1000 reviews be wrong? Actin, alpha-Catenin, and adherens junctions. Cell *123*, 769–772.

Giot, L., Bader, J.S., Brouwer, C., Chaudhuri, A., Kuang, B., Li, Y., Hao, L., Ooi, C.E., Godwin, B., Vitols, E., et al. (2003). A protein interaction map of *Drosophila melanogaster*. Science *302*, 1727–1736.

Groth, A.C., Fish, M., Nusse, R., and Calos, M.P. (2004). Construction of transgenic *Drosophila* by using the site-specific integrase from phage phiC31. Genetics *166*, 1775–1782.

Hamaguchi, M., Matsuyoshi, N., Ohnishi, Y., Gotoh, B., Takeichi, M., and Nagai, Y. (1993). p60v-src causes tyrosine phosphorylation and inactivation of the N-cadherin-catenin cell adhesion system. The EMBO Journal *12*, 307–314.

Harris, B.Z., and Lim, W.A. (2001). Mechanism and role of PDZ domains in signaling complex assembly. Journal of Cell Science *114*, 3219–3231.

Harris, T.J.C., and Peifer, M. (2005). The positioning and segregation of apical cues during epithelial polarity establishment in *Drosophila*. The Journal of Cell Biology *170*, 813–823.

Holaska, J.M., Rais-Bahrami, S., and Wilson, K.L. (2006). Lmo7 is an emerin-binding protein that regulates the transcription of emerin and many other muscle-relevant genes. Human Molecular Genetics *15*, 3459–3472.

Holaska, J.M., and Wilson, K.L. (2006). Multiple roles for emerin: implications for Emery-Dreifuss muscular dystrophy. The Anatomical Record. Part A, Discoveries in Molecular, Cellular, and Evolutionary Biology. *288*, 676–680.

Horikoshi, Y., Suzuki, A., Yamanaka, T., Sasaki, K., Mizuno, K., Sawada, H., Yonemura, S., and Ohno, S. (2009). Interaction between PAR-3 and the aPKC-PAR-6 complex is indispensable for apical domain development of epithelial cells. Journal of Cell Science *122*, 1595–1606.

Huang, J., Zhou, W., Dong, W., Watson, A.M., and Hong, Y. (2009). Directed , efficient , and versatile modifications of the *Drosophila* genome by genomic engineering. Proceedings of the National Academy of Sciences of the United States of America *106*, 8284–8289.

Hurov, J.B., Watkins, J.L., and Piwnica-Worms, H. (2004). Atypical PKC phosphorylates PAR-1 kinases to regulate localization and activity. Current Biology *14*, 736–741.

Ia, K.K., Mills, R.D., Hossain, M., Chan, K.C., Jarasrassamee, B., Jorissen, R.N., and Cheng, H.C. (2010). Structural elements and allosteric mechanisms governing regulation and catalysis of CSK-family kinases and their inhibition of Src-family kinases. Growth Factors *28*, 329-350.

Ishiuchi, T., and Takeichi, M. (2011). Willin and Par3 cooperatively regulate epithelial apical constriction through aPKC-mediated ROCK phosphorylation. Nature Cell Biology *13*, 860–866.

Jacinto, A., Woolner, S., and Martin, P. (2002). Dynamic analysis of dorsal closure in *Drosophila*: from genetics to cell biology. Developmental Cell *3*, 9–19.

Jeleń, F., Oleksy, A., Śmietana, K., and Otlewski, J. (2003). PDZ domains — common players in the cell signaling. Acta Biochimica Polonica *50*, 985–1017.

Jiang, X., Xia, L., Chen, D., Yang, Y., Huang, H., Yang, L., Zhao, Q., Shen, L., Wang, J., and Chen, D. (2008). Otefin , a nuclear membrane protein, determines the fate of germline stem cells in *Drosophila* via interaction with Smad complexes. Developmental Cell *14*, 494–506.

Johnson, K., and Wodarz, A. (2003). A genetic hierarchy controlling cell polarity. Nature Cell Biology *5*, 12–14.

Juarez, M.T., Patterson, R.A., Sandoval-Guillen, E., and McGinnis, W. (2011). Duox, Flotillin-2, and Src42A are required to activate or delimit the spread of the transcriptional response to epidermal wounds in *Drosophila*. PLoS Genetics *7*, e1002424.

Kadrmas, J.L., and Beckerle, M.C. (2004). The LIM domain: from the cytoskeleton to the nucleus. Nature Reviews. Molecular Cell Biology. *5*, 920–931.

Karlsson, O., Thor, S., Norberg, T., Ohlsson, H., and Edlund, T. (1990). Insulin gene enhancer binding protein Isl-1 is a member of a novel class of proteins containing both a homeo- and a Cys-His domain. Nature *344*, 879–882.

Khurana, T., Khurana, B., and Noegel, A.A. (2002). LIM proteins: association with the actin cytoskeleton. Protoplasma *219*, 1–12.

Kim, L., and Wong, T.W. (1998). Growth factor-dependent phosphorylation of the actin-binding protein cortactin is mediated by the cytoplasmic tyrosine kinase FER. The Journal of Biological Chemistry *273*, 23542–23548.

Knust, E., and Bossinger, O. (2002). Composition and formation of intercellular junctions in epithelial cells. Science *298*, 1955–1959.

Krahn, M.P., Bückers, J., Kastrup, L., and Wodarz, A. (2010a). Formation of a Bazooka-Stardust complex is essential for plasma membrane polarity in epithelia. The Journal of Cell Biology *190*, 751–760.

Krahn, M.P., Klopfenstein, D.R., Fischer, N., and Wodarz, A. (2010b). Membrane targeting of Bazooka/PAR-3 is mediated by direct binding to phosphoinositide lipids. Current Biology *20*, 636–642.

Kusakabe, M., and Nishida, E. (2004). The polarity-inducing kinase Par-1 controls *Xenopus* gastrulation in cooperation with 14-3-3 and aPKC. The EMBO Journal *23*, 4190–4201.

Laplante, C., and Nilson, L.A. (2011). Asymmetric distribution of Echinoid defines the epidermal leading edge during *Drosophila* dorsal closure. The Journal of Cell Biology *192*, 335–348.

Laprise, P., Paul, S.M., Boulanger, J., Robbins, R.M., Beitel, G.J., and Tepass, U. (2010). Epithelial polarity proteins regulate *Drosophila* tracheal tube size in parallel to the luminal matrix pathway. Current Biology : CB *20*, 55–61.

Lilien, J., Balsamo, J., Arregui, C., and Xu, G. (2002). Turn-off, drop-out: functional state switching of cadherins. Developmental Dynamics *224*, 18–29.

Lim, W.A., and Pawson, T. (2010). Phosphotyrosine signaling: evolving a new cellular communication system. Cell *142*, 661–667.

Llimargas, M. (2000). Wingless and its signalling pathway have common and separable functions during tracheal development. Development *127*, 4407–4417.

Lu, X., and Li, Y. (1999). *Drosophila Src42A* is a negative regulator of RTK signaling. Developmental Biology *208*, 233–243.

McCaffrey, L.M., and Macara, I.G. (2009). The Par3/aPKC interaction is essential for end bud remodeling and progenitor differentiation during mammary gland morphogenesis. Genes & Development *23*, 1450–1460.

McGill, M.A., McKinley, R.F.A., and Harris, T.J.C. (2009). Independent cadherin-catenin and Bazooka clusters interact to assemble adherens junctions. The Journal of Cell Biology *185*, 787–796.

Morais-de-Sá, E., Mirouse, V., and St Johnston, D. (2010). aPKC phosphorylation of Bazooka defines the apical/lateral border in *Drosophila* epithelial cells. Cell *141*, 509–523.

Murray, M.J., Davidson, C.M., Hayward, N.M., and Brand, A.H. (2006). The Fes/Fer non-receptor tyrosine kinase cooperates with Src42A to regulate dorsal closure in *Drosophila*. Development *133*, 3063–3073.

Müller, H.-A.J. (2000). Genetic control of epithelial cell polarity: lessons from *Drosophila*. Developmental Dynamics *218*, 52–67.

Müller, H.-A.J., and Wieschaus, E. (1996). *armadillo*, *bazooka*, and *stardust* are critical for early stages in formation of the zonula adherens and maintenance of the polarized blastoderm epithelium in *Drosophila*. The Journal of Cell Biology *134*, 149–163.

Nagano, A., Koga, R., Ogawa, M., Kurano, Y., Kawada, J., Okada, R., Hayashi, Y.K., Tsukahara, T., and Arahata, K. (1996). Emerin deficiency at the nuclear membrane in patients with Emery-Dreifuss muscular dystrophy. Nature Genetics *12*, 254–259.

Nakamura, H., Hori, K., Tanaka-Okamoto, M., Higashiyama, M., Itoh, Y., Inoue, M., Morinaka, S., and Miyoshi, J. (2011). Decreased expression of LMO7 and its clinicopathological significance in human lung adenocarcinoma. Experimental And Therapeutic Medicine *2*, 1053–1057.

Nakamura, H., Mukai, M., Komatsu, K., Tanaka-Okamoto, M., Itoh, Y., Ishizaki, H., Tatsuta, M., Inoue, M., and Miyoshi, J. (2005). Transforming growth factor-β1 induces LMO7 while enhancing the invasiveness of rat ascites hepatoma cells. Cancer Letters *220*, 95–99.

Nam, S.-C., and Choi, K.-W. (2003). Interaction of Par-6 and Crumbs complexes is essential for photoreceptor morphogenesis in *Drosophila*. Development *130*, 4363–4372.

Nelson, K.S., Khan, Z., Molnár, I., Mihály, J., Kaschube, M., and Beitel, G.J. (2012). *Drosophila* Src regulates anisotropic apical surface growth to control epithelial tube size. Nature Cell Biology *14*, 518–525.

Neugebauer, J. (2007). Untersuchungen zur Funktion des Gens *CG31534* bei der Entwicklung ektodermaler Epithelien in *Drosophila*. Diplomarbeit an der Georg-August-Universität Göttingen, Göttingen.

Ochoa-Espinosa, A., Baer, M.M., and Affolter, M. (2012). Tubulogenesis: Src42A goes to great lengths in tube elongation. Current Biology *22*, R446–449.

Ooshio, T., Irie, K., Morimoto, K., Fukuhara, A., Imai, T., and Takai, Y. (2004). Involvement of LMO7 in the association of two cell-cell adhesion molecules, nectin and E-cadherin, through afadin and alpha-actinin in epithelial cells. The Journal of Biological Chemistry *279*, 31365–31373.

Ott, E.B., Van den Akker, N.M.S., Sakalis, P.A., Gittenberger-de Groot, A.C., Te Velthuis, A.J.W., and Bagowski, C.P. (2008). The lim domain only protein 7 is important in zebrafish heart development. Developmental Dynamics *237*, 3940–3952.

O'Reilly, A.M., Ballew, A.C., Miyazawa, B., Stocker, H., Hafen, E., and Simon, M.A. (2006). *Csk* differentially regulates *Src64* during distinct morphological events in *Drosophila* germ cells. Development *133*, 2627–2638.

Parsons, S.J., and Parsons, J.T. (2004). Src family kinases , key regulators of signal transduction. Oncogene *23*, 7906–7909.

Pedraza, L.G., Stewart, R.A., Li, D.-M., and Xu, T. (2004). *Drosophila* Src-family kinases function with Csk to regulate cell proliferation and apoptosis. Oncogene *23*, 4754–4762.

Petronczki, M., and Knoblich, J.A. (2001). DmPAR-6 directs epithelial polarity and asymmetric cell division of neuroblasts in *Drosophila*. Nature Cell Biology *3*, 43–49.

Piedra, J., Miravet, S., Castaño, J., Pálmer, H.G., Heisterkamp, N., Herreros, A.G. de, and Duñach, M. (2003). p120 Catenin-associated Fer and Fyn tyrosine kinases regulate beta-catenin Tyr-142 phosphorylation and beta-catenin-alpha-catenin interaction. Molecular and Cellular Biology *23*, 2287–2297.

Pingoud, A., and Jeltsch, A. (2001). Structure and function of type II restriction endonucleases. Nucleic Acids Research *29*, 3705–3727.

Plant, P.J., Fawcett, J.P., Lin, D.C.C., Holdorf, A.D., Binns, K., Kulkarni, S., and Pawson, T. (2003). A polarity complex of mPar-6 and atypical PKC binds, phosphorylates and regulates mammalian Lgl. Nature Cell Biology *5*, 301–308.

Ramrath, A. (2002). Isolierung und Charakterisierung von Bindungspartnern des PDZDomänen-Proteins BAZOOKA aus *Drosophila melanogaster*. Inaugural-Dissertation in Mathematisch-Naturwissenschaftlicher Fakultät der Heinrich-Heine-Universität Düsseldorf, Düsseldorf.

Riento, K., and Ridley, A.J. (2003). Rocks : multifunctional kinases in cell behaviour. Nature Reviews. Molecular Cell Biology. *4*, 446–456.

Rozenblum, E., Vahteristo, P., Sandberg, T., Bergthorsson, J.T., Syrjakoski, K., Weaver, D., Haraldsson, K., Johannsdottir, H.K., Vehmanen, P., Nigam, S., et al. (2002). A genomic map of a 6-Mb region at 13q21-q22 implicated in cancer development: identification and characterization of candidate genes. Human Genetics *110*, 111–121.

Sasaki, M., Tsuji, N., Furuya, M., Kondoh, K., Kamagata, C., Kobayashi, D., Yagihashi, A., and Watanabe, N. (2003). PCD1, a novel gene containing PDZ and LIM domains, is overexpressed in human breast cancer and linked to lymph node metastasis. Anticancer Research *23*, 2717-2721.

Sawyer, J.K., Harris, N.J., Slep, K.C., Gaul, U., and Peifer, M. (2009). The *Drosophila* afadin homologue Canoe regulates linkage of the actin cytoskeleton to adherens junctions during apical constriction. The Journal of Cell Biology *186*, 57–73.

Semenova, E., Wang, X., Jablonski, M.M., Levorse, J., and Tilghman, S.M. (2003). An engineered 800 kilobase deletion of *Uchl3* and *Lmo7* on mouse chromosome 14 causes defects in viability, postnatal growth and degeneration of muscle and retina. Human Molecular Genetics *12*, 1301–1312.

Sewell, W., Sparrow, D.B., Smith, A.J., Gonzalez, D.M., Rappaport, E.F., Dunwoodie, S.L., and Kusumi, K. (2010). Cyclical expression of the Notch/Wnt regulator Nrarp requires modulation by Dll3 in somitogenesis. Developmental Biology *329*, 400–409.

Sheng, M., and Sala, C. (2001). PDZ domains and the organization of supramolecular complexes. Annual Review of Neuroscience *24*, 1–29.

Shindo, M., Wada, H., Kaido, M., Tateno, M., Aigaki, T., Tsuda, L., and Hayashi, S. (2008). Dual function of Src in the maintenance of adherens junctions during tracheal epithelial morphogenesis. Development *135*, 1355–1364.

Simon, M.A., Drees, B., Kornberg, T., and Bishop, J.M. (1985). The nucleotide sequence and the tissue-specific expression of *Drosophila* c-src. Cell *42*, 831–840.

Singh, J., Aaronson, S.A., and Mlodzik, M. (2010). *Drosophila* Abelson kinase mediates cell invasion and proliferation through two distinct MAPK pathways. Oncogene *29*, 4033–4045.

Sotillos, S., Díaz-Meco, M.T., Caminero, E., Moscat, J., and Campuzano, S. (2004). DaPKC-dependent phosphorylation of Crumbs is required for epithelial cell polarity in *Drosophila*. The Journal of Cell Biology *166*, 549–557.

Von Stein, W., Ramrath, A., Grimm, A., Müller-Borg, M., and Wodarz, A. (2005). Direct association of Bazooka/PAR-3 with the lipid phosphatase PTEN reveals a link between the PAR/aPKC complex and phosphoinositide signaling. Development *132*, 1675–1686.

Strong, T.C., and Thomas, J.H. (2011). Maternal and zygotic requirements for *src64* during *Drosophila* cellularization. Genesis *49*, 912–918.

Suzuki, A., Hirata, M., Kamimura, K., Maniwa, R., Yamanaka, T., Mizuno, K., Kishikawa, M., Hirose, H., Amano, Y., Izumi, N., et al. (2004). aPKC acts upstream of PAR-1b in both the establishment and maintenance of mammalian epithelial polarity. Current Biology *14*, 1425–1435.

Suzuki, A., and Ohno, S. (2006). The PAR-aPKC system: lessons in polarity. Journal of Cell Science *119*, 979–987.

Takahashi, F., Endo, S., Kojima, T., and Saigo, K. (1996). Regulation of cell-cell contacts in developing *Drosophila* eyes by *Dsrc41*, a new, close relative of vertebrate c-*src*. Genes & Development *10*, 1645–1656.

Takahashi, K., Matsuo, T., Katsube, T., Ueda, R., and Yamamoto, D. (1998). Direct binding between two PDZ domain proteins Canoe and ZO-1 and their roles in regulation of the Jun N-terminal kinase pathway in *Drosophila* morphogenesis. Mechanisms of Development *78*, 97–111.

Takahashi, M., Takahashi, F., Ui-Tei, K., Kojima, T., and Saigo, K. (2005). Requirements of genetic interactions between *Src42A*, *armadillo* and *shotgun*, a gene encoding E-cadherin, for normal development in *Drosophila*. Development *132*, 2547–2559.

Takeda, H., Nagafuchi, A., Yonemura, S., Tsukita, S., Behrens, J., Birchmeier, W., and Tsukita, S. (1995). V-src kinase shifts the cadherin-based cell adhesion from the strong to the weak state and beta catenin is not required for the shift. The Journal of Cell Biology *131*, 1839–1847.

Tamada, M., Farrell, D.L., and Zallen, J.A. (2012). Abl regulates planar polarized junctional dynamics through β-catenin tyrosine phosphorylation. Developmental Cell *22*, 309–319.

Tanaka-Okamoto, M., Hori, K., Ishizaki, H., Hosoi, A., Itoh, Y., Wei, M., Wanibuchi, H., Mizoguchi, A., Nakamura, H., and Miyoshi, J. (2009). Increased susceptibility to spontaneous lung cancer in mice lacking LIM-domain only 7. Cancer Science *100*, 608–616.

Tanentzapf, G., and Tepass, U. (2003). Interactions between the *crumbs*, *lethal giant larvae* and *bazooka* pathways in epithelial polarization. Nature Cell Biology *5*, 46–52.

Tateno, M., Nishida, Y., and Adachi-Yamada, T. (2000). Regulation of JNK by Src during *Drosophila* development. Science *287*, 324–327.

Tepass, U. (1996). Crumbs, a component of the apical membrane, is required for zonula adherens formation in primary epithelia of *Drosophila*. Developmental Biology *177*, 217–225.

Tepass, U. (2012). The apical polarity protein network in *Drosophila* epithelial cells: regulation of polarity, junctions, morphogenesis, cell growth, and survival. Annual Review of Cell and Developmental Biology *28*, 655–685.

Thibault, S.T., Singer, M.A., Miyazaki, W.Y., Milash, B., Dompe, N.A., Singh, C.M., Buchholz, R., Demsky, M., Fawcett, R., Francis-Lang, H.L., et al. (2004). A complementary transposon tool kit for *Drosophila melanogaster* using *P* and *piggyBac*. Nature Genetics *36*, 283–287.

Thomas, J.H., and Wieschaus, E. (2004). *src64* and *tec29* are required for microfilament contraction during *Drosophila* cellularization. Development *131*, 863–871.

Thomas, S.M., and Brugge, J.S. (1997). Cellular functions regulated by Src family kinases. Annual Review of Cell and Developmental Biology *13*, 513–609.

Tikhmyanova, N., Tulin, A. V, Roegiers, F., and Golemis, E.A. (2010). Dcas supports cell polarization and cell-cell adhesion complexes in development. PloS One *5*, e12369.

Tsai, P.-I., Kao, H.-H., Grabbe, C., Lee, Y.-T., Ghose, A., Lai, T.-T., Peng, K.-P., Van Vactor, D., Palmer, R.H., Chen, R.-H., et al. (2008). Fak56 functions downstream of integrin alphaPS3betanu and suppresses MAPK activation in neuromuscular junction growth. Neural Development *3*.

VanHook, A., and Letsou, A. (2008). Head involution in *Drosophila*: genetic and morphogenetic connections to dorsal closure. Developmental Dynamics *237*, 28–38.

Te Velthuis, A.J.W., and Bagowski, C.P. (2007). PDZ and LIM domain-encoding genes: molecular interactions and their role in development. TheScientificWorldJournal *7*, 1470–1492.

Te Velthuis, A.J.W., Isogai, T., Gerrits, L., and Bagowski, C.P. (2007). Insights into the molecular evolution of the PDZ/LIM family and identification of a novel conserved protein motif. PloS One *2*, e189.

Vicente-Manzanares, M., Ma, X., Adelstein, R.S., and Horwitz, A.R. (2009). Non-muscle myosin II takes centre stage in cell adhesion and migration. Nature Reviews. Molecular Cell Biology. *10*, 778–790.

Walther, R.F., and Pichaud, F. (2010). Crumbs/DaPKC-dependent apical exclusion of Bazooka promotes photoreceptor polarity remodeling. Current Biology *20*, 1065–1074.

Wang, Y., Du, D., Fang, L., Yang, G., Zhang, C., Zeng, R., Ullrich, A., Lottspeich, F., and Chen, Z. (2006). Tyrosine phosphorylated Par3 regulates epithelial tight junction assembly promoted by EGFR signaling. The EMBO Journal *25*, 5058–5070.

Way, J.C., and Chalfie, M. (1988). *mec-3*, a homeobox-containing gene that specifies differentiation of the touch receptor neurons in *C.elegans*. Cell *54*, 5–16.

Wei, S.-Y., Escudero, L.M., Yu, F., Chang, L.-H., Chen, L.-Y., Ho, Y.-H., Lin, C.-M., Chou, C.-S., Chia, W., Modolell, J., et al. (2005). Echinoid is a component of adherens junctions that cooperates with DE-Cadherin to mediate cell adhesion. Developmental Cell *8*, 493–504.

Wimmer, E.A. (2003). Innovations: applications of insect transgenesis. Nature Reviews. Genetics. *4*, 225–232.

Wodarz, A. (2005). Molecular control of cell polarity and asymmetric cell division in *Drosophila* neuroblasts. Current Opinion in Cell Biology *17*, 475–481.

Wodarz, A. (2008). Extraction and immunoblotting of proteins from embryos. Methods in Molecular Biology *420*, 335-345.

Wodarz, A., Grawe, F., and Knust, E. (1993). CRUMBS is involved in the control of apical protein targeting during *Drosophila* epithelial development. Mechanisms of Development *44*, 175–187.

Wodarz, A., Hinz, U., Engelbert, M., and Knust, E. (1995). Expression of crumbs confers apical character on plasma membrane domains of ectodermal epithelia of *Drosophila*. Cell *82*, 67–76.

Wodarz, A., and Huttner, W.B. (2003). Asymmetric cell division during neurogenesis in *Drosophila* and vertebrates. Mechanisms of Development *120*, 1297–1309.

Wodarz, A., Ramrath, A., Grimm, A., and Knust, E. (2000). *Drosophila* atypical protein kinase C associates with Bazooka and controls polarity of epithelia and neuroblasts. The Journal of Cell Biology *150*, 1361–1374.

Wodarz, A., Ramrath, A., Kuchinke, U., and Knust, E. (1999). Bazooka provides an apical cue for Inscuteable localization in *Drosophila* neuroblasts. Nature *402*, 544–547.

Wouda, R.R., Bansraj, M.R.K.S., De Jong, A.W.M., Noordermeer, J.N., and Fradkin, L.G. (2008). Src family kinases are required for WNT5 signaling through the Derailed/RYK receptor in the *Drosophila* embryonic central nervous system. Development *135*, 2277–2287.

Wu, H., and Parsons, J.T. (1993). Cortactin, an 80/85-kilodalton pp60src substrate, is a filamentous actin-binding protein enriched in the cell cortex. The Journal of Cell Biology *120*, 1417–1426.

Yamada, S., Pokutta, S., Drees, F., Weis, W.I., and Nelson, W.J. (2005). Deconstructing the cadherin-catenin-actin complex. Cell *123*, 889–901.

Yamanaka, T., Horikoshi, Y., Sugiyama, Y., Ishiyama, C., Suzuki, A., Hirose, T., Iwamatsu, A., Shinohara, A., and Ohno, S. (2003). Mammalian Lgl forms a protein complex with PAR-6 and aPKC independently of PAR-3 to regulate epithelial cell polarity. Current Biology *13*, 734–743.

Yue, T., Tian, A., and Jiang, J. (2012). The cell adhesion molecule echinoid functions as a tumor suppressor and upstream regulator of the Hippo signaling pathway. Developmental Cell *22*, 255–267.

Ziegenfuss, J.S., Biswas, R., Avery, M.A., Hong, K., Sheehan, A.E., Yeung, Y.-G., Stanley, E.R., and Freeman, M.R. (2008). Draper-dependent glial phagocytic activity is mediated by Src and Syk family kinase signalling. Nature *453*, 935–939.

Zimmerman, S.G., Thorpe, L.M., Medrano, V.R., Mallozzi, C.A., and McCartney, B.M. (2010). Apical constriction and invagination downstream of the canonical Wnt signaling pathway require Rho1 and Myosin II. Developmental Biology *340*, 54–66.